ACOUSTIC SOURCES IN MOTION

by

Ann Patricia Dowling

Dissertation submitted for the degree of Doctor of Philosophy

Sidney Sussex College,
Cambridge

January 1978

Preface

This dissertation describes work done at the Cambridge University Engineering Department between October 1974 and December 1977. During that time I received support from many sources.

I am especially indebted to my supervisor Professor J.E. Ffowcs Williams for his continual guidance and encouragement.

My thanks are also due to Dr. M.E. Goldstein. The work described in Chapter 3 has been published as a joint paper with both Professor Ffowcs Williams and Dr. Goldstein. The part played by my co-authors in the development of this work is detailed in the acknowledgement at the end of Chapter 3.

I have benefited from discussions with Professor Sir James Lighthill and Dr. M.S. Howe and I would like to thank them for their interest and advice.

I am grateful to the Science Research Council, to Girton College, Cambridge and to Sidney Sussex College, Cambridge for their financial support.

I would also like to thank Mrs J. Broadway for doing the numerical calculation mentioned in Chapter 3, and Mrs P. Lister for her careful and accurate typing of the manuscript.

Except where explicitly stated this dissertation is the result of my own work and contains nothing which is the outcome of any work done in collaboration with others. No part of it has been submitted for a degree at any other university.

Sidney Sussex College,
Cambridge
January 1978

A.P. Dowling

Summary

The motion of an acoustic source changes its sound field. Three different fundamental topics concerned with radiation from moving sources are investigated in this thesis. In the first we consider the effect of motion on the sound field of two of the simplest realistic sources, a pulsating and a vibrating body. These two problems are often misrepresented as a moving monopole and dipole respectively. But it is found that for real sources that motion introduces additional coupled multipoles whose combined effect generates previously unexpected features. In general the change in the sound field due to source motion is greater than the effect estimated from previous mathematical models. Moreover, and quite unexpectedly, we have found that the radiation is altered in a direction perpendicular to the flight path.

Our second problem concerns the production of sound by a jet stream. We derive a generalization of Lighthill's acoustic analogy to account for the interaction of the acoustic field with the mean jet flow. We prove that the jet noise problem can be modelled exactly by convected quadrupoles near a vortex sheet. Each moving fluid particle supports a quadrupole whose strength is given by Lighthill's stress tensor and the sound radiates as if it were adjacent to an instability-free vortex sheet. Although we show that the sound field may be expressed in terms of the turbulence stress tensor, sound is also generated by the flow's instability waves as they grow into turbulence, and this sound appears as an exponentially growing precursor to the main field. Some well known features of the mean flow acoustic interaction issue are an immediate consequence of the theory. We examine the case of a round jet in some detail and concentrate on a new aspect. When the jet density is much lower than that of its environment, the mean flow acoustic interaction

results in a considerable amplification of the quadrupole field and the intensity of its sound can scale on an unusually low power of the jet speed. We show that a fourth power law is possible and even a second power law when the density difference is large enough. This may be part of the "excess noise" problem in which the sound of engine produced hot jets is often insensitive to changes in jet speed at low exhaust power.

A modern rotary printing press is a noisy machine. One of the noise sources is the vibration of the paper web as it moves under variable tension between the rollers. Our third problem models this process. We consider a semi-infinite elastic sheet initially at rest with a prescribed displacement. The sound produced by suddenly tugging one end is investigated. It is found that a tension wave travels supersonically through the sheet. There is no motion ahead of this wave but behind it the tensioned sheet supports a vibration. A membrane excited in this way is silent except at the tugged end and at the tension front. The sound field has all the characteristics of a moving line source. The parameters that control the noise output are identified and the dependence of the sound field on these variables is determined.

Table of Contents

	Page Number
Preface	(i)
Summary	(ii)
Table of Contents	(iv)
List of Figures	(v)
CHAPTER 1 INTRODUCTION	1
CHAPTER 2 THE SOUND PRODUCED BY SIMPLE SOURCES IN UNIFORM MOTION	
2.1 Introduction	5
2.2 The sound produced by idealized point sources in uniform motion	8
2.3 The sound produced by a weakly pulsating body in uniform motion	12
2.4 The sound produced by a juddering compact body in uniform motion	26
2.5 Conclusions	40
CHAPTER 3 SOUND PRODUCTION IN A MOVING STREAM	
3.1 Introduction	42
3.2 A generalization of Lighthill's acoustic analogy	47
3.3 The vortex sheet model	61
3.4 The circular cylindrical jet	65
3.5 The slab jet	82
3.6 Conclusions	94
CHAPTER 4 THE SOUND OF A SUDDENLY TENSIONED MEMBRANE	
4.1 Introduction	97
4.2 The sound of a suddenly tensioned membrane	99
4.3 Fluid loading has a dampening effect	116
4.4 Conclusions	122
CHAPTER 5 CONCLUSIONS	124
REFERENCES	129
APPENDIX 3.A THE EFFECT OF RESONANCES	133
APPENDIX 3.B THE RECIPROCAL THEOREM	142
APPENDIX 4.A THE DERIVATION OF THE ELASTIC EQUATIONS OF MOTION	145
APPENDIX 4.B SIMPLIFICATION OF THE INTEGRAL DESCRIBING THE FAR-FIELD DENSITY	149

Table of Figures

		Page Number
2.1	A moving source in a stationary fluid	9
2.2	A stationary source in a moving fluid	11
2.3	A pulsating body of general shape in a moving fluid	13
2.4	The position of the control surface S	23
2.5	A vibrating body in a moving fluid	27
2.6	A juddering sphere	37
3.1	The geometry of the jet	49
3.2	The definition of $G^{\dagger}$	53
3.3	The position of the branch cuts	67
3.4	The position of the curve of steepest descent	70
3.5	New position of the branch cut	70
3.6	A slab jet	83
3.7	Multiple reflexion in a light jet	90
4.1	The initial position of the membrane	100
4.2	The boundary conditions determining the sound field	104
4.3	The Mach wedge	108
4.4	The definition of r_1 and ϕ_1	110
4.5	The position of the wave front	117
3.A	The bounding surface at infinity	134
4.A	The geometry of the plate	146
4.B	The boundary of the region D	150

CHAPTER 1

INTRODUCTION

The frequency and intensity changes in the noise of a train passing through a station or a jet flying overhead leave one in no doubt that a sound field is altered by relative motion between the source and the observer.

In 1900 Wiechert modelled the electric field generated by a moving electron and his basic scheme may be used to determine the effect of source motion on the sound field of acoustic multipoles (Morse & Ingard 1968). The frequency of the sound heard by an observer is modified from its stationary value by the Doppler factor $(1 - M\cos\theta)^{-1}$, where M is the Mach number and θ the angle between the observer and the direction of source motion. This is the well known result that the frequency of the sound emitted by a source approaching the observer is increased, while the frequency of a receding source is decreased. Similarly the intensity of a moving multipole is amplified ahead of the source by an amount depending on the Mach number, while behind it is decreased. There is no effect when $\theta = 90^{o}$; the frequency and intensity of the sound field produced by multipoles is unchanged in a plane at right angles to the direction of motion.

In Chapter 2 we investigate the way in which the radiation from more realistic sources is modified by source motion. The first simple real source we consider is a small pulsating body. This has been modelled as a moving monopole (Lowson 1965), but there is an essential difference between the two problems. In addition to a mass flux, the moving pulsatile body also exerts a fluctuating force on the fluid which generates an additional sound field. Moreover, even for the smallest of physical sources, the retarded time variations over the

body are not negligible, and change the form of the sound field. The radiation from a small vibrating moving sphere is also determined in Chapter 2. In the past this source has been assumed incorrectly to be a dipole (Morse & Ingard 1968) but the presence of additional multipoles destroys such a simple specification of the field. The influence of motion on physically realizable sources seems to be more acute than for the multipoles described in the literature. Source motion can also amplify the sound radiated perpendicular to the direction of motion; this feature has been observed experimentally in the measurement of flight effects on jet noise, but is not demonstrated in the classical mathematical models. Probably the most useful conclusion is that source motion alters the field in a complicated way that depends on the form of the source. We believe that it is essential to have an accurate description of the important sources in a real jet before the effect of flight on aircraft noise can be correctly predicted.

In his pioneering paper Lighthill (1952) rearranged the Navier Stokes equation to show that jet mixing noise may be described by convected quadrupoles emitting into a still fluid, and he determined the exact equivalent sources. Of course, in practice, sound produced within the jet will propagate through turbulent fluid, and such a moving flow can alter the sound field. This interaction between the acoustic field and the mean flow is concealed within Lighthill's 'source terms' and cannot be brought out explicitly in a dimensional analysis. The interaction of sound with its source, an inhomogeneous turbulent flow, is a very complex problem, and is fundamental to an understanding of jet noise. Lush (1971) compared the usual deductions from Lighthill's theory with experiment. He found that there are significant differences between the predicted values and the experimental results whenever an acoustic ray propagates a distance greater than a wavelength through the

shear layer; then proper account must be taken of the effect of flow on the acoustic field.

Lilley (1971 and 1974) has developed a theory whereby the mean velocity variations can be removed from the source term to the wave operator part of the equation. This theory predicts aspects of the sound field of a jet that cannot be obtained directly from the Lighthill theory, but there are certain difficulties associated with the method. The Green function for Lilley's equation is complicated, and it is not clear what initial and boundary conditions should be imposed upon it, because the causal solution has exponential growth at infinity. These instability waves are usually neglected without mention in any analysis of Lilley's equation (Morfey & Tester 1976). Knott (1974) showed that the computational results are relatively insensitive to shear layer details, the variation may be as little as 1 or 2 db. If this is so, the vortex sheet models (Mani 1976, Dash 1976) have a definite advantage for they are the easiest to handle. In Chapter 3 we develop an exact analogy between a vortex sheet and a jet flow. The role of the mean flow instabilities is clarified and the exact equivalent sources determined; a jet may be modelled by moving quadrupoles within an instability-free vortex sheet. The strength of each quadrupole is given by Lighthill's stress tensor measured relative to a uniformly moving jet stream, and the quadrupoles are convected with the fluid flow.

Our exact analogy relates the sound field to the turbulence stress tensor. In an unstable jet sound is generated in part by the flow's instability waves as they grow into turbulence, and this sound appears as a precursor to the main turbulence driven field.

We develop the theory for a general geometry and then apply it to a cylindrical jet of circular cross-section. We derive several well

known results for compact jets; for example we recover Mani's (1976) result that the linear pressure field of the longitudinal quadrupoles is modified by $(1 - M \cos\theta)^{-5}$, so that even at low frequencies the usual results derived from Lighthill's theory are not valid, and the refractive effect of the surrounding fluid alters the amplification factor. We also obtain some new results for the acoustically compact jet of low density. There the sound appears to scale on very low powers of the jet speed. This may be relevant to the 'excess noise' problem, where it is known that the sound of hot jets is less sensitive to variations in speed than Lighthill's eighth power law.

Chapter 4 deals with a different class of problem which at first sight is unrelated to the others; the sound produced when an elastic sheet initially at rest is suddenly tugged. This source is actually not stationary but moves at high speed. In fact a tension front propagates supersonically through the membrane and the jump in normal velocity occurring at this front produces a supersonically moving source. The sound field has all the characteristics of a supersonic line source. The parameters controlling the noise output are determined and the way in which the sound field depends on these parameters is investigated. This problem is thought to bear on the question of how much noise is made by the vibration of the paper web in a rotary printing machine, where the web tension is often changed abruptly by irregularities in the reel surfaces.

The common theme running through these three problems is that in each case the sound field originates in physically realizable sources which move relative to the observer. We find that in every case the field is considerably modified by convection and modified in a way that could hardly have been anticipated without the help of definite solutions.

CHAPTER 2

THE SOUND PRODUCED BY SIMPLE SOURCES IN UNIFORM MOTION

2.1 Introduction

Aircraft flight changes jet noise in a way that is not well understood. An estimate of the influence of forward speed on pure jet noise can be obtained by taking the strength of Lighthill's convected quadrupoles to depend on the relative velocity of the exhaust gases and the surrounding air (Ffowcs Williams 1969). However the series of experiments reported by Hoch & Hawkins (1974) demonstrate that the real situation is not that simple; the reduction of noise at the rear of the jet, ahead of the radiating eddies, is less than that predicted by relative velocity arguments, while the sound in the upstream arc is either unchanged or slightly increased by flight. Hoch & Hawkins in an attempt to explain these results suggest that internal noise sources might be present and influential at higher jet velocities under flight conditions than in a static jet. Internal or 'excess' noise sources are associated with rough flow within the engine. In flight these sources have a forward velocity, and one would expect their sound field to be amplified in the forward arc. This enhancement could mean that sources which are undetectable statically may become significant under flight conditions. But by how much? It is this question that provoked this particular study. Previous analyses had concerned only idealized point multipoles, a choice determined more by mathematical convenience than physical relevance. We attempted to answer the dual question of how to mathematically model a physically realizable source and then to determine the effect of source motion. Our intention was to estimate the nature and the approximate magnitude of flight effects by investigating the sound field of some simple but real sources in motion.

For practical purposes we are often interested in the limit $M^2 << 1$, where M is the Mach number of the source flow. This limit allows a great mathematical simplification; we can study the $O(M)$ kinematic effects of source motion without the complications of varying sound speed etc. which are $O(M^2)$.

The sound produced by multipole point sources in motion has received extensive study in the literature. In 1900 Wiechert determined the field of a moving point electric charge, and showed that motion modifies the amplitude of the electric field by a factor $(1 - M\cos\theta)^{-1}$, where θ is the observation angle referred to the direction of source motion.

There has been much discussion about how this classical result should be applied to acoustic problems, because a different field is obtained when one defines a moving point source as a singularity of the wave equation for the velocity potential rather than, say, the pressure. Warren (1975) recently summarized this difficulty. However, as a moving point source in the pressure wave equation has no physical meaning (Lowson 1965), it is usual to base the definition of the acoustic monopole on the velocity potential. Then the source strength can be interpreted as the volume flux produced by the singularity. The pressure perturbation satisfies a wave equation forced by both a moving monopole, which depends on the change of mass flux, and a coupled dipole describing the associated change of momentum. Source motion modifies this pressure field by a factor $(1 - M\cos\theta)^{-2}$.

A stationary pulsating body radiates like a monopole, and Lowson (1965) states that a moving monopole field is produced by a pulsating sphere in motion. Graham & Graham (1971), however, argue that this conventional moving source cannot represent an expanding and contracting sphere with a uniform velocity, because unlike the sphere

it does not transport the neighbouring fluid with it. Instead they suggest a different model source. Graham & Graham (1971) claim that their source describes the effect of motion on the acoustic field of a small deformable sphere. Goldstein (1975) has shown that the stationary pressure field of that model is modified by a factor $(1 - M\cos\theta)^{-3}$. This is not the result we obtain and we argue that the situation is more intricate than that supposed by Graham & Graham.

We investigate the sound field produced by a pulsating body whose centroid moves with a constant velocity. We find that the influence of motion depends crucially on the geometry of the body through the inertial mass tensor α_{ij}. For a general shape the linear pressure field is amplified from its value when the source is stationary by a factor $(1 + \hat{r}_i \alpha_{ij} M_j)(1 - M\cos\theta)^{-3}$, where $\underset{\sim}{M}$ is a vector in the direction of motion of magnitude M, and $\hat{r}_i$ $(i = 1,2,3)$ are the direction cosines of the path taken by the sound travelling towards the distant observation point. A moving pulsating sphere does not produce a sound field like either a moving monopole or Graham & Graham's source; its pressure field is modified by $(1 - M\cos\theta)^{-3\frac{1}{2}}$. For a general shaped body there is also amplification in a plane perpendicular to the flight path. This is a new result and is quite different from the effect of point multipoles; their field at $\theta = 90^{o}$ is unchanged by motion.

We also study the acoustic far-field produced by an undeformable sphere moving with a small vibration superimposed on an otherwise steady low Mach number velocity. This sound field has previously been assumed (incorrectly) to be modelled by a moving dipole, see for example Morse & Ingard (1968, Chapter 11). The influence of source motion is then completely described by the multiplying factor $(1 - M\cos\theta)^{-2}$. However we show that the effect of motion is far more complicated; the stationary pressure field is amplified by $(1 - M\cos\theta)^{-4}$, and there is an additional omnidirectional term.

2.2 The sound produced by idealized point sources in uniform motion

In this section we summarize the classical results which describe the influence of source motion on the acoustic field of multipoles. It is convenient to have these results listed here so that they can be compared with the effect of the more realistic sources considered later.

A monopole of strength Q, moving with a uniform velocity $\underset{\sim}{U}$, generates a pressure perturbation p that satisfies the inhomogeneous wave equation

$$\nabla^2 p - \frac{1}{c_o^2}\frac{\partial^2 p}{\partial t^2} = -\frac{\partial}{\partial t}\{Q(t)\delta(\underset{\sim}{x}-\underset{\sim}{U}t)\}. \tag{2.1}$$

For $\underset{\sim}{x}$ in the far-field the solution is (the details are given in Morse & Ingard 1968, Chapter 11)

$$p(\underset{\sim}{x},t) = \frac{Q'(t-r/c_o)}{4\pi r(1-M\cos\theta)^2}. \tag{2.2}$$

Equivalently the velocity potential ϕ is given by

$$\phi(\underset{\sim}{x},t) = \frac{-Q(t-r/c_o)}{4\pi r\rho_o(1-M\cos\theta)}, \tag{2.3}$$

where the dash denotes the differentiation of Q with respect to its argument. ρ_o and c_o are the unperturbed values of density and sound speed and r is the distance of the observer at $\underset{\sim}{x}$ from the source at the time it emits, $r = |\underset{\sim}{x}-\underset{\sim}{U}(t-r/c_o)|$. θ is the angle between the path taken by the sound heard at $\underset{\sim}{x}$ and the direction of source motion, as shown in Figure 2.1.

In order to see how the frequency is changed by motion it is convenient to express the time dependence of the argument of Q explicitly;

$$t-r/c_o = t-|\underset{\sim}{x}-\underset{\sim}{U}(t-r/c_o)|/c_o = \frac{t-|\underset{\sim}{x}|/c_o}{1-M\cos\theta} \tag{2.4}$$

correct to order M. This just demonstrates that the frequency of sound emitted by a point source in motion is Doppler shifted.

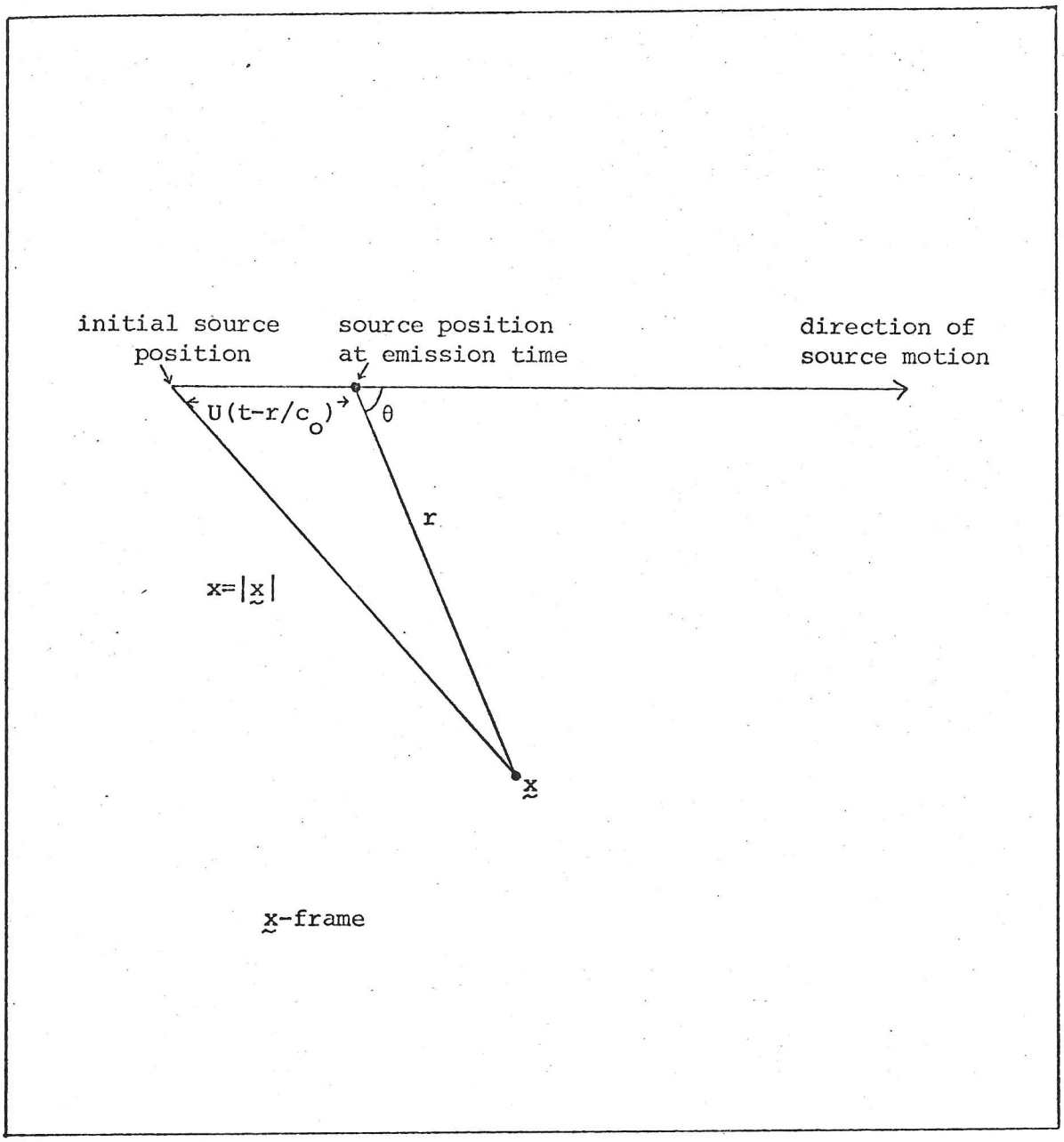

Figure 2.1 A moving source in a stationary fluid

A moving point dipole gives rise to a pressure perturbation p which satisfies

$$\nabla^2 p - \frac{1}{c_o^2}\frac{\partial^2 p}{\partial t^2} = \frac{\partial}{\partial x_i}\{F_i(t)\delta(\underset{\sim}{x}-\underset{\sim}{U}t)\} \quad . \tag{2.5}$$

For large values of $\underset{\sim}{x}$, the solution is (see Crighton 1975)

$$p(\underset{\sim}{x},t) = \frac{\hat{r}_i F_i'(t-r/c_o)}{4\pi r c_o (1-M\cos\theta)^2} \quad , \tag{2.6}$$

or

$$\phi(\underset{\sim}{x},t) = \frac{-\hat{r}_i F_i(t-r/c_o)}{4\pi r c_o \rho_o (1-M\cos\theta)} \quad . \tag{2.7}$$

$\hat{r}_i$ $(i=1,2,3)$ are the direction cosines of the observer from the emission point. When, for example, $\underset{\sim}{F}$ is in the direction of motion, $\hat{r}_i F_i = \cos\theta F$, where $F = |\underset{\sim}{F}|$, and then

$$\phi(\underset{\sim}{x},t) = \frac{-\cos\theta F(t-r/c_o)}{4\pi r c_o \rho_o (1-M\cos\theta)} \quad . \tag{2.8}$$

The acoustic field produced by a point monopole or dipole is modified by source motion in a way that only depends on the value of the Doppler factor, $1-M\cos\theta$. Source motion increases the magnitude of the far pressure field by a factor $(1-M\cos\theta)^{-2}$, and amplifies the velocity potential by $(1-M\cos\theta)^{-1}$.

The corresponding 'wind-tunnel problem' of a stationary point source emitting sound into a uniformly moving stream can be obtained by a simple change of variable. We introduce coordinates $\underset{\sim}{y}$ based on source position

$$\underset{\sim}{y} = \underset{\sim}{x} - \underset{\sim}{U}t \quad . \tag{2.9}$$

In the $\underset{\sim}{y}$-frame, the source is at rest and the fluid is convected past it with a velocity $-\underset{\sim}{U}$, as shown in Figure 2.2.

Far-field kinematic relations correct to order M give

$$y = r(1-M\cos\theta) \tag{2.10}$$

$$\cos\Theta = \frac{\cos\theta - M}{1-M\cos\theta} \tag{2.11}$$

$$\hat{y}_i = \frac{\hat{r}_i}{1-M\cos\theta} \quad \text{for any direction } i \text{ perpendicular to } \underset{\sim}{U} \tag{2.12}$$

and

$$t - y(1+M\cos\Theta)/c_o = t - r/c_o \quad , \tag{2.13}$$

where $y = |\underset{\sim}{y}|$, the distance of the observer from the source, Θ is

the angle between the observer and the direction of fluid motion measured from the source position, and $\hat{y}_i = y_i/y$ are the direction cosines of the observer from the source.

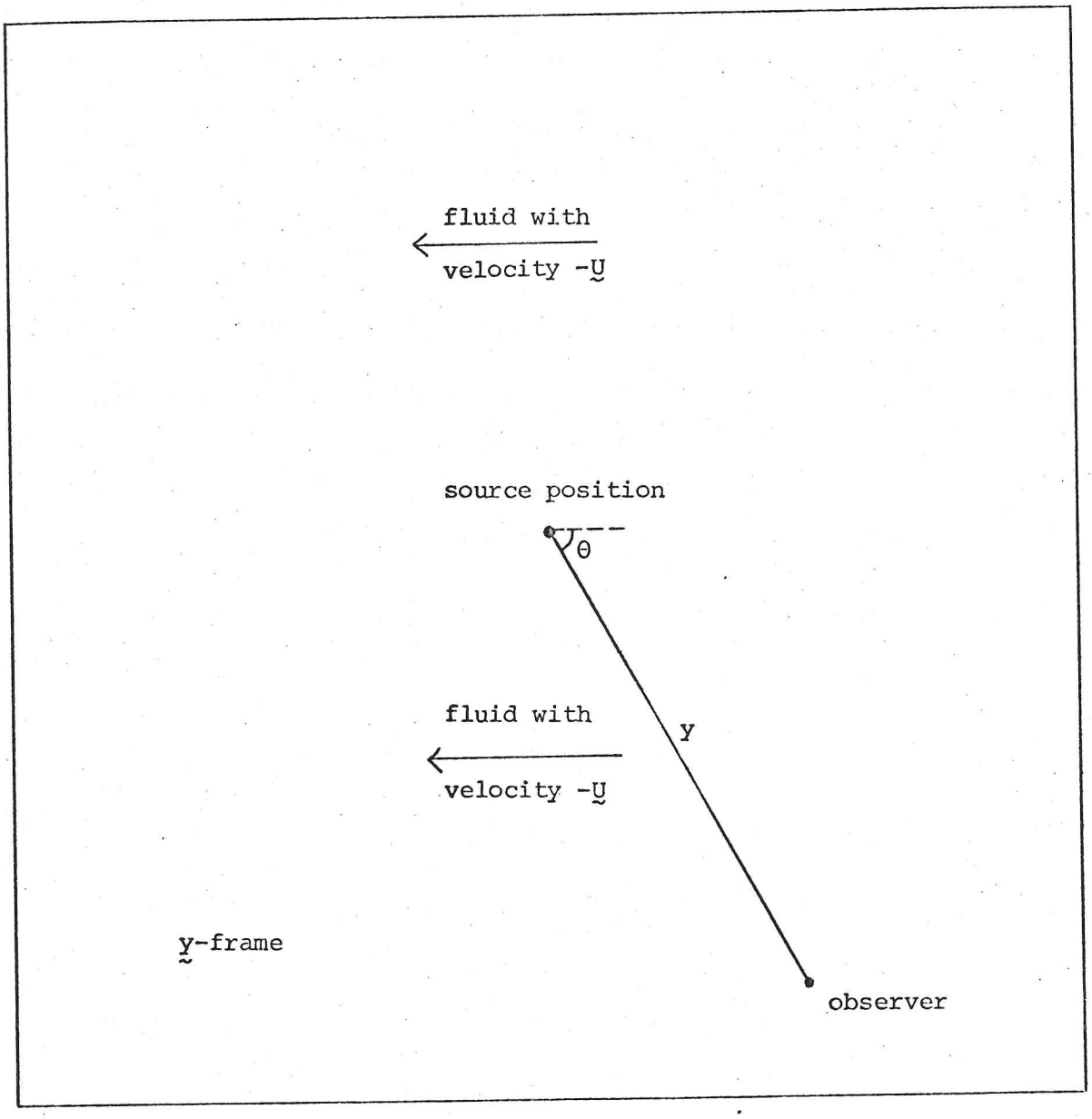

Figure 2.2 A stationary source in a moving fluid

A transformation of equation (2.3) into $\underset{\sim}{y}$ coordinates gives the far-field form of the sound field produced by a stationary monopole surrounded by moving fluid;

$$\phi(\underset{\sim}{y},t) = \frac{-Q(t - y(1 + M\cos\theta)/c_o)}{4\pi y \rho_o} \quad ; \tag{2.14}$$

the retarded time $t - y(1 + M\cos\theta)/c_o$ is appropriate for a disturbance

propagating through a fluid whose velocity is $-\underset{\sim}{U}$ and sound speed c_o. For this source there is no Doppler amplification of the velocity potential.

Similarly from (2.8), a dipole with its axis in the direction of fluid motion gives rise to a far-field of the form

$$\phi(\underset{\sim}{y},t) = \frac{-(\cos\Theta+M)(1-M\cos\Theta)F(t-y(1+M\cos\Theta)/c_o)}{4\pi y c_o \rho_o} . \qquad (2.15)$$

The field is no longer zero in a direction perpendicular to the dipole axis because of the refractive effect of the surrounding fluid. The velocity potential is modified by fluid motion by a factor $(1-M\cos\theta)$.

For a dipole in a direction perpendicular to the mean flow

$$\phi(\underset{\sim}{y},t) = \frac{-\hat{y}_i(1-M\cos\Theta)F_i(t-y(1+M\cos\Theta)/c_o)}{4\pi y c_o \rho_o} . \qquad (2.16)$$

The results of our analysis will contrast with these simple formulae in which all the effects of source motion are contained in Doppler factors.

2.3 The sound produced by a weakly pulsating body in uniform motion

We now investigate the way in which motion alters the sound field of a pulsating body and show that it is significantly different from the effect of motion on a monopole, as described by equations (2.2) and (2.3).

We choose the $\underset{\sim}{x}$-axes so that the motion of the body is in the 1-direction with a speed U. The Mach number M $(= U/c_o)$ is assumed small enough that M^2 is everywhere negligible in comparison with unity. We consider a pulsation which is both linear and compact, and where the shape of the body is unchanged as its size varies. The length of a reference line in the body is denoted by $A(t)$. $A(t)$ is therefore a measure of the size of the body. A compact pulsation is one in which

$\varepsilon = \omega a/c_o << 1$, where a is a typical size of the body, $a = A(0)$ say, ω is an average frequency of the pulsation, $\omega = O(A'/A)$ and the dash denotes differentiation. Since the pulsation is linear $A-a$ and derivatives of A are small and their products may be neglected.

In a moving frame, $\underset{\sim}{y} = \underset{\sim}{x}-\underset{\sim}{U}t$, the centroid of the body is at rest; the corresponding problem is that of a pulsating body surrounded by a stream of fluid whose velocity at infinity is $-\underset{\sim}{U}$ (see Figure 2.3).

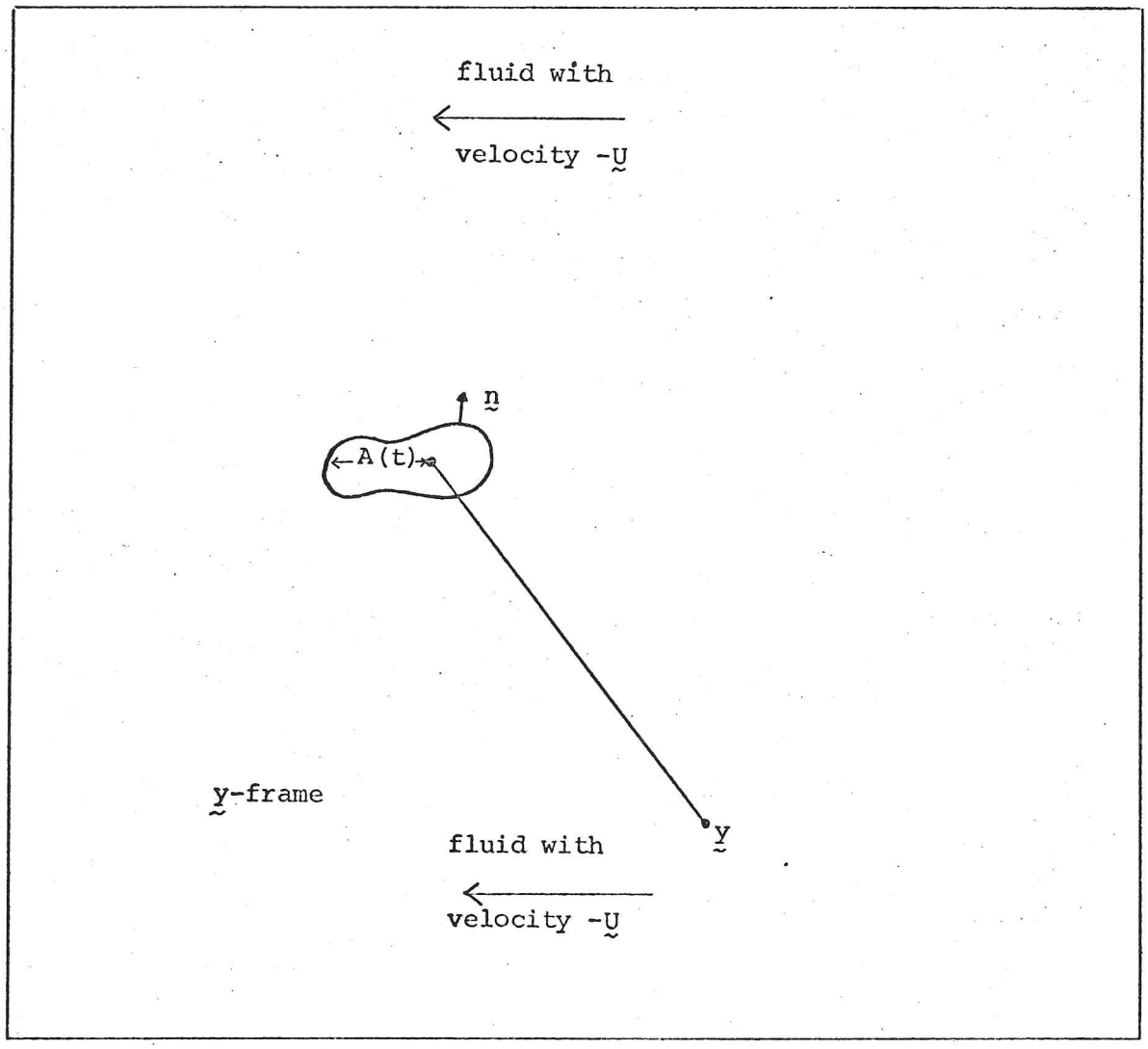

Figure 2.3 A pulsating body of general shape in a moving fluid

The flow is initially irrotational and hence by Kelvin's circulation theorem it remains irrotational and a velocity potential exists. We will divide the velocity potential into two parts and write it as $\bar{\phi} + \phi$,

where $\bar{\phi}$ is the potential of the flow past the mean position of the body surface. $\bar{\phi}$ is therefore independent of time. The additional term, ϕ, due to the effect of the pulsation is small, so that products of it may be neglected. When only terms linear in ϕ are retained the Navier Stokes equations are greatly simplified. The details are given by Taylor (1975) and by Howe (1975). They show that when M^2 is negligible in comparison with unity the time independent potential $\bar{\phi}$ satisfies Laplace's equation in the fluid

$$\nabla^2\bar{\phi} = 0 . \tag{3.1}$$

$\bar{\phi}$ must also be compatible with a condition of zero normal velocity on the average body surface;

$$\underset{\sim}{n}.\nabla\bar{\phi} = 0 \qquad \text{on a body of size } a , \tag{3.2}$$

where $\underset{\sim}{n}$ is the outward normal. Far from the body there is uniform flow in the 1-direction, hence

$$\bar{\phi} \to -Uy_1 \qquad \text{as} \quad |\underset{\sim}{y}| = y \to \infty .$$

The perturbation potential due to the pulsation, ϕ, satisfies a convected wave equation. It is convected with the velocity of the mean potential flow around the body, $\partial\bar{\phi}/\partial y_i$ (again from the work of Taylor (1975) and Howe (1975));

$$\left(\frac{\partial}{\partial t} + \frac{\partial\bar{\phi}}{\partial y_i}\frac{\partial}{\partial y_i}\right)^2\phi - c_o^2\nabla^2\phi = 0 . \tag{3.3}$$

The normal fluid velocity on the real body surface must be equal to the normal velocity of the surface. Therefore the boundary condition for ϕ is

$$\underset{\sim}{n}.\nabla\phi = -\underset{\sim}{n}.\nabla\bar{\phi} + A'g(\underset{\sim}{y}) \qquad \text{on a body of size } A . \tag{3.4}$$

The first term on the right-hand side is proportional to $A-a$, because $\underset{\sim}{n}.\nabla\bar{\phi}$ is zero on a body of size a. The second term is equal to the normal velocity due to the pulsation. g is a function of the geometry of the body. It relates the normal surface velocity to A' at each point. For a sphere $g(\underset{\sim}{y})$ is unity, but in fact the actual form of g is unimportant in the analysis that follows.

There is a second constraint on ϕ; in the far-field it must represent an outward propagating wave.

For a body of arbitrary shape the solution to equation (3.1), which satisfies the boundary conditions, can be expressed as a sum of spherical harmonics. Batchelor (1970, §6.4) shows that the first few terms of the series may be written explicitly as

$$\bar{\phi} = -Uy_1 - \frac{UVa^3(\alpha_{1i}+\delta_{1i})}{4\pi}\frac{y_i}{y^3} + O\left(\frac{Ua^4}{y^3}\right) . \qquad (3.5)$$

V is a number that denotes the volume of a body of the given shape of size 1, so that Va^3 is the mean volume of the body. α_{ij} is the virtual or inertial mass tensor; a function of body geometry that relates the force experienced by a body in a potential flow to its acceleration. α_{ij} describes the 'added mass' of the body due to the inertia of the surrounding fluid. δ_{ij} is the Kronecker δ-function defined by

$$\delta_{ij} = 1 \quad \text{if } i = j$$
$$= 0 \quad \text{otherwise} .$$

Near the body ϕ varies over a length scale proportional to the size of the body, a, but far away compressibility effects are dominant and the relevant measure of length is the wavelength $c_o\omega^{-1}$. For a compact pulsation $\varepsilon = \omega a/c_o << 1$ and these two length scales

become disparate as the compactness ratio ε tends to zero. Then the problem for ϕ is amenable to solution by the method of matched asymptotic expansions (Van Dyke 1975). This can be shown explicitly by rewriting the equations for ϕ in terms of non-dimensional variables. We non-dimensionalize the space coordinate $\underset{\sim}{y}$ with respect to the wavelength $c_o\omega^{-1}$, and time with respect to the time scale of the pulsation ω^{-1}. Then equation (3.3) becomes

$$\left(\frac{\partial}{\partial t} + \frac{\partial \bar{\phi}}{\partial y_i}\frac{\partial}{\partial y_i}\right)^2 \phi - \nabla^2\phi = 0 \quad . \tag{3.6}$$

The same symbols have been used to denote the dimensional and non-dimensional variables. In this equation $\underset{\sim}{y}$ and t are now dimensionless, and

$$\bar{\phi} = -My_1 - \varepsilon^3 \frac{MV(\alpha_{1i}+\delta_{1i})}{4\pi}\frac{y_i}{y^3} + O\left(\frac{M\varepsilon^4}{y^3}\right) \quad . \tag{3.7}$$

We arbitrarily scale ϕ on ac_o, and the obvious choice for A is to non-dimensionalize it with respect to its mean value a, since A/a is only linearly disturbed from unity. Then the boundary condition (3.4) becomes

$$n_i \frac{\partial \phi}{\partial y_i} = -\frac{1}{\varepsilon} n_i \frac{\partial \bar{\phi}}{\partial y_i} + A'g(\underset{\sim}{y}) \qquad \text{on a body of size } \varepsilon A \ , \tag{3.8}$$

where all the parameters are now non-dimensional. Equations (3.6) and (3.8) are to be solved together with the condition that ϕ has outward wave behaviour at infinity.

For small values of ε, we can obtain a solution of the form

$$\phi(\underset{\sim}{y},\varepsilon) = \varepsilon^{\lambda}\phi_{\lambda}(\underset{\sim}{y},\varepsilon) + O(\varepsilon^{\lambda+1}) \ ,$$

where λ, the leading order of the far-field is as yet unknown. This outer expansion tacitly assumes that y is at least of order unity,

and will not be valid near the body where y is small.

From equation (3.6) and the form of $\bar{\phi}$ given in (3.7), we see that ϕ_λ satisfies a uniform convected wave equation

$$\left(\frac{\partial}{\partial t} - M\frac{\partial}{\partial y_1}\right)^2 \phi_\lambda - \nabla^2\phi_\lambda = 0 \quad , \tag{3.9}$$

together with the radiation condition at infinity. Hence

$$\phi^{(\lambda)}(\underset{\sim}{y},\varepsilon) = \varepsilon^\lambda\left\{\frac{f(t-y-My_1)}{y} + \frac{\partial}{\partial y_i}\frac{f_i(t-y-My_1)}{y} + \frac{\partial^2}{\partial y_i \partial y_j}\frac{f_{ij}(t-y-My_1)}{y} + \ldots\right\}, \tag{3.10}$$

where $\phi^{(m)}$ denotes the outer expansion correct to order ε^m. The lowest order of the far-field, λ, and the functions $f_{i\ldots}$ are to be determined from a consideration of the flow in the inner region. The flow near the body scales on a stretched variable $\underset{\sim}{Y}$, where $\underset{\sim}{Y} = \underset{\sim}{y}/\varepsilon$. When this outer expansion is rewritten in terms of the inner coordinate $\underset{\sim}{Y}$

$$\phi^{(\lambda)}(\varepsilon\underset{\sim}{Y},\varepsilon) = \varepsilon^{\lambda-1}\frac{f(t-\varepsilon Y-\varepsilon MY_1)}{Y} + \varepsilon^{\lambda-2}\frac{\partial}{\partial Y_i}\frac{f_i(t-\varepsilon Y-\varepsilon MY_1)}{Y}$$

$$+ \varepsilon^{\lambda-3}\frac{\partial^2}{\partial Y_i \partial Y_j}\frac{f_{ij}(t-\varepsilon Y-\varepsilon MY_1)}{Y} + \ldots \quad ; \tag{3.11}$$

a new power series in ε is obtained. We denote this series truncated after ε^n by $\phi^{(\lambda,n)}$. Once the flow near the body is known, the functions $f_{i\ldots}$ can be found by using Van Dyke's matching procedure to relate the $\phi^{(\lambda,n)}$ to the inner flow variables.

We use the stretched coordinate $\underset{\sim}{Y}$ to describe the flow near the body, and write

$$\phi(\underset{\sim}{y},\varepsilon) \equiv \Phi(\underset{\sim}{Y},\varepsilon) \quad . \tag{3.12}$$

An inner expansion for ϕ can be obtained by expressing Φ in ascending powers of ε

$$\Phi(\underset{\sim}{Y},\varepsilon) = \Phi_o + \varepsilon\Phi_1 + O(\varepsilon^2) \quad . \tag{3.13}$$

When equation (3.6) is rewritten in terms of the variable $\underset{\sim}{Y}$, we find that, correct to order M, $\Phi(\underset{\sim}{Y},\varepsilon)$ is a solution of

$$\frac{\partial^2\Phi}{\partial Y_i \partial Y_i} - 2\varepsilon \frac{\partial\bar{\Phi}}{\partial Y_i}\frac{\partial^2\Phi}{\partial Y_i \partial t} - \varepsilon^2 \frac{\partial^2\Phi}{\partial t^2} = 0 \tag{3.14}$$

with the boundary condition

$$n_i \frac{\partial\Phi}{\partial Y_i} = - n_i \frac{\partial\bar{\Phi}}{\partial Y_i} + \varepsilon A' g(\varepsilon\underset{\sim}{Y}) \qquad \text{on a body of size } A \ , \tag{3.15}$$

where

$$\bar{\Phi}(\underset{\sim}{Y},\varepsilon) = \frac{1}{\varepsilon}\bar{\phi}(\varepsilon\underset{\sim}{Y},\varepsilon) = -MY_1 - \frac{MV(\alpha_{1i}+\delta_{1i})}{4\pi}\frac{Y_i}{Y^3} + O(\frac{M}{Y^3}) \quad . \tag{3.16}$$

By substituting the power series expansion for Φ into both equation (3.14) and the boundary condition (3.15), we obtain a series of equations;

$$\nabla^2\Phi_o = 0 \quad \text{with} \quad n_i \frac{\partial}{\partial Y_i}(\Phi_o+\bar{\Phi}) = 0 \quad \text{on a body of size } A \ , \tag{3.17}$$

and

$$\nabla^2\Phi_1 = 2\frac{\partial\bar{\Phi}}{\partial Y_i}\frac{\partial^2\Phi_o}{\partial Y_i \partial t} \quad \text{with} \quad n_i \frac{\partial\Phi_1}{\partial Y_i} = A' g(\varepsilon\underset{\sim}{Y}) \quad \text{on a body of size } A \ . \tag{3.18}$$

The ideas of classical potential theory can be used to solve (3.17) for the sum $\Phi_o + \bar{\Phi}$. From the form given by Batchelor (1970 §6.4)

$$\Phi_o + \bar{\Phi} = -MY_1 - \frac{MVA^3(\delta_{1i}+\alpha_{1i})}{4\pi}\frac{Y_i}{Y^3} + O(\frac{M}{Y^3}) \quad . \tag{3.19}$$

When the known function $\bar{\Phi}$ determined by (3.16) has been subtracted from this expression and the terms involving A-1 have been linearized we find that

$$\Phi_o = \frac{-3MV(A-1)(\delta_{1i}+\alpha_{1i})}{4\pi}\frac{Y_i}{Y^3} + O(\frac{M}{Y^3}) \quad . \tag{3.20}$$

Therefore the forcing term in the Poisson equation for Φ_1 in (3.18) is $O(M^2A')$ and so gives a contribution to Φ_1 which is M^2 smaller than the term arising from the boundary condition.

The solution of

$$\nabla^2\Phi_1 = 0 \qquad \text{with} \qquad n_i \frac{\partial\Phi}{\partial Y_i} = A'g(\varepsilon\underset{\sim}{Y}) \quad , \tag{3.21}$$

which decays at infinity, may be written as an expansion in spherical harmonics. The coefficient of the leading term is related to the volume flux away from the body (see for example Batchelor 1970 §6.4). The rate of change of volume of the body is $3VA^2A'$. After linearization this is just $3VA'$ because $A-1$ and A' are both small, and so

$$\Phi_1 = -\frac{3VA'}{4\pi Y} + O(\frac{1}{Y^2}) \quad . \tag{3.22}$$

We denote the inner series terminated after ε^n by $\Phi^{(n)}$, i.e. $\Phi^{(0)}(\underset{\sim}{Y},\varepsilon) = \Phi_o$, and $\Phi^{(1)}(\underset{\sim}{Y},\varepsilon) = \Phi_o + \varepsilon\Phi_1$, or alternatively when written in terms of the outer variable $\underset{\sim}{y}$,

$$\Phi^{(0)}(\underset{\sim}{y}/\varepsilon,\varepsilon) = \frac{-\varepsilon^2 3MV(A-1)(\alpha_{1i}+\delta_{1i})}{4\pi}\frac{y_i}{y^3} + O(\varepsilon^3) \quad , \tag{3.23}$$

$$\Phi^{(1)}(\underset{\sim}{y}/\varepsilon,\varepsilon) = \Phi^{(0)}(\underset{\sim}{y}/\varepsilon,\varepsilon) - \frac{\varepsilon^2 3VA'}{4\pi y} + O(\varepsilon^3) \quad , \tag{3.24}$$

and a new power series in ε is obtained. We define a set of functions $\Phi^{(n,m)}$, where $\Phi^{(n,m)}$ is the expansion of $\Phi^{(n)}(\underset{\sim}{y}/\varepsilon,\varepsilon)$ terminated after order ε^m . This inner solution must match to an outer expansion of the form given in (3.11). The matching principle states that

$$\phi^{(\lambda,n)} = \Phi^{(n,\lambda)} \quad , \tag{3.25}$$

where $\phi^{(\lambda,n)}$ has already been defined as the outer expansion correct to order λ , expressed in terms of the inner variables and then

terminated after order ε^n . It is at once apparent that $\lambda = 2$, and that the quadrupoles and all higher multipoles in the outer expansion must be zero. Then (3.11) becomes

$$\phi^{(2)}(\varepsilon\underset{\sim}{Y},\varepsilon) = f_i(t)\,\frac{\partial}{\partial Y_i}\left(\frac{1}{Y}\right) + \varepsilon\left(\frac{f(t)}{Y} - Mf_i'(t)\,\frac{\partial}{\partial Y_i}\left(\frac{Y_1}{Y}\right)\right) + O(\varepsilon^2) \quad . \tag{3.26}$$

When the rule (3.25) is applied to match the expressions (3.23) and (3.24) to (3.26), we find that

$$f_i(t) = \frac{3MV}{4\pi}\,(A-1)(\alpha_{1i}+\delta_{1i}) \tag{3.27}$$

and

$$f(t) = -\frac{3VA'}{4\pi} \quad . \tag{3.28}$$

We have now obtained the far-field solution for ϕ to lowest order in the compactness ratio,

$$\phi(\underset{\sim}{y},t) = -\frac{\varepsilon^2 3V}{4\pi y}\left\{\frac{A'(t-y-My_1)}{y} - M(\alpha_{1i}+\delta_{1i})\,\frac{\partial}{\partial y_i}\,\frac{(A-1)(t-y-My_1)}{y}\right\} . \tag{3.29}$$

After evaluation of the derivative for large y this becomes

$$\phi(\underset{\sim}{y},t) = -\frac{\varepsilon^2 3V}{4\pi y}\left(1 + M(\alpha_{1i}+\delta_{1i})\,\frac{y_i}{y}\right)A'(t-y-My_1) \quad , \tag{3.30}$$

$$= -\frac{\varepsilon^2 3V}{4\pi y}\,\frac{(1+M\alpha_{1i}\hat{y}_i)}{(1-M\cos\theta)}\,A'(t-y-My_1) \quad , \tag{3.31}$$

correct to order M , with $\cos\theta = y_1/y$ and $\hat{y}_i = y_i/y$. Or in dimensional parameters

$$\phi(\underset{\sim}{y},t) = -\frac{3Va^2}{4\pi y}\,\frac{(1+M\alpha_{1i}\hat{y}_i)}{1-M\cos\theta}\,A'(t-(y+My_1)/c_o) \quad . \tag{3.32}$$

Hence, the acoustic field of a pulsating body in a mean flow is quite different from the sound produced by a monopole in a stream. From (2.14) we see that the amplitude of the velocity potential produced

by a monopole is unchanged by the presence of the flow, whereas the field of an expanding and contracting body, described in (3.32), is amplified by a factor $(1+M\alpha_{1i}\hat{y}_i)(1-M\cos\theta)^{-1}$.

The solution to the corresponding problem of a pulsating body moving through a stationary fluid may be obtained by reverting to the $\underset{\sim}{x}$-frame. An application of the kinematic relationships (2.10)-(2.13) shows that

$$\phi(\underset{\sim}{x},t) = -\frac{3Va^2}{4\pi r}\frac{(1+M\alpha_{1i}\hat{r}_i)}{(1-M\cos\theta)^2}A'\left(\frac{t-x/c_o}{1-M\cos\theta}\right) , \tag{3.33}$$

where $x = |\underset{\sim}{x}|$, and $\hat{r}_i$ $(i = 1,2,3)$ are the direction cosines of the observer from the emission point.

In the far-field we can find the pressure perturbation p from a linearized form of Bernoulli's equation;

$$\begin{aligned} p &= -\rho_o\frac{\partial\phi}{\partial t} \\ &= \frac{3Va^2\rho_o(1+M\alpha_{1i}\hat{r}_i)}{4\pi r(1-M\cos\theta)^3}A''\left(\frac{t-x/c_o}{1-M\cos\theta}\right) . \end{aligned} \tag{3.34}$$

The effect of motion on the sound produced by a compact pulsating body is described by (3.34). Source motion increases the amplitude of the far-field pressure by a factor $(1+M\alpha_{1i}\hat{r}_i)(1-M\cos\theta)^{-3}$.

We see that the way in which the motion of a pulsating body alters its sound field depends entirely on the body shape as determined through the inertial mass tensor, and cannot, for an arbitrarily shaped body, be expressed in terms of Doppler factors. The consequence of the motion of this source, unlike the effect of moving point sources, is not in general negligible in a plane at right angles to the direction of motion. A similar result has been obtained by Crighton (1975). He considers the sound scattered by a moving solid body and also finds

that there are effects perpendicular to the direction of motion. The way in which our results depend crucially on the body shape emphasizes how essential it is to have an accurate description of the source before the complete effect of motion can be predicted. The simple and frequently used experimental procedure of taking measurements in a plane perpendicular to the axis of motion and assuming that this eliminates the effect of convection is without rigorous justification.

When the body is symmetric about the 1-axis, or when the 1-axis is an eigenvector of the symmetric tensor α_{ij} ,

$$\alpha_{1i} = \alpha\delta_{1i} \tag{3.35}$$

where α is the corresponding eigenvalue.

The far-field pressure is then given by

$$p(\underset{\sim}{x},t) = \frac{3Va^2\rho_o}{4\pi r}\frac{(1+\alpha M\cos\theta)}{(1-M\cos\theta)^3}A''\left(\frac{t-x/c_o}{1-M\cos\theta}\right) \tag{3.36}$$

$$= \frac{3Va^2\rho_o}{4\pi r(1-M\cos\theta)^{3+\alpha}}A''\left(\frac{t-x/c_o}{1-M\cos\theta}\right) \tag{3.37}$$

correct to order M .

Since α is positive the effect of source motion described here is always greater than that for a monopole. The minimum effect is for a flat plate moving parallel to its own plane. For such a plate $\alpha = 0$, and source motion modifies the pressure field by $(1-M\cos\theta)^{-3}$. This agrees with the result obtained by Ffowcs Williams & Lovely (1975).

For a sphere $\alpha = \frac{1}{2}$, and if we take the reference length to be the radius $V = 4\pi/3$, so that

$$p(\underset{\sim}{x},t) = \frac{a^2\rho_o}{r(1-M\cos\theta)^{3\frac{1}{2}}}A''\left(\frac{t-x/c_o}{1-M\cos\theta}\right) , \tag{3.38}$$

where a is the initial value of the radius; the pressure is amplified

by three and a half Doppler factors.

This result for a sphere can also be obtained from Lighthill's theory. We introduce a control surface S, where S is the surface of a sphere of radius b moving with a speed U in the 1-direction. The fixed radius b is to be just large enough to enclose the pulsating sphere at all times, as shown in Figure 2.4. Since the pulsation is linear, $b-A$ is small.

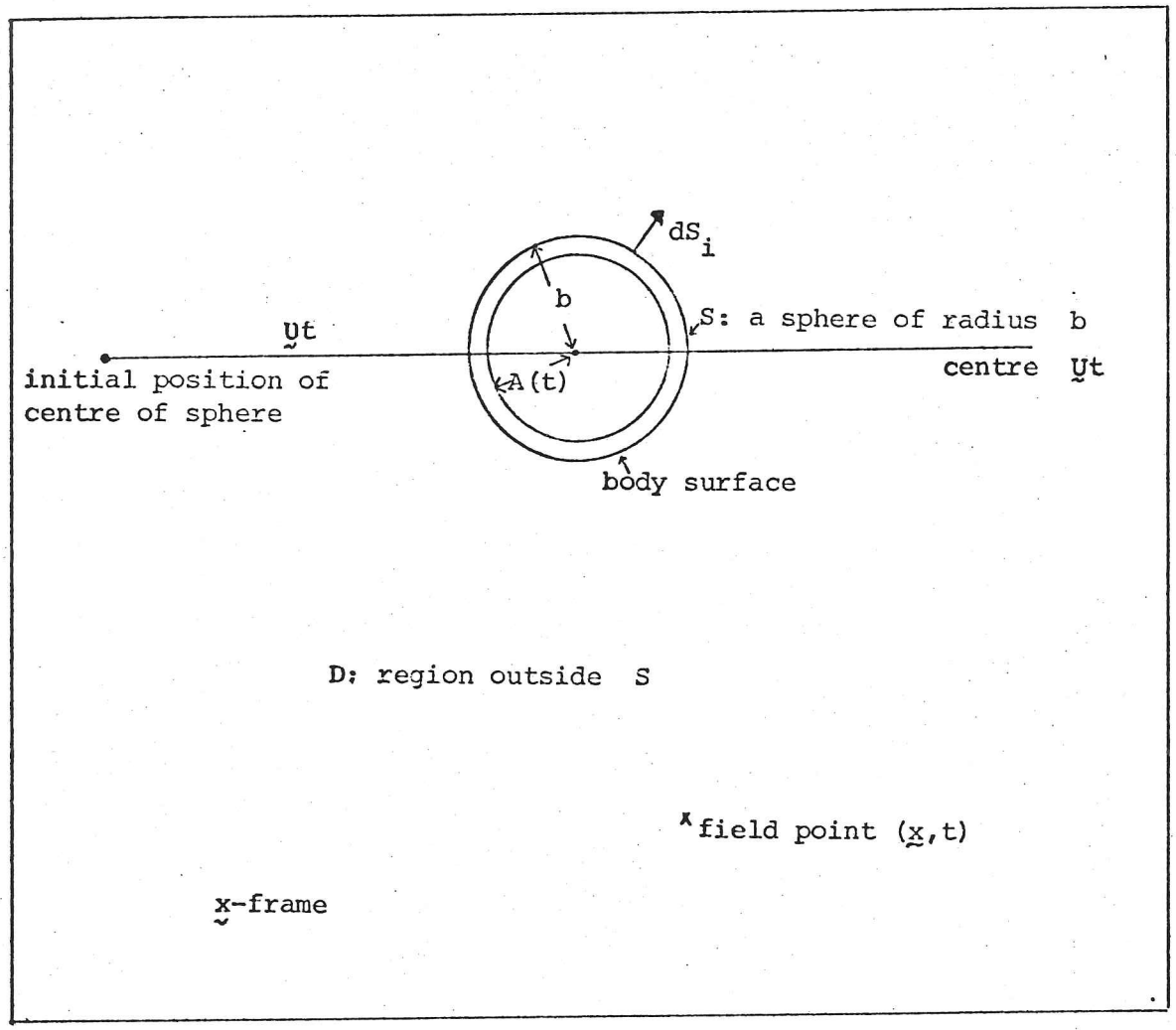

Figure 2.4 The position of the control surface S

For $\underset{\sim}{x}$ in the far-field the Lighthill theory applied in the region D outside S gives (see for example Ffowcs Williams 1976a)

$$4\pi p(\underset{\sim}{x},t) = \frac{\partial^2}{\partial x_i \partial x_j}\int_D \left[\frac{T_{ij}}{r(1-M\cos\theta)}\right] d^3\underset{\sim}{\eta} - \frac{\partial}{\partial x_i}\int_S \left[\frac{p_{ij}+\rho u_i(u_j-U_j)}{r(1-M\cos\theta)}\right] dS_j(\underset{\sim}{\eta})$$

$$+ \frac{\partial}{\partial t}\int_S \left[\frac{\rho_o u_i + (\rho-\rho_o)(u_i-U_i)}{r(1-M\cos\theta)}\right] dS_i(\underset{\sim}{\eta}) \quad . \tag{3.39}$$

T_{ij} is the Lighthill stress tensor, $T_{ij} = \rho u_i u_j + p_{ij} - c_o^2(\rho-\rho_o)\delta_{ij}$, $\underset{\sim}{u}$ is the fluid velocity, p_{ij} the stress tensor (in an inviscid fluid $p_{ij} = p\delta_{ij}$) and ρ is the actual fluid density. dS_i is a vector in the direction of the outward normal to S of magnitude dS. $\underset{\sim}{\eta}$ is a coordinate measured from the centroid of the body, and the square brackets denote that the function they enclose is to be evaluated at a retarded time τ, where τ satisfies

$$\tau = t - |\underset{\sim}{x}-\underset{\sim}{\eta}-\underset{\sim}{U}\tau|/c_o \quad . \tag{3.40}$$

For large x

$$\tau \simeq \frac{t-x/c_o+\hat{f}_i\eta_i/c_o}{1-M\cos\theta} \quad ; \tag{3.41}$$

the retarded time τ is a function of $\underset{\sim}{\eta}$ and varies across the body.

For a sphere we can find the inner expansion for ψ, the total velocity potential in the $\underset{\sim}{x}$-frame, by solving equations (3.17) and (3.18) correct to order M. In dimensional variables,

$$\psi = \bar{\phi} + U\eta_1 + \phi = -\frac{A'a^2}{\eta} - \tfrac{1}{2}UA^3\frac{\eta_1}{\eta^3} + O\left(\frac{A''a^2}{c_o}\right) \quad , \tag{3.42}$$

where $\eta = |\underset{\sim}{\eta}|$.

This expansion describes the flow near the surface S. $\underset{\sim}{u}$, the flow velocity in the $\underset{\sim}{x}$-frame, is given by

$$u_i = \frac{\partial\psi}{\partial\eta_i} \tag{3.43}$$

and from the compressible form of Bernoulli's equation

$$\int \frac{dp}{\rho} = -\left.\frac{\partial\psi}{\partial t}\right|_{\underset{\sim}{\eta}} + U\frac{\partial\psi}{\partial\eta_1} - \tfrac{1}{2}u^2 \qquad (3.44)$$

$$= c_o^2(\rho-\rho_o)/\rho_o = p/\rho_o \text{ , correct to order } M \text{ .}$$

When $O(M^2)$ is neglected, the monopole term is

$$= \frac{\partial}{\partial t}\int_{\eta=b} \rho_o\left[\frac{A'}{r(1-M\cos\theta)} + \frac{UA^3}{b^4}\frac{\eta_1}{r(1-M\cos\theta)}\right] dS(\underset{\sim}{\eta}) \text{ .}$$

From an expansion of the retarded time we see

$$= \frac{\partial}{\partial t}\left\{\frac{4\pi a^2\rho_o A'}{r(1-M\cos\theta)} + \frac{4\pi a^2\rho_o M\cos\theta A'}{r}\right\} \qquad (3.45)$$

+ higher time derivatives and products of $A-a$.

$$= \frac{4\pi a^2\rho_o}{r(1-M\cos\theta)^3} A''\left(\frac{t-x/c_o}{1-M\cos\theta}\right) \text{ .} \qquad (3.46)$$

Evaluation of the dipole term gives

$$-\frac{\partial}{\partial x_i}\int_S \left[\frac{p\delta_{ij}+\rho u_i(u_j-U_j)}{r(1-M\cos\theta)}\right] n_j dS(\underset{\sim}{\eta}) = \frac{2\pi a^2\rho_o M\cos\theta}{r} A''\left(\frac{t-x/c_o}{1-M\cos\theta}\right) \text{ .} \qquad (3.47)$$

Also we note that

$$\frac{\partial^2}{\partial x_i\partial x_j}\int_D \left[\frac{T_{ij}}{r(1-M\cos\theta)}\right] d^3\underset{\sim}{\eta} \simeq O\left(\frac{a^2\rho_o M^2 A''}{r}\right) \text{ .} \qquad (3.48)$$

When these terms are added together we recover the previous result;

$$p(\underset{\sim}{x},t) = \frac{a^2\rho_o}{r(1-M\cos\theta)^{3\frac{1}{2}}} A''\left(\frac{t-x/c_o}{1-M\cos\theta}\right) \text{ .} \qquad (3.49)$$

This method helps to explain why there is a difference between a moving monopole and a pulsating compact body. A moving body producing a mass flux necessarily has a fluctuating force and momentum associated with it. These additional sources are significant being

only of order M smaller than the monopole due to the mass flux, and prohibit any simple specification of the field.

2.4 The sound field produced by a juddering compact body in uniform motion

We next consider the noise produced by a rigid body moving through an inviscid fluid at rest, when the velocity of the body is only slightly perturbed from a uniform value $\underset{\sim}{U}$. An aircraft travelling through a patch of turbulence moves more or less in this way; in addition to the mean forward flight of the plane there is a 'cobble-stone' effect caused by the turbulent air flow and the ride becomes 'bouncy'. This type of motion also occurs in helicopter or turbine blades, where the circular motion of the blades is superimposed on the uniform forward velocity of the aircraft. Morse & Ingard (1968) state that a compact body juddering in this way is equivalent to a fluctuating point force and may be modelled by a moving dipole. That point of view is widely believed but we show it is actually not true; the sound field produced by such a body motion is completely different from that of a moving dipole.

We introduce moving coordinates centred at the mean position of the body, $\underset{\sim}{y} = \underset{\sim}{x} - \underset{\sim}{U}t$. In this frame the body vibrates linearly, and the fluid far from the body has a velocity $-\underset{\sim}{U}$, as shown in Figure 2.5. This type of motion is similar to that of an anchored buoy bobbing on the sea surface in a current or to the flutter of an aerofoil in a wind-tunnel.

The flow is irrotational, and we write the velocity potential as $\bar{\phi} + \phi$, where $\bar{\phi}$ describes the flow past the mean position of the body, and ϕ represents the effect of the vibration and is small. We take the mean fluid flow to be in the 1-direction with speed $-U$ and

only of order M smaller than the monopole due to the mass flux, and prohibit any simple specification of the field.

2.4 The sound field produced by a juddering compact body in uniform motion

We next consider the noise produced by a rigid body moving through an inviscid fluid at rest, when the velocity of the body is only slightly perturbed from a uniform value $\underset{\sim}{U}$. An aircraft travelling through a patch of turbulence moves more or less in this way; in addition to the mean forward flight of the plane there is a 'cobble-stone' effect caused by the turbulent air flow and the ride becomes 'bouncy'. This type of motion also occurs in helicopter or turbine blades, where the circular motion of the blades is superimposed on the uniform forward velocity of the aircraft. Morse & Ingard (1968) state that a compact body juddering in this way is equivalent to a fluctuating point force and may be modelled by a moving dipole. That point of view is widely believed but we show it is actually not true; the sound field produced by such a body motion is completely different from that of a moving dipole.

We introduce moving coordinates centred at the mean position of the body, $\underset{\sim}{y} = \underset{\sim}{x} - \underset{\sim}{U}t$. In this frame the body vibrates linearly, and the fluid far from the body has a velocity $-\underset{\sim}{U}$, as shown in Figure 2.5. This type of motion is similar to that of an anchored buoy bobbing on the sea surface in a current or to the flutter of an aerofoil in a wind-tunnel.

The flow is irrotational, and we write the velocity potential as $\bar{\phi} + \phi$, where $\bar{\phi}$ describes the flow past the mean position of the body, and ϕ represents the effect of the vibration and is small. We take the mean fluid flow to be in the 1-direction with speed $-U$ and

restrict our attention to the particular geometry of a sphere of radius a, with its centre at the variable point $\underset{\sim}{l}(t)$.

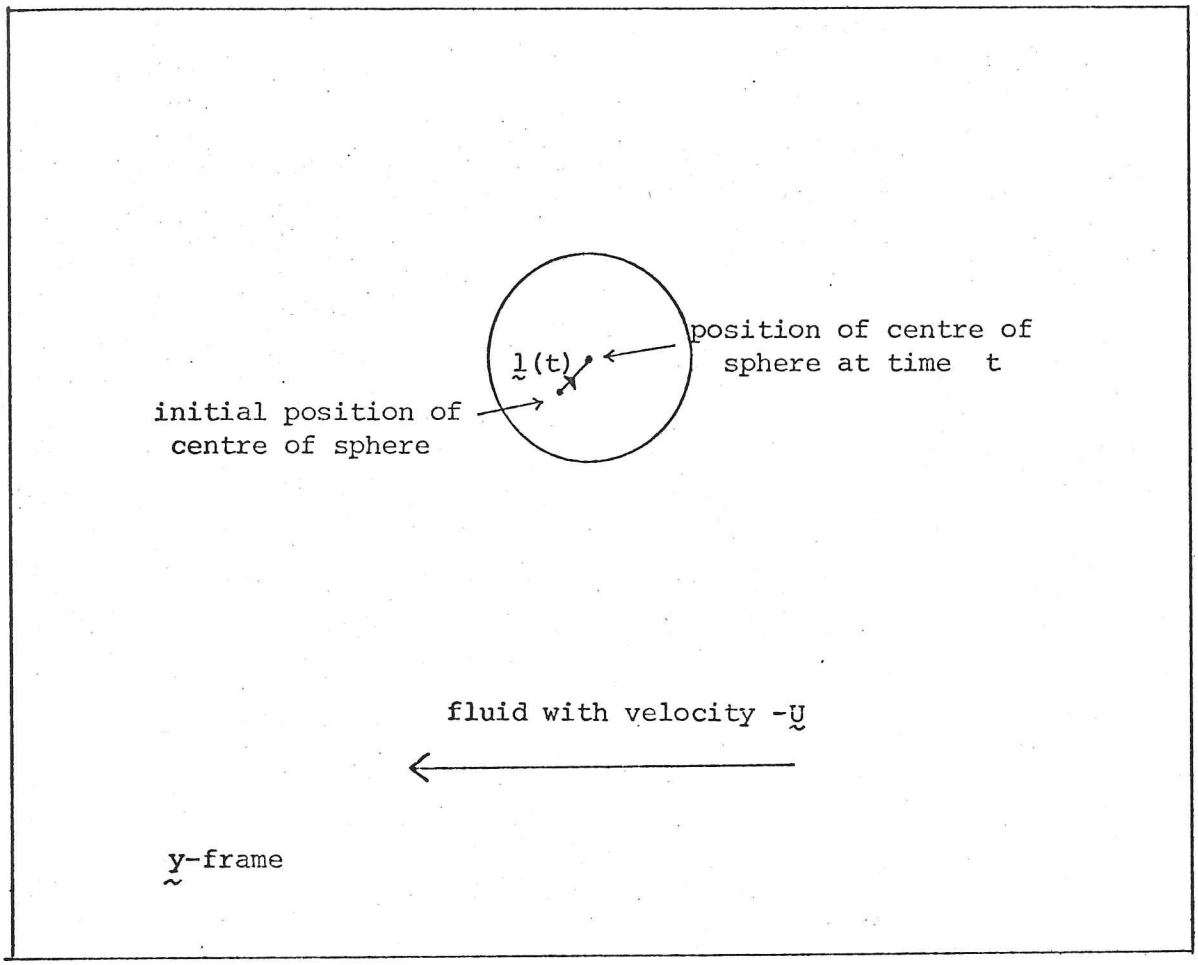

Figure 2.5 A vibrating body in a moving fluid

The Navier Stokes equation linearized in ϕ and correct to order M reduces to equations (3.1) and (3.3). From (3.1) $\bar{\phi}$ satisfies

$$\nabla^2\bar{\phi} = 0 \quad \text{with} \quad \underset{\sim}{n}.\nabla\bar{\phi} = 0 \quad \text{on} \quad y = a \; . \tag{4.1}$$

Far from the body the fluid has a uniform velocity $-U$ in the 1-direction, and so

$$\bar{\phi} \to -Uy_1 \quad \text{as} \quad y \to \infty \; .$$

This problem for $\bar{\phi}$ can be solved immediately,

$$\bar{\phi} = -Uy_1 - \tfrac{1}{2}Ua^3 y_1/y^3 \quad , \tag{4.2}$$

this describes steady potential flow around a sphere of radius a, with its centre at the origin.

The perturbation potential ϕ satisfies (3.3), a convected wave equation,

$$\left(\frac{\partial}{\partial t} + \frac{\partial \bar{\phi}}{\partial y_i}\frac{\partial}{\partial y_i}\right)^2 \phi - c_o^2 \nabla^2 \phi = 0 \quad . \tag{4.3}$$

On the surface of the sphere, the normal velocity of the fluid must be equal to that of the body;

$$\underset{\sim}{n}.\nabla\phi = -\underset{\sim}{n}.\nabla\bar{\phi} + \underset{\sim}{n}.\underset{\sim}{l}'(t) \qquad \text{on} \qquad |\underset{\sim}{y}-\underset{\sim}{l}(t)| = a \quad , \tag{4.4}$$

and in the distant field ϕ represents an outward propagating wave.

As before, there are two length scales involved in the problem for ϕ, the radius of the sphere, a, and the wavelength, $c_o\omega^{-1}$, where ω is the frequency of the judder, i.e. $\omega \sim O(l'/l)$. For a compact body $\omega a/c_o = \varepsilon << 1$, and the problem for ϕ is suitable for solution by the method of matched asymptotic expansions.

When all the variables are non-dimensionalized as in §2.3 the equation for ϕ is

$$\left(\frac{\partial}{\partial t} + \frac{\partial \bar{\phi}}{\partial y_i}\frac{\partial}{\partial y_i}\right)^2 \phi - \nabla^2 \phi = 0 \quad . \tag{4.5}$$

The boundary condition on the sphere becomes

$$n_i \frac{\partial \phi}{\partial y_i} = -\frac{1}{\varepsilon} n_i \frac{\partial \bar{\phi}}{\partial y_i} + n_i l_i' \qquad \text{on} \qquad |\underset{\sim}{y}-\varepsilon\underset{\sim}{l}| = \varepsilon \quad , \tag{4.6}$$

where all the variables are now dimensionless. $\underset{\sim}{l}$ has been non-

dimensionalized with respect to a and

$$\bar{\phi} = - My_1 - \tfrac{1}{2}\varepsilon^3 My_1/y^3 \quad . \tag{4.7}$$

Away from the body we can obtain a solution for small values of ε of the form

$$\phi(\underset{\sim}{y},\varepsilon) = \varepsilon^\lambda \phi_\lambda(\underset{\sim}{y}) + O(\varepsilon^{\lambda+1}) \quad .$$

When this series is substituted into equation (4.5) we find that ϕ_λ satisfies a uniform convected wave equation;

$$\left(\frac{\partial}{\partial t} - M\frac{\partial}{\partial y_1}\right)^2 \phi_\lambda - \nabla^2\phi_\lambda = 0 \quad . \tag{4.8}$$

The solution is (cf. equation (3.10))

$$\phi^{(\lambda)}(\underset{\sim}{y},\varepsilon) = \varepsilon^\lambda \left\{ \frac{f(t-y-My_1)}{y} + \frac{\partial}{\partial y_i}\frac{f_i(t-y-My_1)}{y} + \frac{\partial^2}{\partial y_i \partial y_j}\frac{f_{ij}(t-y-My_1)}{y} + \ldots \right\}, \tag{4.9}$$

where $\phi^{(\lambda)} = \varepsilon^\lambda \phi_\lambda$; the outer expansion correct to the lowest order λ .

Alternatively, in terms of the inner variable $\underset{\sim}{Y}$,

$$\phi^{(\lambda)}(\varepsilon\underset{\sim}{Y},\varepsilon) = \varepsilon^{\lambda-1}\frac{f(t-\varepsilon Y-\varepsilon MY_1)}{Y} + \varepsilon^{\lambda-2}\frac{\partial}{\partial Y_i}\frac{f_i(t-\varepsilon Y-\varepsilon MY_1)}{Y} + \varepsilon^{\lambda-3}\frac{\partial^2}{\partial Y_i \partial Y_j}\frac{f_{ij}(t-\varepsilon Y-\varepsilon MY_1)}{Y} + \ldots \quad . \tag{4.10}$$

This produces a new power series in ε , and we denote the expansion terminated after ε^n by $\phi^{(\lambda,n)}$. The functions $f_{i\ldots}$ and the value of λ must be determined by a consideration of the flow in the inner region.

Near the body the flow scales on a stretched coordinate $\underset{\sim}{Y} = \underset{\sim}{y}/\varepsilon$. We introduce $\Phi(\underset{\sim}{Y},\varepsilon) = \phi(\underset{\sim}{y},\varepsilon)$, and when equation (4.5) is written in terms of the variable $\underset{\sim}{Y}$ it becomes

$$\nabla^2\Phi - 2\varepsilon \frac{\partial\bar{\Phi}}{\partial Y_i} \frac{\partial^2\Phi}{\partial Y_i \partial t} - \varepsilon^2 \frac{\partial^2\Phi}{\partial t^2} = 0 \quad , \tag{4.11}$$

with the boundary condition

$$n_i \frac{\partial\Phi}{\partial Y_i} = - n_i \frac{\partial\bar{\Phi}}{\partial Y_i} + \varepsilon n_i \ell_i' \qquad \text{on} \quad |\underset{\sim}{Y}-\underset{\sim}{\ell}| = 1 \quad , \tag{4.12}$$

where

$$\bar{\Phi} = - MY_1 - \tfrac{1}{2}MY_1/Y^3 \quad . \tag{4.13}$$

We express the solution as a power series in the small parameter ε , $\Phi = \Phi_o + \varepsilon\Phi_1 + \varepsilon^2\Phi_2 \ldots$. A series of equations can be obtained by substituting this form for Φ into (4.11) and the boundary condition (4.12),

$$\nabla^2\Phi_o = 0 \quad , \quad n_i \frac{\partial}{\partial Y_i}(\Phi_o+\bar{\Phi}) = 0 \qquad \text{on} \quad |\underset{\sim}{Y}-\underset{\sim}{\ell}| = 1 \quad , \tag{4.14}$$

$$\nabla^2\Phi_1 = 2 \frac{\partial\bar{\Phi}}{\partial Y_i} \frac{\partial^2\Phi_o}{\partial Y_i \partial t} \quad , \quad n_i \frac{\partial\Phi_1}{\partial Y_i} = n_i \ell_i' \qquad \text{on} \quad |\underset{\sim}{Y}-\underset{\sim}{\ell}| = 1 \quad , \tag{4.15}$$

and

$$\nabla^2\Phi_2 = 2 \frac{\partial\bar{\Phi}}{\partial Y_i} \frac{\partial^2\Phi_1}{\partial Y_i \partial t} + \frac{\partial^2\Phi_o}{\partial t^2} \quad , \quad n_i \frac{\partial\Phi_2}{\partial Y_i} = 0 \qquad \text{on} \quad |\underset{\sim}{Y}-\underset{\sim}{\ell}| = 1 \quad . \tag{4.16}$$

Equation (4.14) describes a simple problem for the potential $\Phi_o + \bar{\Phi}$. It states that $\Phi_o + \bar{\Phi}$ is the potential of the incompressible flow around a stationary sphere whose centre is instantaneously at $\underset{\sim}{\ell}$. The solution which tends to $-MY_1$ as $Y \to \infty$ is

$$\Phi_o + \bar{\Phi} = - MY_1 - \tfrac{1}{2}M \frac{Y_1 - \ell_1}{|\underset{\sim}{Y}-\underset{\sim}{\ell}|^3} \quad . \tag{4.17}$$

After subtracting $\bar{\Phi}$ and linearizing in $\underset{\sim}{\ell}$, we find that

$$\Phi_o = \tfrac{1}{2}M\ell_i \left(\frac{\delta_{i1}}{Y^3} - \frac{3Y_iY_1}{Y^5} \right) \quad . \tag{4.18}$$

Therefore the contribution to Φ_1 from the particular integral of the Poisson equation in (4.15) is of order M^2 smaller than the term

arising from the boundary condition, and the solution (linearized in $\underset{\sim}{U}$) is

$$\Phi_1 = -\tfrac{1}{2}U_i' Y_i / Y^3 \quad , \tag{4.19}$$

the potential of incompressible flow around a sphere with velocity $\underset{\sim}{U}'$.

The forcing terms in the problem for Φ_2 have now been determined, and when they are written explicitly (4.16) becomes

$$\nabla^2 \Phi_2 = \tfrac{1}{2} M U_i'' \left\{ \frac{3\delta_{i1}}{Y^3} + \frac{\delta_{i1}}{Y^6} - \frac{9 Y_i Y_1}{Y^5} + \frac{3 Y_i Y_1}{Y^8} \right\} \tag{4.20}$$

with $$n_i \frac{\partial \Phi_2}{\partial Y_i} = 0 \qquad \text{on} \quad |\underset{\sim}{Y} - \underset{\sim}{U}| = 1 \quad .$$

We can consider the components of the acceleration separately because the judder is linear. First we solve the inner flow for a vibration with an arbitrary displacement and velocity, but where the acceleration is in the direction of the stream, $U_i'' = U_1'' \delta_{i1}$. Then equation (4.20) is

$$\nabla^2 \Phi_2 = M U_1'' \left\{ - \frac{3 P_2(\cos\Theta)}{Y^3} + \frac{P_2(\cos\Theta)}{Y^6} + \frac{1}{Y^6} \right\} . \tag{4.21}$$

P_2 is the Legendre function of second order, $P_2(\cos\Theta) = \tfrac{1}{2}(3\cos^2\Theta - 1)$, and $\cos\Theta = Y_1 / Y$. It is easy to verify that

$$\Phi_2 = M U_1'' \left\{ - \frac{1}{3Y} + \frac{1}{12 Y^4} + P_2(\cos\Theta) \left(\frac{1}{2Y} - \frac{7}{18 Y^3} + \frac{1}{6 Y^4} \right) \right\} \tag{4.22}$$

satisfies both equation (4.21) and the boundary condition. Φ_o and Φ_1 describe incompressible flow around the moving sphere. Φ_2 is the lowest order term in the expansion of Φ that takes account of the compressibility of the inner field.

We denote the inner expansion correct to order ε^n by $\Phi^{(n)}(\underset{\sim}{Y}, \varepsilon)$; $\Phi^{(0)} = \Phi_o$, $\Phi^{(1)} = \Phi^{(0)} + \varepsilon \Phi_1$, and $\Phi^{(2)} = \Phi^{(1)} + \varepsilon^2 \Phi_2$.

When expressed in terms of the outer variable $\underset{\sim}{y}$,

$$\Phi^{(0)}(\underset{\sim}{y}/\varepsilon,\varepsilon) = \tfrac{1}{2}\varepsilon^3 M l_i \left(\frac{\delta_{i1}}{y^3} - \frac{3y_i y_1}{y^5}\right) , \tag{4.23}$$

$$\Phi^{(1)}(\underset{\sim}{y}/\varepsilon,\varepsilon) = \Phi^{(0)}(\underset{\sim}{y}/\varepsilon,\varepsilon) - \tfrac{1}{2}\varepsilon^3 l_i' y_i/y^3 , \tag{4.24}$$

and

$$\Phi^{(2)}(\underset{\sim}{y}/\varepsilon,\varepsilon) = \Phi^{(1)}(\underset{\sim}{y}/\varepsilon,\varepsilon) + \varepsilon^3 M l_1'' \left(-\frac{7}{12} + \frac{3}{4}\cos^2\theta\right)/y + O(\varepsilon^5) . \tag{4.25}$$

$\Phi^{(n)}(\underset{\sim}{y}/\varepsilon,\varepsilon)$ is a new power series in ε . As in §2.3 we define $\Phi^{(n,m)}$ to be the expansion of $\Phi^{(n)}(\underset{\sim}{y}/\varepsilon,\varepsilon)$ terminated at ε^m .

The matching rule relates the functions $\Phi^{(n,m)}$ to the outer expansion of ϕ by

$$\Phi^{(n,m)} = \phi^{(m,n)} , \tag{4.26}$$

where $\phi^{(m,n)}$ is the outer expansion correct to order ε^m , expressed in terms of the inner variable and then truncated after order ε^n .

When equations (4.23)-(4.25) are compared with the outer solution given in (4.10), we see at once that $\lambda = 3$, and that the highest order multipoles in the outer expansion are quadrupole. Hence

$$\phi^{(3)}(\varepsilon\underset{\sim}{Y},\varepsilon) = f_{ij}(t)\frac{\partial^2}{\partial Y_i \partial Y_j}\left(\frac{1}{Y}\right) + \varepsilon\left\{f_i(t)\frac{\partial}{\partial Y_i}\left(\frac{1}{Y}\right) - Mf_{ij}'(t)\frac{\partial^2 \cos\theta}{\partial Y_i \partial Y_j}\right\}$$

$$+ \varepsilon^2\left\{\frac{f(t)}{Y} - Mf_i'(t)\frac{\partial(\cos\theta)}{\partial Y_i} + \tfrac{1}{2}f_{ij}''(t)\frac{\partial^2(Y+2MY_1)}{\partial Y_i \partial Y_j}\right\} . \tag{4.27}$$

The functions $f_{i\ldots}$ can be evaluated from the matching rule. For example

$$\phi^{(3,0)} = f_{ij}\frac{\partial^2}{\partial Y_i \partial Y_j}\left(\frac{1}{Y}\right) = \Phi^{(0,3)} ,$$

and from the expression (4.23) for $\Phi^{(0)}$,

$$f_{1i} = -\tfrac{1}{2}M l_i , \text{ with all other components zero} . \tag{4.28}$$

Similarly the condition $\Phi^{(3,1)} = \Phi^{(1,3)}$ shows that

$$f_i = \tfrac{1}{2} \ell_i' \quad . \tag{4.29}$$

The strength of the monopole term f is determined from $\Phi^{(2)}$. $\Phi^{(2)}$ is only non-zero because the fluid is compressible; even for this compact source the compressibility of the inner field must be considered in order to evaluate the outer field correctly. The matching procedure gives

$$f = \frac{M}{6} \ell_1'' \quad . \tag{4.30}$$

We have now derived the outer expansion

$$\phi(\underset{\sim}{y},t) = \varepsilon^3 \left\{ \frac{M}{6y} \ell_1''(t-y-My_1) + \frac{1}{2} \frac{\partial}{\partial y_i} \frac{\ell_i'(t-y-My_1)}{y} - \frac{M}{2} \frac{\partial^2}{\partial y_1 \partial y_i} \frac{\ell_i(t-y-My_1)}{y} \right\} \quad . \tag{4.31}$$

The largest contribution to the sound field comes from the dipole, with a smaller effect from the weaker monopole and quadrupole.

After the evaluation of the derivatives for large values of y,

$$\phi(\underset{\sim}{y},t) = \frac{\varepsilon^3}{y} \left\{ \frac{M}{6} - \frac{1}{2} \cos\Theta - \frac{1}{2} M - \frac{1}{2} M\cos^2\Theta \right\} \ell_1''(t-y-My_1) \quad , \tag{4.32}$$

since we are considering the case where $\underset{\sim}{\ell}''$ is parallel to the 1-axis. The velocity potential depends only on the acceleration of the sphere at the emission time

$$\phi(\underset{\sim}{y},t) = \frac{\varepsilon^3}{y} \left(- \frac{1}{2} \frac{\cos\Theta + M}{1-M\cos\Theta} + \frac{M}{6} \right) \ell_1''(t-y-My_1) \quad , \tag{4.33}$$

correct to order M.

When rewritten in terms of dimensional variables

$$\phi(\underset{\sim}{y},t) = \frac{a^3}{yc_o} \left(- \frac{1}{2} \frac{\cos\Theta + M}{1-M\cos\Theta} + \frac{M}{6} \right) \ell_1''(t-(y+My_1)/c_o) \quad . \tag{4.34}$$

The kinematic relations (2.10)-(2.13) can be used to derive the perturbed velocity potential in the $(\underset{\sim}{x},t)$ frame, where the fluid at

infinity is at rest and the sphere has a mean velocity $\underset{\sim}{U}$.

$$\phi(\underset{\sim}{x},t) = \frac{a^3}{rc_o}\left(-\frac{1}{2}\frac{\cos\theta}{(1-M\cos\theta)^3} + \frac{M}{6}\right) l_1''\left(\frac{t-x/c_o}{1-M\cos\theta}\right) \quad . \tag{4.35}$$

This result tells us that the sound field produced by a body juddering in the direction of the mean flow is completely different from (2.8), the sound of a moving dipole. The effect of motion on this field is much larger. The source motion amplifies the velocity potential by a factor $(1-M\cos\theta)^{-3}$ and there is an additional omnidirectional term, which means that the acoustic field in a plane perpendicular to the direction of motion is also modified.

We will now consider the other component of the acceleration of the sphere; acceleration perpendicular to the mean flow. With no loss of generality we can take this to be in the 2-direction; $l_i'' = l_2''\delta_{2i}$, while the velocity and displacement are arbitrary.

Then Φ_o and Φ_1 are the same as in (4.18) and (4.19),

$$\Phi_o = \frac{1}{2} M l_i \left(\frac{\delta_{i1}}{Y^3} - \frac{3Y_iY_1}{Y^5}\right) \quad , \tag{4.36}$$

and

$$\Phi_1 = -\frac{1}{2} l_i' \frac{Y_i}{Y^3} \quad . \tag{4.37}$$

Φ_2 is to be determined from equation (4.20) which, when $\underset{\sim}{l}''$ is parallel to the 2-axis, reduces to

$$\nabla^2\Phi_2 = \frac{3}{2} M l_2'' Y_1 Y_2 \left(-\frac{3}{Y^5} + \frac{1}{Y^8}\right) \quad . \tag{4.38}$$

The solution of this equation which satisfies $n_i \partial\Phi_2/\partial Y_i = 0$ on $|\underset{\sim}{Y}-\underset{\sim}{l}| = 1$ is

$$\Phi_2 = M l_2'' Y_1 Y_2 \left(\frac{3}{4Y^3} + \frac{1}{4Y^6} - \frac{7}{12Y^5}\right) \quad . \tag{4.39}$$

When the matching principle is used to relate the total inner field to an outer field of the form given in equation (4.10) we find that $\lambda = 3$ and again all multipoles of higher order than quadrupole are zero. The matching gives

$$f_{1i} = -\tfrac{1}{2}M l_i \ , \quad \text{with all other components of } f_{ij} \text{ zero} \ ,$$

$$f_i = \tfrac{1}{2} l_i' \ ,$$

and $f = 0$.

Therefore to lowest order in ε the outer solution is

$$\phi(\underset{\sim}{y},t) = \varepsilon^3 \left\{ \frac{\partial}{\partial y_i} \frac{l_i'(t-y-My_1)}{2y} - M \frac{\partial^2}{\partial y_1 \partial y_i} \frac{l_i(t-y-My_1)}{2y} \right\} . \tag{4.40}$$

After the derivatives have been evaluated for large y ,

$$\begin{aligned} \phi(\underset{\sim}{y},t) &= -\frac{\varepsilon^3}{2y} \hat{y}_2 (1+M\cos\Theta)\, l_2''(t-y-My_1) \\ &= -\frac{\varepsilon^3 \hat{y}_2}{2y(1-M\cos\Theta)} l_2''(t-y-My_1) \end{aligned} \tag{4.41}$$

correct to order M , where $\hat{y}_2 = y_2/y$. In dimensional parameters

$$\phi(\underset{\sim}{y},t) = -\frac{a^3 \hat{y}_2}{2yc_o(1-M\cos\Theta)} l_2''(t-(y+My_1)/c_o) \ . \tag{4.42}$$

Again we notice that this is not the same as the acoustic field of a dipole with its axis perpendicular to the mean flow, as given in equation (2.16). The velocity potential generated by a sphere vibrating in the 2-direction has an extra multiplying factor $(1-M\cos\Theta)^{-2}$.

We can use the relations (2.10)-(2.13) to determine the potential in the $\underset{\sim}{x}$-frame in which the flow far from the body is at rest,

$$\phi(\underset{\sim}{x},t) = -\frac{a^3 \hat{f}_2}{2rc_o(1-M\cos\theta)^3} l_2''\left(\frac{t-x/c_o}{1-M\cos\theta}\right) \ . \tag{4.43}$$

Source motion modifies the velocity potential by a factor $(1-M\cos\theta)^{-3}$. This is again larger than the effect of motion on a dipole.

The acoustic field generated by a sphere juddering with an arbitrary acceleration $\underset{\sim}{l}''$ can be obtained by adding the velocity potential produced by its two components determined in (4.35) and (4.43). We find that for an arbitrary vibration

$$\phi(\underset{\sim}{x},t) = \frac{a^3}{rc_o}\left\{\frac{-\hat{r}_i}{2(1-M\cos\theta)^3} l_i''\left(\frac{t-x/c_o}{1-M\cos\theta}\right) + \frac{M}{6} l_1''\left(\frac{t-x/c_o}{1-M\cos\theta}\right)\right\} . \qquad (4.44)$$

In the linear acoustic field the pressure perturbation p is $-\rho_o \partial\phi/\partial t$,

$$p = \frac{a^3\rho_o}{rc_o}\left\{\frac{\hat{r}_i}{2(1-M\cos\theta)^4} l_i'''\left(\frac{t-x/c_o}{1-M\cos\theta}\right) - \frac{M}{6} l_1'''\left(\frac{t-x/c_o}{1-M\cos\theta}\right)\right\} . \qquad (4.45)$$

Lighthill's theory gives the same result. The pressure perturbation at a point $\underset{\sim}{x}$ in the linear acoustic field can be expressed in terms of integrals over B, the surface of the sphere, and a volume integral throughout the fluid (see for example Ffowcs Williams & Hawkings 1969)

$$4\pi p(\underset{\sim}{x},t) = \frac{\partial^2}{\partial x_i \partial x_j}\int_{\mathcal{D}}\left[\frac{T_{ij}}{r(1-M\cos\theta-l_k'\hat{r}_k/c_o)}\right] d^3\underset{\sim}{\eta}$$

$$- \frac{\partial}{\partial x_i}\int_B\left[\frac{p_{ij}n_j}{r(1-M\cos\theta-l_k'\hat{r}_k/c_o)}\right] dS(\underset{\sim}{\eta}) + \frac{\partial}{\partial t}\int_B\left[\frac{\rho_o u_i n_i}{r(1-M\cos\theta-l_k'\hat{r}_k/c_o)}\right] dS(\underset{\sim}{\eta}) , \qquad (4.46)$$

where T_{ij} is Lighthill's stress tensor, $\rho u_i u_j + p_{ij} - c_o^2(\rho-\rho_o)\delta_{ij}$. The square brackets mean that the function they enclose is to be evaluated at the retarded time τ appropriate for waves travelling from the source to $\underset{\sim}{x}$ with speed c_o;

$$\tau = t - r/c_o = t - |\underset{\sim}{x}-\underset{\sim}{\eta}-\underset{\sim}{U}\tau-\underset{\sim}{l}|/c_o .$$

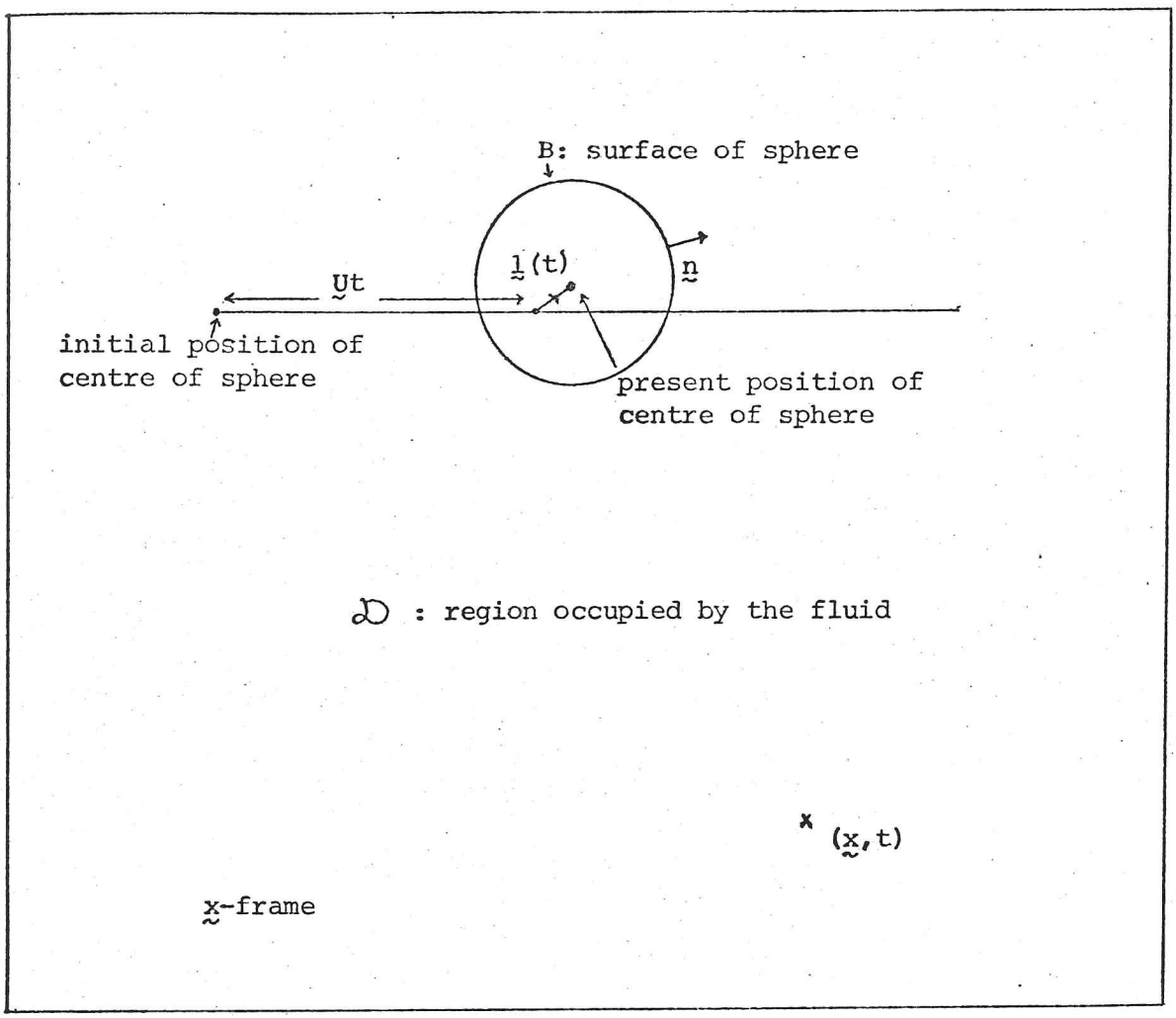

Figure 2.6 A juddering sphere

Therefore τ varies over the range of integration. For large x,

$$\tau = \frac{t - x/c_o + \hat{f}_i n_i/c_o}{1 - M\cos\theta - l'_k \hat{f}_k/c_o} \quad . \tag{4.47}$$

The normal fluid velocity on the surface of the sphere is equal to the component of the velocity of the body in that direction. In the $\underset{\sim}{x}$-frame this is $l'_i n_i + U n_1$. After linearizing in $\underset{\sim}{l}$, we find that correct to order M the monopole term is

$$\frac{\partial}{\partial t}\int_B \rho_o \left[\frac{l'_i n_i + U n_1}{r(1-M\cos\theta)} + \frac{M l'_i \hat{f}_i n_1}{r}\right] dS(\underset{\sim}{\eta}) \quad . \tag{4.48}$$

The variation of $l'_i(\tau)$ over the body can be expanded as a Taylor series

$$l'_i(\tau) = l'_i\left(\frac{t-x/c_o}{1-M\cos\theta}\right) + \frac{\hat{f}_i \eta_i}{c_o(1-M\cos\theta)}\, l''_i\left(\frac{t-x/c_o}{1-M\cos\theta}\right) + \ldots$$

With this form for $\ell_i'(\tau)$ in (4.48) it is easy to evaluate the integral over the surface of the sphere, and we find that the monopole term becomes

$$\frac{4\pi a^3 \rho_o}{3rc_o}(1+4M\cos\theta)\hat{r}_i \ell_i'''\left(\frac{t-x/c_o}{1-M\cos\theta}\right) \tag{4.49}$$

correct to order M.

The dipole strength depends on the pressure perturbation near the sphere. Equations (4.17) and (4.19) give an expansion of the velocity potential valid in this inner region. The potential in the $\underset{\sim}{x}$-frame, ψ, is $U\eta_1 + \bar{\phi} + \phi$. Hence, in dimensional parameters

$$\psi = -\frac{1}{2}U\frac{a^3\eta_1}{\eta^3} - \frac{1}{2}\ell_i'\frac{a^3\eta_i}{\eta^3} + O\left(\frac{a^2}{c_o}M\ell''\right) , \tag{4.50}$$

where $\underset{\sim}{\eta}$ is measured from the point $\underset{\sim}{U}t + \underset{\sim}{\ell}$, the position of the centre of the sphere.

In the $\underset{\sim}{x}$-frame the fluid velocity u_i is $\partial\psi/\partial\eta_i$ and the pressure can be determined from the compressible form of Bernoulli's equation;

$$\begin{aligned}\int \frac{dp}{\rho} &= -\left.\frac{\partial\psi}{\partial t}\right|_{\underset{\sim}{\eta}} + (U_j+\ell_j')\frac{\partial\psi}{\partial\eta_j} - \frac{1}{2}u^2 \\ &= \frac{1}{2}\ell_i''\eta_i + U\ell_i'\left(-\frac{5}{4}\delta_{i1} + \frac{9}{4}\frac{\eta_i\eta_1}{a^2}\right) + U^2\left(-\frac{5}{8} + \frac{9}{8}\frac{\eta_1^2}{a^2}\right) \quad \text{on } \eta = a .\end{aligned} \tag{4.51}$$

For a homentropic flow, variations in the sound speed are $O(M^2)$ (Taylor 1975), so that

$$\int \frac{dp}{\rho} = c_o^2 \log(\rho/\rho_o) \tag{4.52}$$

and from equation (4.51) we see that if M^2 is neglected in comparison with unity

$$p = c_o^2(\rho-\rho_o) = \rho_o \int \frac{dp}{\rho} . \tag{4.53}$$

When this expression for the pressure perturbation is substituted into the dipole term, the surface integral can be evaluated to give

$$-\frac{\partial}{\partial x_i}\int_B \left[\frac{p_{ij}n_j}{r(1-M\cos\theta-\ell_k'\hat{r}_k/c_o)}\right] dS(\underset{\sim}{\eta}) = \frac{4\pi a^3\rho_o}{rc_o}\left(\ell_i'''\hat{r}_i\left(\frac{1}{6}+\frac{19}{30}M\cos\theta\right)-\frac{4}{15}M\ell_1'''\right). \tag{4.54}$$

The density, velocity and pressure in the volume source term T_{ij} are estimated by their values in the inner field. It is impossible to give a formal justification of this approximation, but it is equivalent to Lighthill's basic conjecture that the sound itself, i.e. the outer field, is a negligible source of sound.

The quadrupole source strength can be integrated to show

$$\frac{\partial^2}{\partial x_i\partial x_j}\int_{\mathcal{D}}\left[\frac{T_{ij}}{r(1-M\cos\theta-\ell_k'\hat{r}_k/c_o)}\right] d^3\underset{\sim}{\eta} = \frac{4\pi a^3\rho_o}{rc_o}M\left(\frac{\cos\theta}{30}\hat{r}_i\ell_i''''+\frac{1}{10}\ell_1''''\right). \tag{4.55}$$

Adding the contributions from the three terms together we find

$$p(\underset{\sim}{x},t) = \frac{a^3\rho_o}{rc_o}\left(\frac{\hat{r}_i\ell_i'''}{2(1-M\cos\theta)^4}-\frac{1}{6}M\ell_1'''\right). \tag{4.56}$$

This expression for the far-field pressure perturbation is the same as that obtained earlier in equation (4.45).

It is at first sight surprising that Lighthill's method requires less information about the inner field than the method of matched asymptotic expansions! When applying the matching principle we need to know Φ_2, the order ε^2 term in the inner potential in order to determine the outer field. In fact $\Phi_2 \sim a^2M|\underset{\sim}{\ell}''|/c_o$, and the effect of the derivatives in Lighthill's theory ensures that in this method Φ_2 gives rise to a negligible far-field; it only produces a contribution to the pressure field of order $a^3\rho_oM^2\ell'''/(rc_o)$ or $a^4\rho_oM\ell^{iv}/(rc_o^2)$. We can understand this by considering the way in which Φ_2 enters the matching procedure. Although $\varepsilon^2\Phi_2$ is small in magnitude near the body,

it decays slowly with distance from the sphere (see equations (4.22) and (4.39)) and so in the 'matching region' it is comparable with the other terms in the inner expansion, and must be evaluated to obtain the outer field. The Lighthill theory is different. The structure of the Navier Stokes equation is used to express the acoustic field in terms of integrals over the source region. The main sources, the monopole and dipole, depend only on the flow on the surface of the body and there the $\varepsilon^2\Phi_2$ is negligible in comparison with the lower order terms.

The derivation of the acoustic field from a substitution of the 'inner flow' into Lighthill's exact form cannot be rigorously justified but this method is instructive because it gives an understanding of why the sound field of a compact juddering body is different from that of a point force. We have shown that for a juddering sphere, no matter how small, it is incorrect to neglect the variation in retarded time across the body in the way suggested by Ffowcs Williams & Hawkings (1969). Some of the terms arising from the retarded time variation are only of order M smaller than the leading acoustic field and change its directivity. Source motion also induces an additional quadrupole. The total pressure field is significantly different from that of a moving dipole and cannot be simply specified in terms of multipoles.

2.5 Conclusions

The motion of a 'real' source alters the sound field in a more striking way than previously thought possible. The motion of elementary point sources had formed the models on which convective effects were assessed and we now see that this is inadequate because motion also alters the source type.

We have investigated the far-field form of the acoustic field produced by a moving pulsating body of arbitrary shape, and have shown

that its pressure field is amplified from its value at rest by a factor $(1+\hat{r}_i \alpha_{ij} M_j)(1-M\cos\theta)^{-3}$, where α_{ij} is the inertial mass tensor, and $\underset{\sim}{M}$ is a vector in the direction of the body motion of strength M . When $\underset{\sim}{M}$ lies along an eigenvector of the symmetric tensor α_{ij} , the amplifying factor is $(1-M\cos\theta)^{-3-\alpha}$, where α is the corresponding eigenvalue. However, when $\underset{\sim}{M}$ is not in the direction of an eigenvector of α_{ij}, the far-field may be amplified even for points which lie in a plane perpendicular to the direction of motion. We see that a moving pulsating body cannot be modelled by a moving monopole source. This is because a moving pulsating body, producing a mass flux, necessarily has a momentum flux associated with it. Hence the sound field produced is that of a moving monopole and a coupled dipole. Moreover, the strength of the dipole is only a Mach number smaller than the monopole and so affects the amplification factor.

The distant form of the acoustic field produced by the oscillation of a compact sphere about a mean uniform motion has also been determined. The effect of motion is complicated; the stationary pressure field is modified by a factor $(1-M\cos\theta)^{-4}$ and there is an additional omni-directional term.

The way in which motion alters the sound field produced by real sources depends very much on the type and shape of the source. In general the modification made to the pressure field cannot be expressed simply. It depends on details of the source structure and those details must be known before the modification due to convection can be calculated.

The results derived in this chapter have been published previously (Dowling 1976) but they are obtained here by a different, and we think more elegant, method.

CHAPTER 3

SOUND PRODUCTION IN A MOVING STREAM

3.1 Introduction

Ever since the experimental work of Lush (1971) there has been no doubt that the interaction of aerodynamic sound with the moving flow, whose mixing provided its source, is an important element of the jet noise problem. Lush found that although Lighthill's (1952) theory gives good overall agreement for the sound intensity it wrongly predicts the convective amplification at high frequencies near the jet axis. Many of the features described by Ribner (1964) as refraction of sound by gradients in mean flow and refractive index were confirmed in Lush's work, so putting experimental observation and intuitive reasoning in the lead of any formal theory.

Of course, it was always evident that some refraction of sound passing through an inhomogeneous flow was inevitable, and Lighthill (1952) argued that such effects should be treated separately after the sound generation problem had been solved. Jet refraction problems have been worked by Gottlieb (1960) and Schubert (1972), with evidence that flow can deform any sound wave passing through it. Only Lighthill's (1952) theory could treat the sound generation problem exactly, but that theory was incapable of explicitly displaying the refractive effects. Theories that bring out the flow acoustic interaction explicitly are invariably approximate and difficult to handle, so that the consequences of the necessary approximations remain obscure. For example, Gottlieb's work concerned a plane vortex sheet modelling of a jet, while Schubert described waves propagating through a laminar flow. Zones of silence arise in such flows and the upstream deflection of an initially downstream propagating ray is impossible. But some upstream deflection

is quite probable for high frequency waves in an actual jet as concentrated eddies can bend rays in a different and more extreme manner from that found in parallel laminar flows (cf. Broadbent 1977).

Phillips (1960) was the first to attempt an exact description of sound generation by turbulent shear layers in which the flow interaction was made explicit. That work was extended by Pao (1969) and Lilley (1971). Primarily aimed at the supersonic problem it left obscure the important issues that Mani (1976) emphasized; the Lighthill analogy does not seem to provide even an approximate low speed estimate of the full convection effects on the sound generated by sources shrouded in a jet flow. Mani's analysis was only based on an intuitive modelling of the flow, some support for the model being deduced from Lilley's (1974) theory. The results agree so well with experiment, even in those areas where Lush pointed to the deficiencies of the Lighthill theory, that one is led to suspect a more fundamental justification is possible; that is essentially what this chapter is about.

A substantial amount of recent theoretical work on the interaction between the mean flow, the turbulence and the acoustic field is based on the idea that the unsteady stream can be thought of as a weak perturbation to a parallel laminar inviscid flow with a velocity and density profile equal to that of the mean jet. The motion is governed by a compressible version of the Rayleigh equation, whose inhomogeneous form is the Lilley (1974) equation. This method is formally exact, but it is not easy to apply. One difficulty is that the source terms are complicated, and in general they are only described approximately. Morfey & Tester (1976) show that equivalent ways of expressing the source (both correct to quadratic order in the fluctuating quantities) can lead to completely different estimates for the sound field; so obviously the greatest care must be taken not to use a misleading description of the source terms.

The Green function for the Lilley equation is not easy to obtain. It is a solution to a third order differential equation with variable coefficients, and in general must be evaluated numerically, although simple solutions can be obtained in the low frequency (Goldstein 1975) and high frequency (Balsa 1976) limits. In addition to these practical difficulties there are fundamental unresolved problems associated with this method. Non-trivial solutions of the homogeneous compressible Rayleigh equation exist, indeed they are the ones so extensively studied in examining the stability of laminar flows, and to obtain a unique solution to Lilley's equation we need some way of deciding what combination of these modes should be incorporated within the Green function, or equivalently what initial and boundary conditions should be prescribed. The intuitive choice is to pick a causal Green function, but for an unstable profile strict causality is incompatible with boundedness at infinity (Jones 1973); the causal solution contains instability waves which are invariably neglected in an analysis of Lilley's equation. Another difficulty in principle concerns the idea of evaluating the field as a weak perturbation about a laminar flow with the mean jet profile. Real turbulent jets are highly disturbed; the instantaneous velocity vector deviates from the axial direction by more than $\pi/4$ quite frequently (Acton 1976). Fluctuations in a low Mach number jet are on the same time scale as the sound they produce, during which time the sound travels many shear layer thicknesses. Any single sound wave therefore interacts with a geometrically contorted shear layer, quite unlike the mean shear layer, and the interaction is complete long before the shear layer has wobbled enough to resemble the mean. It might be thought that the mean effect of acoustic shear interaction could be approximated by a single passage of sound through a 'mean' shear layer. But that too seems unlikely, at least at high frequencies, because, for example, shadow zones exist in the laminar shear layer problem which

would be penetrated by rays in an actual jet (Dowling 1975). The Lilley theory does however account for the major effects of refraction remarkably well. The existence of quiet zones is an obvious area in which the qualitative similarity is good, and away from the shadow zone there is quantitative agreement. But in many respects Mani's vortex sheet modelling of the jet problem seems as good as that more laboriously obtained when the jet flow is given a mean velocity and temperature profile (Morfey & Tester 1976), which suggests that in these areas where the laminar flow theories are successful, the details of the profile are actually unimportant. In that case, the best model will be that which is most easily handled and it is difficult to imagine any simpler model than a vortex sheet. It is this analytical tractability that might give Mani's model its edge; its weakness lies in its inability to define the sources. Mani tries to determine the source terms in his model from Lilley's theory. But in doing so he has to discard a singular source term which would actually dominate in any physical realization of that model. Mani also argues that there are efficient monopoles arising from mean density gradients in a hot jet; that is now known to be incorrect (cf. Kempton 1977) and is in fact obtained from an erroneous application of Lilley's equation (cf. Morfey & Tester 1976). Because it is not based on an exact analogy Mani's theory cannot provide a convincing procedure for handling the more subtle and difficult problems such as vortex sheet instability and the apparent singularities encountered at the Mach wave condition in supersonic jets.

In this chapter we develop an exact analogy between a vortex sheet simulation of a jet flow and the real thing, and show that the equivalent source required in the analogy is a convected quadrupole distribution, each quadrupole having a strength determined by Lighthill's stress tensor measured relative to a uniformly moving jet stream. This result is

essentially that already given by Ffowcs Williams (1974), but we now give a more rigorous derivation of the theory.

In our exact analogy we require that the linear model should share the real flow's finite level of acoustic activity. Any instability of the model flow must therefore be avoided and this causes a precursor ahead of the wave front. We believe that this is entirely reasonable for, in addition to the turbulence producing sound, the sound waves will also provoke any real unstable shear layer to support rapidly growing waves that later break into turbulence. Any theory that attributes the source of that sound to the turbulence must therefore allow for the sound's prior existence. The turbulence provides the dominant source, while the contribution made by instability waves growing into turbulence necessarily precedes it. The analogy, which is exact, allows both these elements to be specified through Lighthill's stress tensor and the bounded Green function for a vortex sheet simulation of the flow.

We first develop the theory in a general way and illustrate its application for a cylindrical jet of circular cross-section and then derive from the theory some important known results for an acoustically compact jet flow. We contend that this theory provides a justification for the correctness of Mani's (1976) vortex sheet modelling. The sources needed for that model are however quite different from those used by Mani, which in any case are now known to misrepresent the effects of mean density gradients. It is our belief that this theory allows all the power and simplicity of Lighthill's analogy to be applied to real jet flows in which there are significant mean flow acoustic interactions; these interactions are made explicit in an analytically tractable way.

We also give some new results for the acoustically compact jet of low density. There it seems that sound will scale on very low powers of jet speed. We think that this may well be part of the excess noise

problem where sound is known not to conform with the simple scaling of Lighthill's free quadrupole model.

3.2 A generalization of Lighthill's acoustic analogy

Our development is based on Lighthill's (1952) equation

$$\frac{\partial^2 \rho'}{\partial \tau^2} - c_0^2 \frac{\partial^2 \rho'}{\partial y_i^2} = \frac{\partial^2 T_{ij}}{\partial y_i \partial y_j}, \tag{2.1}$$

where $T_{ij} = \rho v_i v_j + p_{ij} - c_0^2 \rho' \delta_{ij}$; (2.2)

v_i is the fluid velocity, ρ the density, and $\rho' = (\rho - \rho_0)$. p_{ij} is the compressive stress tensor, $p_{ij} = (p - p_0)\delta_{ij} - e_{ij}$, with p the pressure and e_{ij} the viscous stress. ρ_0, c_0 and p_0 are the unperturbed values of density, sound speed and pressure. It is well known that this equation is a direct consequence of the continuity and momentum equations

$$\frac{\partial \rho}{\partial \tau} + \frac{\partial}{\partial y_i}(\rho v_i) = 0, \tag{2.3}$$

$$\frac{\partial}{\partial \tau}(\rho v_i) + \frac{\partial}{\partial y_j}(T_{ij} + c_0^2 \rho' \delta_{ij}) = 0. \tag{2.4}$$

Lighthill's formulation of the aerodynamic sound problem is most appropriate when the sound generated by the flow propagates through a medium which is homogeneous and at rest relative to the observer. When some of the fluid is heated or has a uniform velocity, T_{ij} contains terms which depend linearly on the sound field. Equation (2.1)* is still formally exact, and if T_{ij} were known exactly would lead to the correct answer for the density perturbation ρ'. However T_{ij} can only be determined from a solution of the full Navier Stokes equation and for the turbulent jets of technological interest this represents a daunting

---

*Equations referred to are always within the same chapter.

prospect; at present it is only feasible to obtain a dimensional analysis of the sound field based on the time averaged properties of Lighthill's stress tensor (Lighthill 1952). Ffowcs Williams (1977) shows that this procedure can lead to erroneous predictions when there are extensive linear terms in T_{ij} .

In a region of moving fluid it is more natural to recast the Lighthill theory in terms of a convected wave operator. We choose a coordinate system so that the mean velocity is in the 1-direction with speed U_1 . When the mass equation is rewritten using the convected derivative $\frac{D_1}{D\tau} \equiv \frac{\partial}{\partial \tau} + U_1 \frac{\partial}{\partial y_1}$, it becomes

$$\frac{D_1 \rho}{D\tau} + \frac{\partial}{\partial y_i}(\rho v_i') = 0, \tag{2.5}$$

where $v_i' = v_i - U_1 \delta_{i1}$.

Similarly the momentum balance can be expressed as

$$\frac{D_1}{D\tau}(\rho v_i') + \frac{\partial}{\partial y_j}(T_{ij}' + c_1^2 \rho_1' \delta_{ij}) = 0. \tag{2.6}$$

T_{ij}' is Lighthill's stress tensor based on the relative velocity v_i' ,

$$T_{ij}' = \rho v_i' v_j' + p_{ij} - c_1^2 \rho_1' \delta_{ij} , \tag{2.7}$$

$$\rho_1' = (\rho - \rho_1) .$$

ρ_1 and c_1 are the mean values of the density and sound speed. If the jet is hot they will be different from ρ_0 and c_0 .

Equations (2.5) and (2.6) combine to give

$$\frac{D_1^2 \rho_1'}{D\tau^2} - c_1^2 \frac{\partial^2 \rho_1'}{\partial y_i^2} = \frac{\partial^2 T_{ij}'}{\partial y_i \partial y_j}, \tag{2.8}$$

the form of the Lighthill theory relevant in a hot, moving fluid. If $U_1 = 0$, and $\rho_1 = \rho_0$, $c_1 = c_0$ equation (2.8) reduces to the more

usual expression (2.1).

In practice a moving stream of air is generated by the stirring and heating action of external surfaces within the fluid. In order to describe this situation we suppose that the fluid occupies all space outside a surface $\Sigma(\tau)$, which may in fact consist of several closed surfaces. For example, $\Sigma(\tau)$ may be the surfaces of the compressor blades in a jet engine, where the motion of the blades and the subsequent combustion of the compressed gas produces a hot, fast-moving stream that emerges into the ambient fluid. We introduce a control surface $S(\tau)$, convected with the fluid particles, and such that it encloses most of the energetic flow and all the surfaces $\Sigma(\tau)$, as shown in Figure 3.1.

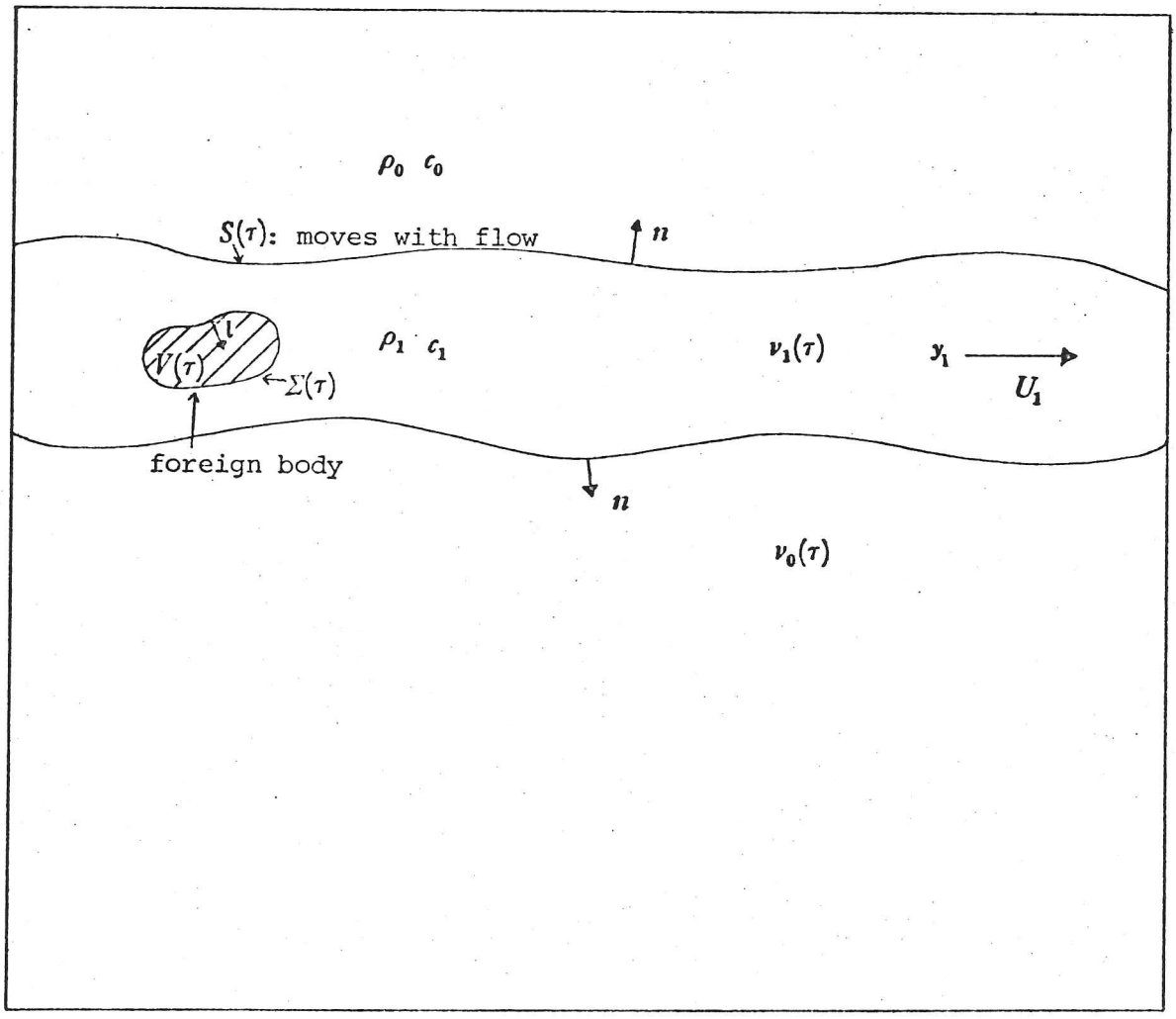

Figure 3.1 The geometry of the jet

We denote the region within $S(\tau)$ by $\nu_1(\tau)$. The hot jet in ν_1 has a mean velocity U_1 in the downstream direction, and a characteristic sound speed c_1 and density ρ_1 . It is therefore reasonable to use equation (2.8) to describe its aero-acoustics. In the region $\nu_0(\tau)$, outside the surface $S(\tau)$, most of the fluid is unheated and at rest, and the formulation (2.1) is a more useful description of the flow. The shape of the regions $\nu_0(\tau)$ and $\nu_1(\tau)$ is arbitrary. But in the analysis that follows we will assume that $\nu_1(\tau)$ is finite, or at most infinite in one dimension, for example, an infinitely long tube with a bounded cross-sectional area, as illustrated in Figure 3.1.

To simplify the procedure of using different equations to describe the flow in the two regions ν_0 and ν_1 , we define a function $g(\mathbf{y},\tau)$, by $g=0$ on the surface $S(\tau)$, g positive in ν_0 and negative in ν_1 . The Heaviside function $H(g)$ is consequently unity in the region ν_0 and zero in ν_1 . Derivatives of H are non-zero only on the surface $S(\tau)$, and because $S(\tau)$ is convected with the flow, they are related by

$$\partial H/\partial\tau + v_i \partial H/\partial y_i = 0. \tag{2.9}$$

$\partial H/\partial y_i$ is a vector perpendicular to $S(\tau)$, positive in the direction leading from ν_1 into the exterior unbounded region ν_0 and

$$\int_\infty \frac{\partial H}{\partial y_i} K(\mathbf{y},\tau)\,\mathrm{d}^3\mathbf{y}\,\mathrm{d}\tau = \int \mathrm{d}\tau \int_{S(\tau)} n_i K(\mathbf{y},\tau)\,\mathrm{d}S(\tau), \tag{2.10}$$

for any function $K(\mathbf{y},\tau)$, where n is the normal to the surface $S(\tau)$ in the direction shown in Figure 3.1.

We only wish to use equation (2.1) to describe the flow in the region ν_0 , where H is non-zero, and so we multiply (2.1) by H . It is a straightforward matter to transfer H through the differential

operators, and to use (2.3) and (2.4) to obtain;

$$\left\{\frac{\partial^2}{\partial\tau^2}-c_0^2\frac{\partial^2}{\partial y_i^2}\right\}(H\rho')=\frac{\partial^2(HT_{ij})}{\partial y_i\partial y_j}-\frac{\partial}{\partial y_j}\left(p_{ij}\frac{\partial H}{\partial y_i}\right)+\rho_0\frac{\partial}{\partial\tau}\left(v_i\frac{\partial H}{\partial y_i}\right), \tag{2.11}$$

which is essentially equation (2.8) of Ffowcs Williams & Hawkings (1969) paper. $H\rho'$ is a function defined over all space; it is equal to the density fluctuation $\rho-\rho_0$ in v_0 and zero elsewhere.

Next we consider the fluid in the region v_1. The Navier Stokes equation (2.8) is, of course, only valid in the region exterior to the surface $\Sigma(\tau)$. We therefore introduce H_V a Heaviside function which is unity in $V(\tau)$, the region within the surface $\Sigma(\tau)$, and zero elsewhere. Then if $\Sigma(\tau)$ is impermeable

$$\partial H_V/\partial\tau+v_i\,\partial H_V/\partial y_i=0. \tag{2.12}$$

Also

$$\int_\infty(\partial H_V/\partial y_i)\,K(\boldsymbol{y},\tau)\,\mathrm{d}^3y\,\mathrm{d}\tau=\int\mathrm{d}\tau\int_{\Sigma(\tau)}l_iK(\boldsymbol{y},\tau)\,\mathrm{d}\Sigma, \tag{2.13}$$

for any function $K(\boldsymbol{y},\tau)$, where $\boldsymbol{l}$ is the normal to the surface $\Sigma(\tau)$ in the direction shown in Figure 3.1.

$\bar{H}(g)=1-H(g)$ is equal to unity in v_1, and zero in v_0. Hence $\bar{H}-H_V$ is non-zero only for points in the fluid in v_1, where (2.8) is valid. A direct repetition of the argument leading from (2.1) to (2.11), with (2.8) replacing (2.1) and $\bar{H}-H_V$ instead of H shows that

$$\left\{\frac{\mathrm{D}_1^2}{\mathrm{D}\tau^2}-c_1^2\frac{\partial^2}{\partial y_i^2}\right\}(\bar{H}-H_V)\rho_1'=\frac{\partial^2}{\partial y_i\partial y_j}\{T'_{ij}(\bar{H}-H_V)\}-\frac{\partial}{\partial y_j}\left\{p_{ij}\left(\frac{\partial\bar{H}}{\partial y_i}-\frac{\partial H_V}{\partial y_i}\right)\right\}+\rho_1\frac{\mathrm{D}_1}{\mathrm{D}\tau}\left\{v_i'\left(\frac{\partial\bar{H}}{\partial y_i}-\frac{\partial H_V}{\partial y_i}\right)\right\}. \tag{2.14}$$

We will deal exclusively with the exact viscous non-linear

equations of fluid motion described by (2.11) and (2.14). We recognize by common observation that the solution for the far-field density perturbation $H\rho'$ is limited by several constraints. Firstly, the jet flow must be driven by an externally applied force distribution acting through the surface $\Sigma(\tau)$. This force is non-zero only for a finite time, which ensures that there is no flow at infinity in any one of the four space-time coordinates. Secondly waves will tend to travel towards infinity from the neighbourhood of the surface $\Sigma(\tau)$ driving the mean flow.

We choose to work with a reciprocal Green function that is bounded at infinity

$$G^\dagger(\mathbf{y},\tau|\mathbf{x},t) = H(\mathbf{y},\tau)\, G_0^\dagger(\mathbf{y},\tau|\mathbf{x},t) + \bar{H}(\mathbf{y},\tau)\, G_1^\dagger(\mathbf{y},\tau|\mathbf{x},t)$$

and decays as τ becomes large and positive, has incoming wave behaviour outside the surface $S(\tau)$ in the variables $\mathbf{y}$ and τ, and is consistent with the equations

$$H\left\{\frac{\partial^2 G_0^\dagger}{\partial y_i^2} - \frac{1}{c_0^2}\frac{\partial^2 G_0^\dagger}{\partial \tau^2}\right\} = -H\delta(\mathbf{x}-\mathbf{y}, t-\tau) \tag{2.15}$$

and

$$\bar{H}\left\{\frac{\partial^2 G_1^\dagger}{\partial y_i^2} - \frac{1}{c_1^2}\frac{\mathrm{D}_1^2}{\mathrm{D}\tau^2} G_1^\dagger\right\} = 0\,. \tag{2.16}$$

These conditions do not uniquely define $G^\dagger$ and we will later exploit its arbitrariness.

We only require a weak form of causality; $G^\dagger \to 0$ as $\tau \to \infty$, we do not insist that $G^\dagger$ satisfies the strict causality conditions $G^\dagger = \mathrm{D}_1 G^\dagger/\mathrm{D}\tau = 0$ for $t < \tau$, that are usually imposed on a reciprocal Green function. Indeed it is well known (Jones 1973) that in certain model problems a Green function bounded at infinity is incompatible with strict causality.

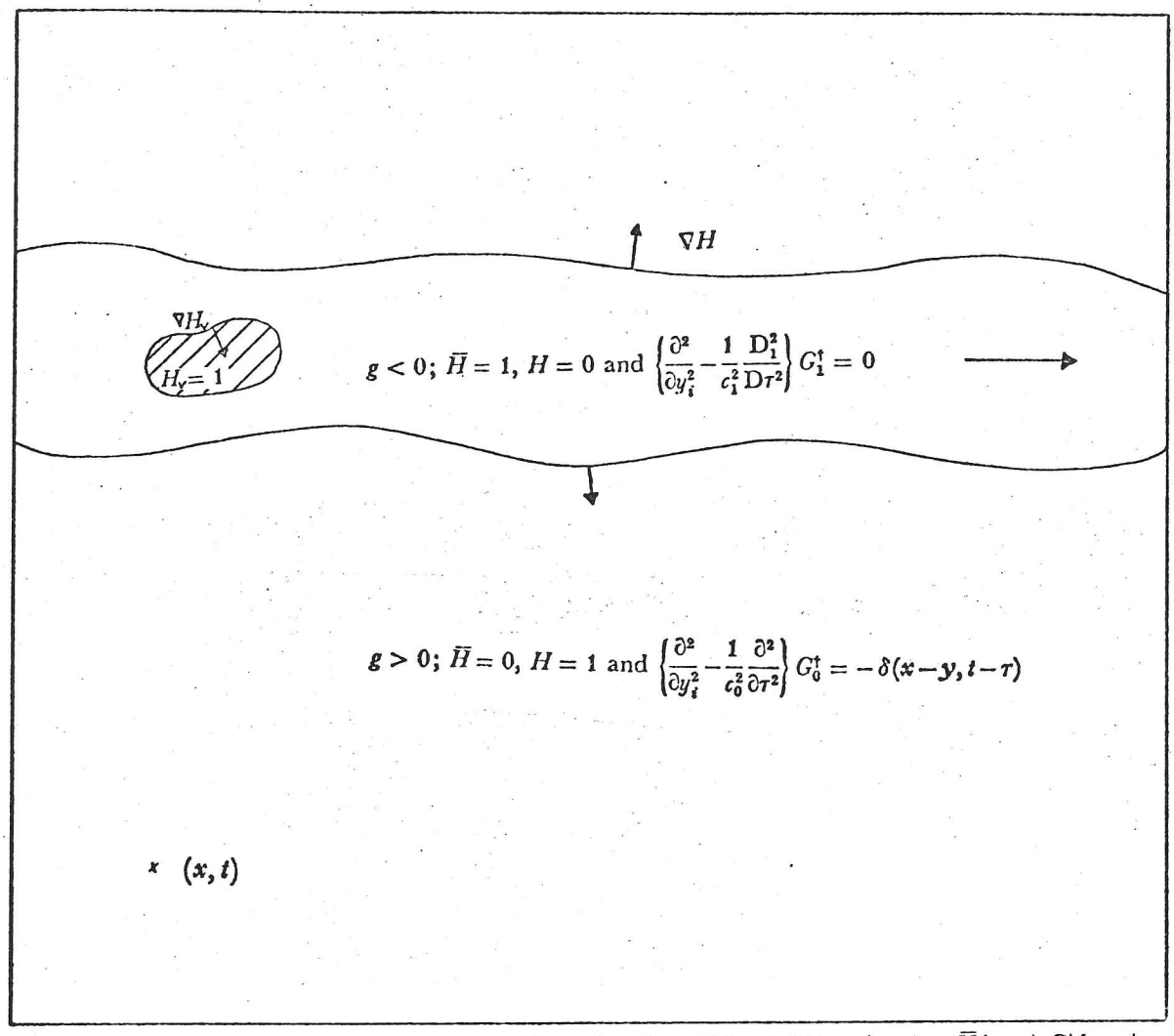

Figure 3.2 The definition of $G^\dagger(y,\tau|x,t) = H(y,\tau)\,G_0^\dagger(y,\tau|x,t) + \bar{H}(y,\tau)\,G_1^\dagger(y,\tau|x,t)$

$G^\dagger$ can be used to determine $H\rho'$

$$H\rho'(x,t) = \int_\infty \rho'(y,\tau)\,H\delta(x-y,t-\tau)\,\mathrm{d}^3y\,\mathrm{d}\tau$$

$$= -\int_\infty H\rho'(y,\tau)\left\{\frac{\partial^2 G_0^\dagger}{\partial y_i^2} - \frac{1}{c_0^2}\frac{\partial^2 G_0^\dagger}{\partial \tau^2}\right\}\mathrm{d}^3y\,\mathrm{d}\tau. \qquad (2.17)$$

This result follows from equation (2.15) and the definition of the δ-function. The integration ranges over all four dimensional (y,τ) space. For large $|y|$, ρ' is an outgoing acoustic wave, and outside the surface $S(\tau)$ $G_0^\dagger$ has incoming wave behaviour. ρ' is zero at $\tau = -\infty$, and $G_0^\dagger$ decays as $\tau \to \infty$. This ensures that when (2.17) is integrated by parts the contributions from the end-points at infinity

vanish. Hence

$$H\rho' = \int_\infty \frac{G_0^\dagger}{c_0^2}\left\{\frac{\partial^2}{\partial\tau^2} - c_0^2\frac{\partial^2}{\partial y_i^2}\right\}(H\rho')\,\mathrm{d}^3y\,\mathrm{d}\tau\ . \tag{2.18}$$

Alternatively this equation may be obtained by noting that the real density perturbation ρ' vanishes for large $(|y|, |\tau|)$.

We can use (2.11) to write

$$c_0^2 H\rho'(x,t) = \int_\infty G_0^\dagger\left\{\frac{\partial^2(HT_{ij})}{\partial y_i\,\partial y_j} - \frac{\partial}{\partial y_j}\left(p_{ij}\frac{\partial H}{\partial y_i}\right) + \rho_0\frac{\partial}{\partial\tau}\left(v_i\frac{\partial H}{\partial y_i}\right)\right\}\mathrm{d}^3y\,\mathrm{d}\tau \tag{2.19}$$

$$= \int_\infty \left\{HT_{ij}\frac{\partial^2 G_0^\dagger}{\partial y_i\,\partial y_j} + p_{ij}\frac{\partial H}{\partial y_i}\frac{\partial G_0^\dagger}{\partial y_j} - \rho_0 v_i\frac{\partial H}{\partial y_i}\frac{\partial G_0^\dagger}{\partial\tau}\right\}\mathrm{d}^3y\,\mathrm{d}\tau, \tag{2.20}$$

after partial integration.

This equation gives the density at (x,t) in terms of an integral of a Green function with 'sources'. The first term describes the sound produced by Lighthill's volume quadrupoles. An application of (2.10) shows that the last two terms are surface integrals. The strength of the surface sources is linear in the field variable. Such linear surface sources can often appear to be much more efficient generators of sound than they actually are - especially when one does not know the source strength accurately enough to account for phase cancellations (Ffowcs Williams 1974). Therefore (2.20) could lead to an incorrect estimate of the acoustic field generated by the flow. We will try to eliminate these misleading surface terms by considering the flow in the region v_1 . We multiply equation (2.16) by $(\bar{H}-H_V)\rho_1'(y,\tau)$ and integrate over all space

$$0 = \int_\infty (\bar{H}-H_V)\rho_1'\left\{\frac{\partial^2 G_1^\dagger}{\partial y_i^2} - \frac{1}{c_1^2}\frac{\mathrm{D}_1^2 G_1^\dagger}{\mathrm{D}\tau^2}\right\}\mathrm{d}^3y\,\mathrm{d}\tau. \tag{2.21}$$

For the moment we will restrict our attention to the case where $\bar{H}G^\dagger$ and

its derivatives decay algebraically at infinity. The more general situation where resonances are excited and Green's function is only bounded within the jet will be considered later. In the case dealt with here the differential operators can be transferred onto the field quantity $(\bar{H}-H_V)\rho_1'$ by integration by parts.

$$0=\int_\infty G_1^\dagger\left\{\frac{\partial^2}{\partial y_i^2}-\frac{1}{c_1^2}\frac{\mathrm{D}_1^2}{\mathrm{D}\tau^2}\right\}(\bar{H}-H_V)\rho_1'\,\mathrm{d}^3y\,\mathrm{d}\tau. \tag{2.22}$$

We substitute (2.14) into (2.22) and rearrange by partial integration; the condition that $\bar{H}G^\dagger$ vanishes as any one of the variables tends to $\mp$ infinity again ensures that end-point contributions are zero.

$$0=\int_\infty\left\{(\bar{H}-H_V)\,T_{ij}'\frac{\partial^2 G_1^\dagger}{\partial y_i\partial y_j}+p_{ij}\frac{\partial G_1^\dagger}{\partial y_j}\left(\frac{\partial\bar{H}}{\partial y_i}-\frac{\partial H_V}{\partial y_i}\right)-\rho_1\frac{\mathrm{D}_1 G_1^\dagger}{\mathrm{D}\tau}v_i'\left(\frac{\partial\bar{H}}{\partial y_i}-\frac{\partial H_V}{\partial y_i}\right)\right\}\mathrm{d}^3y\,\mathrm{d}\tau. \tag{2.23}$$

This equation is multiplied by $\beta(x,t)$, an arbitrary function of (x,t) and the result added to (2.20) to obtain the exact equation

$$c_0^2H\rho'(x,t)=\int_\infty\left\{HT_{ij}\frac{\partial^2 G_0^\dagger}{\partial y_i\partial y_j}+\beta(\bar{H}-H_V)\,T_{ij}'\frac{\partial^2 G_1^\dagger}{\partial y_i\partial y_j}-\beta p_{ij}\frac{\partial H_V}{\partial y_i}\frac{\partial G_1^\dagger}{\partial y_j}+\beta\rho_1\frac{\mathrm{D}_1 G_1^\dagger}{\mathrm{D}\tau}v_i'\frac{\partial H_V}{\partial y_i}\right\}\mathrm{d}^3y\,\mathrm{d}\tau+\Phi(x,t), \tag{2.24}$$

where

$$\Phi(x,t)=\int_\infty\left\{\frac{\partial\bar{H}}{\partial y_i}p_{ij}\left(\beta\frac{\partial G_1^\dagger}{\partial y_j}-\frac{\partial G_0^\dagger}{\partial y_j}\right)+\rho_0 v_i\frac{\partial\bar{H}}{\partial y_i}\frac{\partial G_0^\dagger}{\partial\tau}-\beta\rho_1 v_i'\frac{\partial\bar{H}}{\partial y_i}\frac{\mathrm{D}_1 G_1^\dagger}{\mathrm{D}\tau}\right\}\mathrm{d}^3y\,\mathrm{d}\tau. \tag{2.25}$$

The first two terms in equation (2.24) describe sound generation by volume quadrupole sources, the third and fourth terms the field generated by the force and velocity distributions on $\Sigma(\tau)$. $\Phi(x,t)$ represents linear source terms on the control surface $S(\tau)$. The presence of these linear terms prevents (2.24) from giving a useful estimate of the acoustic field. We now exploit the arbitrariness in $G^\dagger$ in order to eliminate these terms. $G^\dagger$ is not completely specified until we impose two jump conditions on $S(\tau)$.

From equation (2.9) $v_i' \partial \bar{H}/\partial y_i$ may be rewritten as $-D_1 \bar{H}/D\tau$ and then the last term in (2.25) integrated by parts to obtain

$$-\beta\rho_1 \int_\infty v_i' \frac{\partial \bar{H}}{\partial y_i} \frac{D_1 G_1^\dagger}{D\tau} d^3y\, d\tau = -\beta\rho_1 \int_\infty \bar{H} \frac{D_j^2 G_1^\dagger}{D\tau^2} d^3y\, d\tau. \tag{2.26}$$

We define a function $\Gamma(y,\tau)$ in ν_1 by

$$\bar{H}\partial^2\Gamma/\partial\tau^2 = \bar{H} D_1^2 G_1^\dagger/D\tau^2, \quad \bar{H}\,\partial\Gamma/\partial\tau \to 0 \quad \text{as} \quad |\tau| \to \infty . \tag{2.27}$$

Hence

$$-\beta\rho_1 \int_\infty \bar{H} \frac{D_1^2 G_1^\dagger}{D\tau^2} d^3y\, d\tau = -\beta\rho_1 \int_\infty \bar{H} \frac{\partial^2 \Gamma}{\partial\tau^2} d^3y\, d\tau$$

$$= -\beta\rho_1 \int_\infty v_i \frac{\partial \bar{H}}{\partial y_i} \frac{\partial \Gamma}{\partial \tau} d^3y\, d\tau. \tag{2.28}$$

When this expression is substituted into Φ, we obtain

$$\Phi(x,t) = \int_\infty \frac{\partial \bar{H}}{\partial y_i} \left\{ (p-p_0) \left(\beta \frac{\partial G_1^\dagger}{\partial y_i} - \frac{\partial G_0^\dagger}{\partial y_i} \right) - e_{ij} \left(\beta \frac{\partial G_1^\dagger}{\partial y_j} - \frac{\partial G_0^\dagger}{\partial y_j} \right) + v_i \left(\rho_0 \frac{\partial G_0^\dagger}{\partial \tau} - \beta\rho_1 \frac{\partial \Gamma}{\partial \tau} \right) \right\} d^3y\, d\tau$$

$$= \int_{-\infty}^{\infty} \int_{S(\tau)} \left\{ (p-p_0) \left(\frac{\partial G_0^\dagger}{\partial n} - \beta \frac{\partial G_1^\dagger}{\partial n} \right) + n_i e_{ij} \left(\beta \frac{\partial G_1^\dagger}{\partial y_j} - \frac{\partial G_0^\dagger}{\partial y_j} \right) - n_i v_i \left(\rho_0 \frac{\partial G_0^\dagger}{\partial \tau} - \beta\rho_1 \frac{\partial \Gamma}{\partial \tau} \right) \right\} dS\, d\tau \tag{2.29}$$

$G^\dagger$ and Γ are uniquely determined once we specify two jump conditions across $S(\tau)$. We want to choose conditions that minimize the misleading linear source term Φ, and therefore impose

$$\rho_0 \partial G_0^\dagger/\partial\tau = \beta\rho_1 \partial\Gamma/\partial\tau \quad \text{and} \quad \partial G_0^\dagger/\partial n = \beta\, \partial G_1^\dagger/\partial n, \tag{2.30}$$

for y on all parts of $S(\tau)$ where $v_i n_i \neq 0$, $p_{ij} \neq 0$. Then only the viscous term remains in Φ and

$$c_0^2 H\rho'(x,t) = \int_{-\infty}^{\infty}\int_{\nu_0(\tau)} T_{ij}\frac{\partial^2 G_0^\dagger}{\partial y_i \partial y_j}\,\mathrm{d}^3y\,\mathrm{d}\tau + \beta\int_{-\infty}^{\infty}\int_{\nu_1(\tau)-V(\tau)} T'_{ij}\frac{\partial^2 G_1^\dagger}{\partial y_i \partial y_j}\,\mathrm{d}^3y\,\mathrm{d}\tau$$

$$+\beta\int_{-\infty}^{\infty}\int_{\Sigma(\tau)} l_i\left(\rho_1 v'_i\frac{\mathrm{D}_1 G_1^\dagger}{\mathrm{D}\tau} - p_{ij}\frac{\partial G_1^\dagger}{\partial y_j}\right)\mathrm{d}\Sigma\,\mathrm{d}\tau$$

$$-\int_{-\infty}^{\infty}\int_{S(\tau)} n_i e_{ij}\frac{\partial}{\partial y_j}(G_0^\dagger - \beta G_1^\dagger)\,\mathrm{d}S\,\mathrm{d}\tau. \qquad (2.31)$$

This equation is exact.

So far it has been assumed that all the external driving surfaces $\Sigma(\tau)$ are in ν_1, but this expression can easily be modified to include the effect of surfaces $\Sigma^\dagger(\tau)$ in ν_0 (provided none of the surfaces intersect $S(\tau)$) by the addition of the term,

$$\int_{-\infty}^{\infty}\int_{\Sigma^\dagger(\tau)} l_i\left(\rho_0 v_i\frac{\partial G_0^\dagger}{\partial\tau} - p_{ij}\frac{\partial G_0^\dagger}{\partial y_j}\right)\mathrm{d}\Sigma^\dagger\mathrm{d}\tau.$$

We have obtained this formulation of the aerodynamic sound problem by embedding the sound sources in the moving fluid to eliminate an extensively distributed linear source within the jet, while at the same time using a particular Green function to prevent the occurrence of any confusing linear surface sources. It applies to any real flow. When $U_1 = 0$, $\beta = 1$, $\rho_1 = \rho_0$ and $c_1 = c_0$, equation (2.31) reduces to the Ffowcs Williams & Hawkings (1969) statement of Lighthill's aerodynamic sound theory. But in the general case the first term in (2.31) represents the sound generated by the usual Lighthill quadrupole source, T_{ij}, in the exterior region ν_0, while the second term represents the generation of sound by a stress tensor based on relative velocity and density in the interior region ν_1. The third term describes the sound produced by the action of the surface $\Sigma(\tau)$ and the last represents the sound generation by tangential viscous stresses acting across the surface $S(\tau)$. At the high Reynolds numbers of interest in

aerodynamic sound problems the latter term is negligible in comparison with the remaining inertial terms, and we have succeeded in eliminating all significant linear surface sources; a requisite for obtaining a good estimate of the sound field.

In establishing the representation (2.31), we have assumed that the influence of a point source at (x,t) does not extend to infinity; we have considered $G^\dagger$ for which $\bar{H}G^\dagger$ decays algebraically for large $|y,\tau|$. This assumption will not be true whenever the reciprocal source at (x,t) can trigger a neutrally stable free mode of the vortex sheet determining $G^\dagger$. Waves can then propagate along the vortex sheet without a fast decay, and even at infinity $\bar{H}G^\dagger$ will not be negligible. We can easily extend the analysis to deal with such cases. The details are given in Appendix 3.A. In fact the only effect of these modes is to ensure that the vortex sheet sources vanish at infinity.

We find

$$c_0^2 H\rho'(x,t) = \iint \left\{ HT_{ij}\frac{\partial^2 G_0^\dagger}{\partial y_i \partial y_j} + \beta\left((\bar{H}-H_V)\,T'_{ij} - (\bar{H}_0 - H_{V0})(\rho_0 U_1^2 \delta_{i1}\delta_{j1} - c_1^2(\rho_0-\rho_1)\,\delta_{ij})\right)\frac{\partial^2 G_1^\dagger}{\partial y_i \partial y_j}\right\} \mathrm{d}^3y\,\mathrm{d}\tau$$

$$+ \iint \beta\left\{\rho_1\left(U_1\frac{\partial H_{V0}}{\partial y_1} - \frac{\mathrm{D}_1 H_V}{\mathrm{D}\tau}\right)\frac{\mathrm{D}_1 G_1^\dagger}{\mathrm{D}\tau} - \frac{\partial H_V}{\partial y_i}p_{ij}\frac{\partial G_1^\dagger}{\partial y_j}\right\} \mathrm{d}^3y\,\mathrm{d}\tau$$

$$- \int_{-\infty}^{\infty}\int_{S(\tau)} n_i\, e_{ij}\frac{\partial}{\partial y_j}(G_0^\dagger - \beta G_1^\dagger)\,\mathrm{d}S\,\mathrm{d}\tau, \qquad (2.32)$$

where $\bar{H}_0$ is the Heaviside function which is unity for points within $\nu_1^{(0)}$, the region enclosed by the position of the fluid surface S at $\tau = -\infty$, and zero elsewhere. Similarly H_{V0} is unity within the initial position of the surface $\Sigma(\tau)$. The integrand decays as any one of the variables tends to infinity,

$$G^\dagger \to 0 \quad \text{as} \quad \tau \to \infty,$$

and

$$(\bar{H}-H_V)\,T'_{ij}\to(\bar{H}_0-H_{V0})\,(\rho_0 U_1^2\delta_{i1}\delta_{j1}-c_1^2(\rho_0-\rho_1)\,\delta_{ij}),$$

$$\frac{\mathrm{D}_1 H_V}{\mathrm{D}\tau}\to U_1\frac{\partial H_{V0}}{\partial y_1}\quad\text{as}\quad |\boldsymbol{y}|,\,-\tau\to\infty,$$

because initially the fluid is at rest and unheated, and far from the sources there is no flow.

When $G^\dagger$ decays at infinity (2.32) reduces to the previous representation (2.31).

The reciprocal Green function $G^\dagger$ which appears in this equation is the incoming wave solution to equations (2.15) and (2.16), that satisfies the two jump conditions (2.30) across $S(\tau)$, vanishes as $\tau\to\infty$, and is bounded within ν_1 as $|\boldsymbol{y}|,-\tau\to\infty$.

The function $\beta(\boldsymbol{x},t)$ is arbitrary, but it is easy to see that the density fluctuation described by (2.32) does not depend on the choice of β. Since, if G^* is the solution to the boundary value problem with $\beta=1$, and $G^\dagger$ denotes the solution for any other value of β, it follows from equations (2.15) and (2.30) that these solutions must be related by

$$G_0^\dagger = G_0^*\quad\text{for}\quad \boldsymbol{y}\text{ in }\nu_0,$$

$$\beta G_1^\dagger = G_1^*\quad\text{for}\quad \boldsymbol{y}\text{ in }\nu_1.$$

Hence $G_0^\dagger$ and $\beta G_1^\dagger$ are invariant under the choice of β. These are the functions that appear in equation (2.32), and therefore $H\rho'(\boldsymbol{x},t)$ must be independent of β. We have only introduced this function to facilitate the interpretation of the jump conditions.

The sound generated by the surface distributions that excite the flow is usually quite distinct from the jet noise problem associated with the turbulence. At this stage we restrict ourselves to the problem

of sound generation by free turbulence and discard the integrals over the surface $\Sigma(\tau)$. By doing this, for a jet engine driven flow for example, all engine noise and any interaction of the field with diffracting surfaces is lost, and (2.32) reduces to a description of the sound produced by turbulence in the vicinity of a substantial region of uniformly moving fluid. At a sufficiently high Reynolds number all the surface terms have been eliminated and the aerodynamic sound equation becomes

$$c_0^2 H\rho'(x,t) = \int_{-\infty}^{\infty}\int_{\nu_0(\tau)} T_{ij}\frac{\partial^2 G_0^\dagger}{\partial y_i\,\partial y_j}\,\mathrm{d}^3y\,\mathrm{d}\tau + \beta\int_{-\infty}^{\infty}\int_{\nu_1(\tau)} T'_{ij}\frac{\partial^2 G_1^\dagger}{\partial y_i\,\partial y_j}\,\mathrm{d}^3y\,\mathrm{d}\tau$$

$$-\beta\int_{-\infty}^{\infty}\int_{\nu_1^{(0)}}\{\rho_0 U_1^2\delta_{i1}\delta_{j1} - c_1^2(\rho_0-\rho_1)\,\delta_{ij}\}\frac{\partial^2 G_1^\dagger}{\partial y_i\,\partial y_j}\,\mathrm{d}^3y\,\mathrm{d}\tau. \qquad (2.33)$$

$\nu_0(\tau)$ and $\nu_1(\tau)$ are material volumes consisting of the same fluid particles. In terms of the Eulerian coordinates y , $\nu_0(\tau)$ and $\nu_1(\tau)$ are changing functions of time. However they are fixed regions when written in terms of Lagrangian coordinates η , where η denotes a particular fluid element. We therefore choose to express the first two integrals in terms of these material coordinates. The Jacobian of the transformation from Eulerian to Lagrangian coordinates is ρ^*/ρ , ρ^* being the density of the fluid particle identified by η at the time when the Lagrangian and Eulerian coordinates coincide, i.e. at the time when $\eta = y$.

Our description of the induced field is then provided by the Lagrangian form of equation (2.33)

$$c_0^2 H\rho'(x,t) = \int_{-\infty}^{\infty}\int_{\nu_0} \rho^*(\eta)\left\{\frac{T_{ij}}{\rho}\right\}\frac{\partial^2 G_0^\dagger}{\partial y_i\,\partial y_j}\,\mathrm{d}^3\eta\,\mathrm{d}\tau + \beta\int_{-\infty}^{\infty}\int_{\nu_1}\rho^*(\eta)\left\{\frac{T'_{ij}}{\rho}\right\}\frac{\partial^2 G_1^\dagger}{\partial y_i\,\partial y_j}\,\mathrm{d}^3\eta\,\mathrm{d}\tau$$

$$-\beta\int_{-\infty}^{\infty}\int_{\nu_1^{(0)}}\{\rho_0 U_1^2\delta_{i1}\delta_{j1} - c_1^2(\rho_0-\rho_1)\,\delta_{ij}\}\frac{\partial^2 G_1^\dagger}{\partial y_i\,\partial y_j}\,\mathrm{d}^3y\,\mathrm{d}\tau. \qquad (2.34)$$

This is the sound generated by a moving distribution of

quadrupoles of strength density per unit mass T_{ij}/ρ in ν_0 , T'_{ij}/ρ in ν_1 .. The use of Lagrangian coordinates emphasizes the importance of the kinematics of the flow in determining the source terms because now for small density fluctuations the main source term is $v_i v_j$ rather than $\rho v_i v_j$ in ν_0 , $v'_i v'_j$ instead of $\rho v'_i v'_j$ in ν_1 , and the source strength is independent of the fluid density.

We have developed a representation for the acoustic field in terms of 'source terms' and the reciprocal Green function. It is possible to estimate the source terms but it would be a formidable task to calculate $G^\dagger$, because the jump conditions on $G^\dagger$ are imposed on a surface $S(\tau)$ which moves with the actual flow. For real turbulent flows such a surface will become highly irregular. Indeed it is even difficult at this stage to arrive at a physical interpretation of $G^\dagger$. Fortunately for the nearly parallel flows of technological interest, it is possible to construct the reciprocal Green function and we will now demonstrate that it is Green's function appropriate to an instability-free (and therefore only weakly causal) vortex sheet modelling of the flow.

3.3 The vortex sheet model

For most real flows the turbulent non-linear fluid motion is concentrated within the high mean velocity region. It is appropriate to choose $\nu_1(\tau)$ so that it coincides with this source region, and then the only disturbance to the flow in ν_0 is caused by acoustic waves propagating through it, and so the fluctuations are linear. This is equivalent to choosing the control surface $S(\tau)$ sufficiently far away from the jet so that it lies in the acoustic field. In this case, $T_{ij} = 0$ in ν_0 and equation (2.34) simplifies;

$$c_0^2 H\rho'(x,t) = \beta \int d\tau \left\{ \int_{\nu_1} \frac{\rho^* T'_{ij}}{\rho} \frac{\partial^2 G_1^\dagger}{\partial y_i \partial y_j} d^3\eta - \int_{\nu_1(\tau)} (\rho_0 U_1^2 \delta_{i1}\delta_{j1} - c_1^2(\rho_0 - \rho_1)\delta_{ij}) \frac{\partial^2 G_1^\dagger}{\partial y_i \partial y_j} d^3 y \right\}. \quad (3.1)$$

The flow parameters on the surface $S(\tau)$ are small, and also $S(\tau)$ is only linearly disturbed from its initial position S_0. We can therefore linearize the boundary terms in equation (2.29) by transferring them from $S(\tau)$ to the fixed surface S_0. The problem of determining the Green function is now more tractable, since $G^\dagger$ can be defined by jump conditions across a fixed surface;

$$\rho_0 \partial G_0^\dagger/\partial\tau = \beta\rho_1 \partial\Gamma/\partial\tau \quad \text{and} \quad \partial G_0^\dagger/\partial n = \beta\, \partial G_1^\dagger/\partial n \quad \text{on} \quad S_0. \tag{3.2}$$

We can use (2.27) to eliminate Γ from these equations and obtain

$$\rho_0 \frac{\partial^2 G_0^\dagger}{\partial\tau^2} = \beta\rho_1 \frac{\mathrm{D}_1^2 G_1^\dagger}{\mathrm{D}\tau^2} \quad \text{and} \quad \frac{\partial G_0}{\partial n} = \beta \frac{\partial G_1^\dagger}{\partial n} \quad \text{on} \quad S_0. \tag{3.3}$$

We now consider a particular geometry and take S_0, the initial position of S, to be a cylindrical surface doubly infinite in the y_1-direction. Then in the problem for $G^\dagger$ there is no characteristic scale for either the time or the distance in the y_1-direction. Hence $G_0^\dagger$ and $G_1^\dagger$ can depend on t, τ, x_1, and y_1 only in the combination $t-\tau$, and x_1-y_1, so that

$$\frac{\partial G_0^\dagger}{\partial\tau} = -\frac{\partial G_0^\dagger}{\partial t}, \quad \frac{\mathrm{D}_1 G_0^\dagger}{\mathrm{D}\tau} = -\left\{\frac{\partial}{\partial t} + U_1 \frac{\partial}{\partial x_1}\right\} G_0^\dagger, \tag{3.4}$$

and the derivatives of $G_1^\dagger$ satisfy the same relationship.

We restrict our attention to the case where the observation point $\boldsymbol{x}$ is in the far-field. Then because $G^\dagger$ represents an incoming wave in $(\boldsymbol{y},\tau)$, it has the form of an outgoing wave in the variables $(\boldsymbol{x},t)$ and

$$\frac{\partial G^\dagger}{\partial x_1} = -\frac{1}{c_0}\frac{\partial G^\dagger}{\partial\tau}\frac{\partial|\boldsymbol{x}|}{\partial x_1} = -\frac{x_1}{|\boldsymbol{x}|\, c_0}\frac{\partial G^\dagger}{\partial t}. \tag{3.5}$$

Hence

$$\frac{\mathrm{D}_1 G_0^\dagger}{\mathrm{D}\tau} = -(1-M_r)\frac{\partial G_0^\dagger}{\partial t} = (1-M_r)\frac{\partial G_0^\dagger}{\partial\tau},$$

and similarly

$$\frac{D_1 G_1^\dagger}{D\tau} = (1 - M_r)\frac{\partial G_1^\dagger}{\partial \tau},$$

where $M_r = M\, x_1/|x|$, and $M \equiv U_1/c_0$ is the Mach number of the mean flow based on U_1, the mean velocity in ν_1, and c_0, the sound speed in ν_0.

By using these relations, the boundary conditions (3.3) can be put in the form

$$G_0^\dagger = BG_1^\dagger, \qquad \rho_1 \frac{D_1^2}{D\tau^2}\frac{\partial G_0^\dagger}{\partial n} = \rho_0 B \frac{\partial^2}{\partial \tau^2}\frac{\partial G_1^\dagger}{\partial n}, \tag{3.6}$$

with $B = \beta(1 - M_r)^2 \rho_1/\rho_0$. We have, however, shown that the final result for the acoustic field is independent of our choice of β, and so we can put

$$\beta = \frac{\rho_0}{\rho_1(1 - M_r)^2}, \qquad \text{which means } B = 1. \tag{3.7}$$

Now the jump conditions (3.6) are more familiar. They are in fact the usual acoustic boundary conditions

$$G_0^\dagger = G_1^\dagger, \qquad \rho_1 \frac{D_1^2}{D\tau^2}\frac{\partial G_0^\dagger}{\partial n} = \rho_0 \frac{\partial^2}{\partial \tau^2}\frac{\partial G_1^\dagger}{\partial n}, \tag{3.8}$$

describing continuity of pressure and particle displacement across a linearly disturbed vortex sheet. These conditions are obtained because we chose $S(\tau)$ to be a material surface. A fixed control surface will lead to different jump conditions with no obvious physical interpretation. The analogy between a real jet flow and sources adjacent to a vortex sheet requires that the equivalent sources are attached to the fluid particles and move with the flow.

The reciprocal Green function $G^\dagger(y, \tau | x, t)$ can be related to the direct Green function $G(x, t | y, \tau)$, where G represents the field produced by a source within the vortex sheet at a point (y, τ). G is

a bounded, weakly causal, outgoing wave solution to the equations

$$\left\{\frac{\partial^2}{\partial x_i^2}-\frac{1}{c_0^2}\frac{\partial^2}{\partial t^2}\right\}G(x,t|y,\tau)=0 \quad \text{if} \quad x \text{ is in } \nu_0^{(0)} \text{ and } y \text{ in } \nu_1^{(0)} \tag{3.9}$$

$$\left\{\frac{\partial^2}{\partial x_i^2}-\frac{1}{c_1^2}\frac{D_1^2}{Dt^2}\right\}G(x,t|y,\tau)=-\delta(x-y,t-\tau) \quad \text{if} \quad x \text{ and } y \text{ are in } \nu_1^{(0)}. \tag{3.10}$$

In these equations, $\frac{D_1}{Dt}\equiv\frac{\partial}{\partial t}+U_1\frac{\partial}{\partial x_1}$, and $\nu_0^{(0)}$ and $\nu_j^{(0)}$ are the fixed regions separated by the cylindrical surface S_0. G satisfies vortex sheet jump conditions across S_0;

$$G_0=G_1 \qquad \text{and} \qquad \rho_1\frac{D_1^2}{Dt^2}\frac{\partial G_0}{\partial n}=\rho_0\frac{\partial^2}{\partial t^2}\frac{\partial G_1}{\partial n}, \tag{3.11}$$

where G_0 denotes the limit of G as x tends towards S_0 through $\nu_0^{(0)}$, and G_1 the limit of G as x approaches S_0 from $\nu_1^{(0)}$.

G is simply the sound field produced by an acoustic point source located in an infinite 'instability-free' cylindrical jet, with a 'top-hat' velocity profile. It is shown in Appendix 3.B that it is related to the reciprocal Green function $G^\dagger$ by

$$G(x,t|y,\tau)=\beta G_1^\dagger(y,\tau|x,t), \tag{3.12}$$

for x in the radiation field in $\nu_0^{(0)}$ and y in $\nu_1^{(0)}$.

The appearance of this weakly causal Green function in (3.1) means that the information about the turbulence reaches the far-field sooner than it would if it just propagated from the turbulent sources with a uniform speed c_0. We believe that this is reasonable. The representation (3.1) describes the way in which the sound field depends on the turbulence, but it is not the simple relationship between the observed sound and its 'source'. In an unstable jet sound waves can cause turbulence, and then later that turbulence can become a source of sound. Equation (3.1) must therefore describe the more complicated

interdependence of the turbulence and sound field. It is difficult to see how the strictly causal Green function could be used in such a representation because of problems associated with the convergence of the integrals.

3.4 The circular cylindrical jet

In order to illustrate the vortex sheet analogy we now consider a simple geometry for which it is possible to obtain $G^{\dagger}$ explicitly. We investigate a turbulent round jet of radius a, with mean flow U_1 in the 1-direction, emitting sound into a linearly disturbed fluid. It is convenient to introduce cylindrical coordinates, and we write

$$\boldsymbol{x} = (R, \Phi, x_1), \quad \boldsymbol{y} = (\sigma, \phi, y_1).$$

Then from (3.1) and (3.7)

$$c_0^2 H\rho'(\boldsymbol{x},t) = \frac{\rho_0}{\rho_1(1-M_r)^2}\int \mathrm{d}\tau\left\{\int_{v_1} \frac{\rho^* T'_{ij}}{\rho}\frac{\partial^2 G_1^{\dagger}}{\partial y_i \partial y_j}\mathrm{d}^3\eta - \int_{v_1(a)} (\rho_0 U_1^2 \delta_{i1}\delta_{j1} - c_1^2(\rho_0-\rho_1)\delta_{ij})\frac{\partial^2 G_1^{\dagger}}{\partial y_i \partial y_j}\mathrm{d}^3 y\right\}, \tag{4.1}$$

where

$$\left\{\frac{\partial^2}{\partial y_i^2} - \frac{1}{c_0^2}\frac{\partial^2}{\partial \tau^2}\right\} G_0^{\dagger}(\boldsymbol{y},\tau|\boldsymbol{x},t) = -\delta(\boldsymbol{x}-\boldsymbol{y}, t-\tau) \quad \text{for} \quad \sigma > a,$$

$$\left\{\frac{\partial^2}{\partial y_i^2} - \frac{1}{c_1^2}\frac{\mathrm{D}_1^2}{\mathrm{D}\tau^2}\right\} G_1^{\dagger}(\boldsymbol{y},\tau|\boldsymbol{x},t) = 0 \quad \text{for} \quad \sigma < a, \tag{4.2}$$

together with the vortex sheet jump conditions

$$G_0^{\dagger} = G_1^{\dagger}, \quad \rho_1 \frac{\mathrm{D}_1^2}{\mathrm{D}\tau^2}\frac{\partial G_0^{\dagger}}{\partial \sigma} = \rho_0 \frac{\partial^2}{\partial \tau^2}\frac{\partial G_1^{\dagger}}{\partial \sigma} \quad \text{on} \quad \sigma = a. \tag{4.3}$$

However $G^{\dagger}$ differs from the vortex sheet Green function found by Morgan (1975) in that it is devoid of instabilities because

$$\bar{H}G^{\dagger} \sim O(1) \quad \text{as} \quad |\boldsymbol{y},\tau| \to \infty.$$

This system of equations can be solved most simply by taking Fourier transforms in y_1, τ and ϕ. (Actually the angular dependence is expanded as a Fourier series.) If we denote the transform of $G_1^\dagger$ by $\bar{G}_1$ then

$$\bar{G}_1(\sigma, k, n, \omega|x, t) = \int_{\phi=0}^{2\pi}\int_{y_1=-\infty}^{\infty}\int_{\tau=-\infty}^{\infty} G_1^\dagger(y, \tau|x, t)\exp\{-i(ky_1+\omega\tau+n\phi)\}\,dy_1\,d\tau\,d\phi$$

and

$$G_1^\dagger(\mathbf{y}, \tau|x, t) = \frac{1}{(2\pi)^3}\int_{-\infty}^{\infty}\int_{-\infty}^{\infty}\sum_{n=-\infty}^{\infty}\bar{G}_1(\sigma, k, n, \omega|x, t)\exp\{i(ky_1+\omega\tau+n\phi)\}\,dk\,d\omega.$$

$\bar{G}_0(\sigma, k, n, \omega|x, t)$ satisfies

$$\frac{1}{\sigma}\frac{d}{d\sigma}\left(\sigma\frac{d\bar{G}_0}{d\sigma}\right)+\left(\frac{\omega^2}{c_0^2}-k^2-\frac{n^2}{\sigma^2}\right)\bar{G}_0 = -\frac{\delta(\sigma-R)}{\sigma}\exp\{-i(kx_1+\omega t+n\Phi)\}, \tag{4.4}$$

which has the solution

$$\bar{G}_0 = -\frac{\exp\{-i(kx_1+\omega t+n\Phi)\}}{RW(f_1, f_2)}\begin{cases} f_1(\sigma)f_2(R) & \text{for } \sigma \leqslant R \\ f_1(R)f_2(\sigma) & \text{for } \sigma \geqslant R. \end{cases} \tag{4.5}$$

f_1 and f_2 are two Bessel functions chosen to satisfy the boundary conditions and W is their Wronskian evaluated at R (see for example Morse & Feshbach 1953, Page 826). The general form of f_1 is

$f_1(\sigma) = J_n(\gamma_0\sigma) + D_n H_n^{(1)}(\gamma_0\sigma)$, where $\gamma_0^2 = \omega^2/c_0^2 - k^2$ and D_n is to be determined from the jump conditions on $\sigma = a$. $G_0^\dagger$ behaves like an incoming wave at infinity in the (y, τ) coordinates so that

$f_2(\sigma) = H_n^{(1)}(\gamma_0\sigma)$, if the root of γ_0 is chosen so that when real γ_0 has the sign of ω. When γ_0 is complex its imaginary part must be positive to ensure that $G_0^\dagger$ is bounded at infinity. Both these conditions are satisfied by the Riemann sheet Imaginary $\gamma_0 > 0$ with a branch cut along Imaginary $\gamma_0 = 0$ as shown in Figure 3.3.

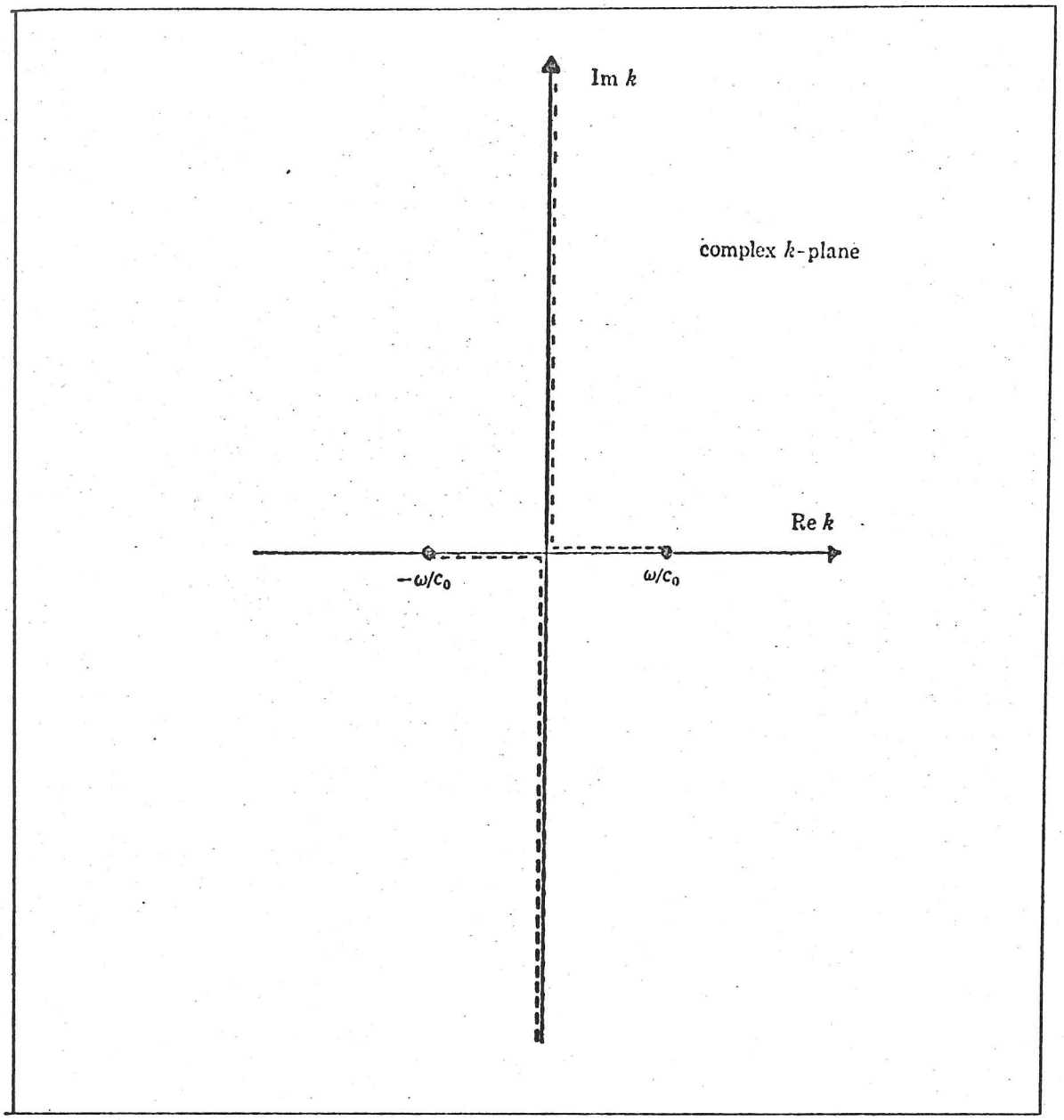

Figure 3.3 The position of the branch cuts

We note that $W(f_1,f_2) = W(J_n(\gamma_0 R), H_n^{(1)}(\gamma_0 R))$ is $2i/\pi R$.

The Fourier transform of the second equation in (4.2) gives

$$\frac{1}{\sigma}\frac{d}{d\sigma}\left(\sigma\frac{d\bar{G}_1}{d\sigma}\right)+\left(\frac{(\omega+U_1k)^2}{c_1^2}-k^2-\frac{n^2}{\sigma^2}\right)\bar{G}_1 = 0 \quad \text{in} \quad \sigma < a. \tag{4.6}$$

$\bar{G}_1$ must be finite at $\sigma = 0$, and hence

$$\bar{G}_1(\sigma,k,n,\omega|x,t) = E_n J_n(\gamma\sigma), \quad \text{where} \quad \gamma = \{(\omega+U_1k)^2/c_1^2-k^2\}^{\frac{1}{2}}.$$

E_n can be determined by applying the jump conditions (4.3) at $\sigma = a$ to obtain

$$\bar{G}_1(\sigma, k, n, \omega|x, t) = \frac{\rho_1(\omega + U_1 k)^2 H_n^{(1)}(\gamma_0 R)\, J_n(\gamma\sigma)}{F_n(\omega, k)} \exp\{-\mathrm{i}(kx_1 + \omega t + n\Phi)\}, \tag{4.7}$$

where $F_n(\omega, k) = a\{\rho_0 \omega^2 \gamma J_n'(\gamma a)\, H_n^{(1)}(\gamma_0 a) - \rho_1(\omega + U_1 k)^2 \gamma_0 J_n(\gamma a)\, H_n^{(1)\prime}(\gamma_0 a)\}$,

and the prime denotes differentiation with respect to the argument.

Inversion of the Fourier transform gives

$$G_1^{\dagger}(y, \tau|x, t) = \frac{1}{(2\pi)^3} \iint \sum_{n=-\infty}^{\infty} \frac{\rho_1(\omega + U_1 k)^2 H_n^{(1)}(\gamma_0 R) J_n(\gamma\sigma)}{F_n(\omega, k)} \exp \mathrm{i}\{k(y_1 - x_1) + \omega(\tau - t) + n(\phi - \Phi)\}\, \mathrm{d}k\, \mathrm{d}\omega, \tag{4.8}$$

where the ω-integral is to be taken along the weakly causal contour, which lies above the poles and branch cuts on the real ω-axis in order to satisfy the condition $G^{\dagger} \to 0$ as $\tau \to \infty$.

We now introduce θ, the angle between the distant observation point and the direction of flow, defined by $R = |x| \sin\theta$ and $x_1 = |x| \cos\theta$. Then $H_n^{(1)}(\gamma_0 R) = H_n^{(1)}(\gamma_0 \sin\theta |x|)$ and for x in the far-field we can expand $H_n^{(1)}$ by its asymptotic form for large arguments and write

$$H_n^{(1)}(\gamma_0 R) \sim \left(\frac{2}{\pi\gamma_0 \sin\theta |x|}\right)^{\frac{1}{2}} \exp \mathrm{i}\{\gamma_0 \sin\theta |x| - \tfrac{1}{2}n\pi - \tfrac{1}{4}\pi\} \quad \text{if} \quad \gamma_0 \sin\theta \neq 0.$$

Hence

$$G_1^{\dagger}(y, \tau|x, t) \sim \frac{1}{(2\pi)^3} \int_{-\infty}^{\infty} \sum_{n=-\infty}^{\infty} \exp \mathrm{i}\{\omega(\tau - t) + n(\phi - \Phi - \tfrac{1}{2}\pi) - \tfrac{1}{4}\pi\}\, \mathrm{d}\omega$$

$$\times \int \left(\frac{2}{\pi\gamma_0 \sin\theta |x|}\right)^{\frac{1}{2}} \frac{\rho_1(\omega + U_1 k)^2 J_n(\gamma\sigma)}{F_n(\omega, k)} \exp\{\mathrm{i}ky_1 + |x|\, h(k, \omega)\}\, \mathrm{d}k. \tag{4.9}$$

For large $|x|$ the k-integral is in a form suitable for evaluation by the method of stationary phase. The stationary point of

$h(k,\omega) = -ik\cos\theta + i\gamma_0 \sin\theta$ on the Riemann sheet Imaginary $\gamma_0 > 0$ occurs at $k = -\omega\cos\theta/c_0$, and the path of steepest descent is therefore a curve C in the complex k-plane defined by $-ik\cos\theta + i\gamma_0\sin\theta - i\omega/c_0 = -u^2$, where u is real on C. A sketch of the curve C is shown in Figure 3.4. We see that the steepest descent curve C crosses the branch cuts as they are defined at present. It is therefore convenient to redefine the cuts as shown in Figure 3.5; then in the shaded region $\mathrm{Im}\,\gamma_0 < 0$. We now make the usual approximation in the method of steepest descents and write

$$\int_C \left(\frac{2}{\pi\gamma_0 \sin\theta|x|}\right)^{\frac{1}{2}} \frac{\rho_1(\omega + U_1 k)^2}{F_n(\omega,k)} J_n(\gamma\sigma) \exp\{iky_1 + |x|\, h(k,\omega)\}\,dk$$
$$= \frac{2\rho_1\omega^2(1-M_r)^2 J_n(\gamma\sigma)}{|x|\, F_n(\omega, -\omega\cos\theta/c_0)} \exp i\{\omega(|x| - y_1\cos\theta)/c_0 - \tfrac{1}{4}\pi\}, \qquad (4.10)$$

where now $\gamma_0 = \omega\sin\theta/c_0$, $\gamma = \omega\left\{\frac{(1-M_r)^2}{c_1^2} - \frac{\cos^2\theta}{c_0^2}\right\}^{\frac{1}{2}}$

and $M_r = U_1\cos\theta/c_0$.

The integral along the real k-axis can be determined by relating it to the known integral along C. In doing this we will pick up contributions from any poles lying between the two curves. $F_n(\omega,k)$ has no zeros for ω and k real with $|k|c_0 < |\omega|$, because for this range of k, γ is either real or purely imaginary, in both cases $\gamma J_n'(\gamma a)/J_n(\gamma a)$ is real. But γ_0 is also real and therefore the imaginary part of $\gamma_0 H_n^{(1)\prime}(\gamma_0 a)/H_n^{(1)}(\gamma_0 a)$ is always non-zero, and so there are no poles on the axis with $|k|c_0 < |\omega|$. This argument does not apply when $|k|c_0 \geqslant |\omega|$, but the residue at these poles and at any pole off the axis is exponentially small for large $|x|$. Therefore when x is in the far-field

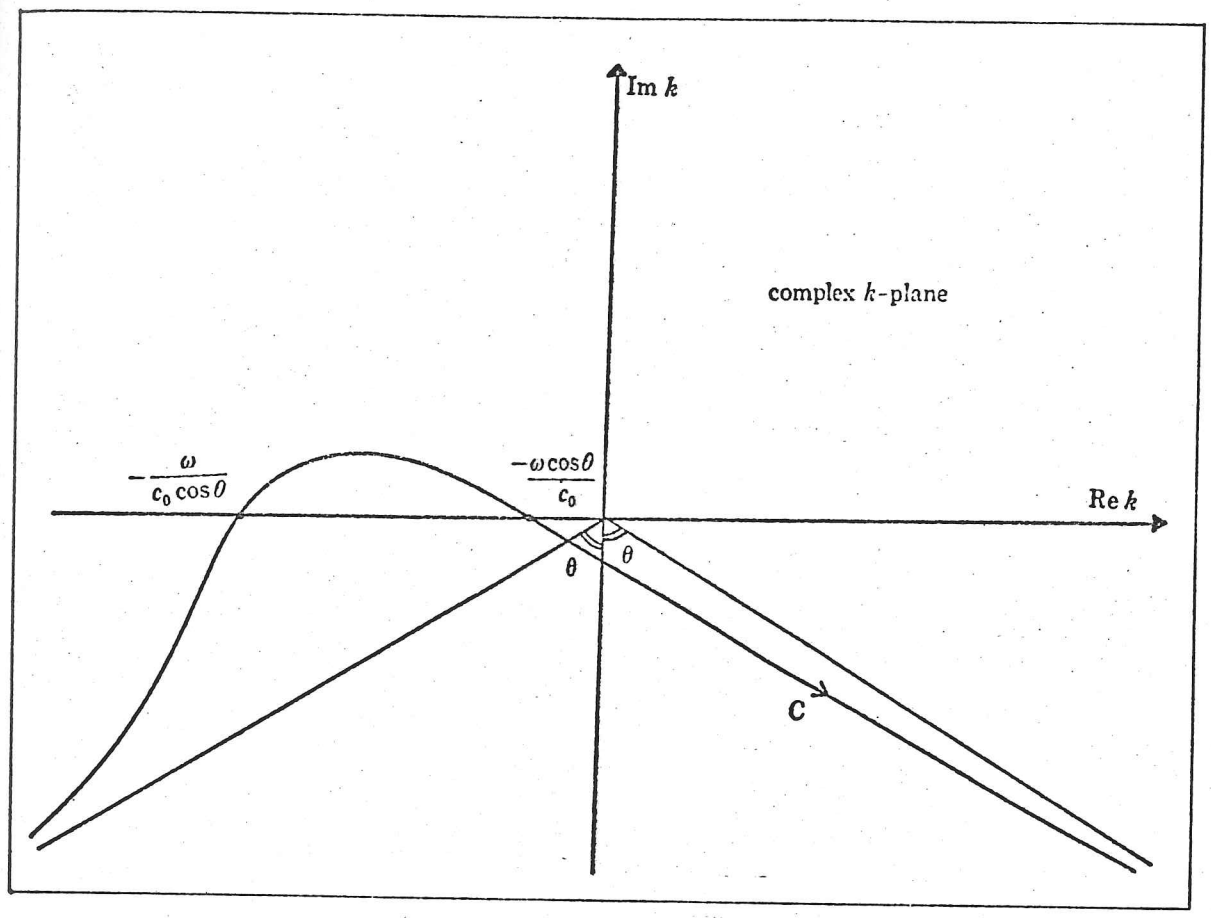

Figure 3.4 The position of the curve of steepest descent

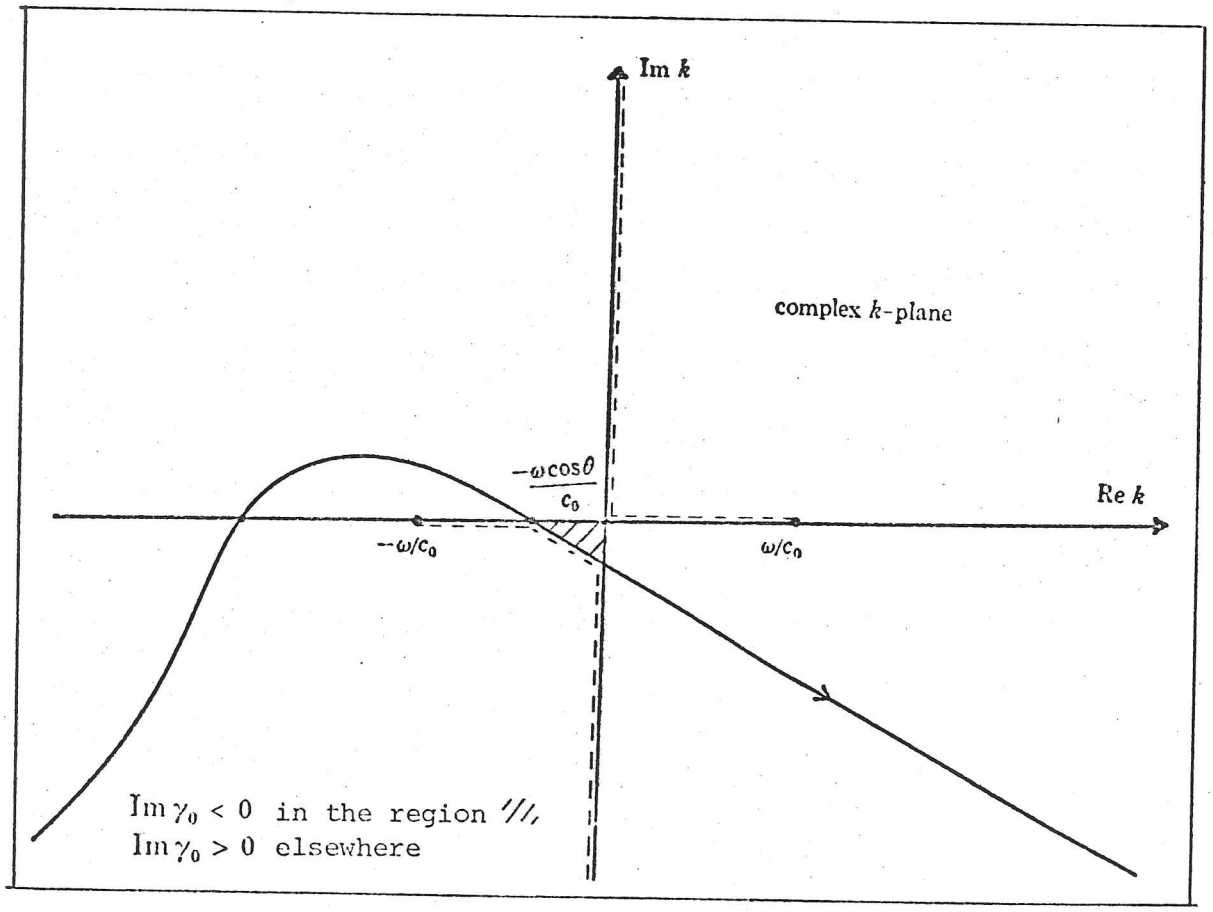

Figure 3.5 New position of the branch cut

$$G_1^\dagger(\boldsymbol{y},\tau|\boldsymbol{x},t)=\frac{\rho_1(1-M_r)^2}{4\pi^3|\boldsymbol{x}|\mathrm{i}}\int\sum_{n=-\infty}^{\infty}\frac{\omega^2 J_n(\gamma\sigma)}{F_n(\omega,-\omega\cos\theta/c_0)}\exp\mathrm{i}\{\omega(\tau-t^*)+n(\phi-\Phi-\tfrac{1}{2}\pi)\}\,\mathrm{d}\omega,\tag{4.11}$$

where t^* is the retarded time appropriate to waves travelling to $\boldsymbol{x}$ at speed c_0, $t^*=t-(|\boldsymbol{x}|-y_1\cos\theta)/c_0$.

By a similar argument we find

$$G_0^\dagger(\boldsymbol{y},\tau|\boldsymbol{x},t)=\frac{1}{8\pi^2|\boldsymbol{x}|}\int\sum_{n=-\infty}^{\infty}\left\{J_n(\gamma_0\sigma)+\frac{B_n(\omega)\,H_n^{(1)}(\gamma_0\sigma)}{F_n(\omega,-\omega\cos\theta/c_0)}\right\}\exp\mathrm{i}\{\omega(\tau-t^*)+n(\phi-\Phi-\tfrac{1}{2}n)\}\,\mathrm{d}\omega,\tag{4.12}$$

with $B_n(\omega)=a\omega^2\{\rho_1(1-M_r)^2\gamma_0 J_n'(\gamma_0 a)\,J_n(\gamma a)-\rho_0\gamma J_n(\gamma_0 a)\,J_n'(\gamma a)\}$.

This shows that $G_0^\dagger$ and $G_1^\dagger$ have outward wave behaviour for large $|\boldsymbol{x}|$. Alternatively the k-integral could have been evaluated for large values of $|\boldsymbol{y}|$ by the same method to verify that $G_0^\dagger$ has inward wave behaviour in the variables $(\boldsymbol{y},\tau)$.

The far-field at a point $\boldsymbol{x}$ depends on $F_n(\omega,-\omega\cos\theta/c_0)$; only elements of $F_n(\omega,k)$ whose component of phase velocity in the direction of the observer is equal to c_0 can propagate towards $\boldsymbol{x}$, i.e. (ω,k) for which $c_0=-\omega\cos\theta/k$. In particular this means that only components with a supersonic phase speed affect the far-field. We have already noted that $F_n(\omega,-\omega\cos\theta/c_0)$ has no zeros for real ω. This shows that a neutrally stable mode of the vortex sheet jet cannot be excited by a reciprocal source at $\boldsymbol{x}$, whenever $\boldsymbol{x}$ is in the far-field, or alternatively any resonances excited by sources within the jet do not propagate into the far-field.

When $\tau-t^*-a\sin\theta/c_0$ is positive we can evaluate $G_1^\dagger$ by closing the ω-contour in (4.11) with a large semi-circle in the upper

half plane;

$$G_1^{\dagger} = \sum_{n=-\infty}^{\infty} \sum_j Q_j \exp\, i\omega_j\left(\tau - t^* - a\sin\theta/c_0\right) , \tag{4.13}$$

where the sum is over the poles, ω_j , in the upper half plane and $Q_j \exp\, i\omega_j\left(\tau - t^* - a\sin\theta/c_0\right)$ is the residue at ω_j .

When the vortex sheet is unstable, and such poles do exist $G_1^{\dagger}$ can be non-zero for $\tau - t^* - a\sin\theta/c_0 > 0$ and is therefore not strictly causal.

The imaginary part of ω_j is positive and the contribution from each pole decays exponentially for large τ . As $\tau \to \infty$, the form of $G_1^{\dagger}$ will be dictated by the pole in the upper half plane with the smallest imaginary part, since its residue will have the slowest decay. We define K by

$$Ka/c_0 = \text{minimum } (\text{Im}\,\omega_j).$$

It is easy to see from the form of F_n that K is a function of $\cos\theta, M, n$ and the ratios $c_1/c_0, \rho_1/\rho_0$. We have determined the value of K at a Mach number $M = 2$, $\cos\theta = \frac{2}{3}, \rho_1 = \rho_0$ and $c_1 = c_0$ for the symmetric mode $n = 0$, by evaluating F_0 numerically and investigating the position of its zeros. We found the value of K to be .8 .

We can now see the meaning of the expression 'weakly causal'. There is a 'precursor' ahead of the wave front, that is at a point (x, t) such that $t^* < \tau - a\sin\theta/c_0$. The precursor decays exponentially ahead of this front, and will in fact be negligible for $t^* < \tau - a\sin\theta/c_0 - Ka/c_0$. Therefore, for this example of the symmetric mode, sound will only be heard up to a jet diameter or so ahead of the front.

Green's function $G^{\dagger}$ could be used in the representation (4.1) to determine the sound produced by a circular cylindrical jet. In the

general case this estimate for the sound field must be determined numerically; this has been done heuristically by Mani (1976). We have now developed a formal theory which supports Mani's general procedure. This analogy also gives an exact description of the sources and a clearer understanding of the causality question.

The compact jet

We now restrict our detailed analysis to the compact case which is algebraically more straightforward. By 'compact' we mean a jet with a diameter small in comparison with the acoustic wavelength.

From equation (4.1)

$$H\rho'(\boldsymbol{x},t) = \frac{\rho_0}{\rho_1(1-M_r)^2 c_0^2}\int\{\bar{H}T'_{ij} - \bar{H}_0(\rho_0 U_1^2\delta_{i1}\delta_{j1} - c_1^2(\rho_0-\rho_1)\,\delta_{ij})\}\frac{\partial^2 G_1^\dagger}{\partial y_i\,\partial y_j}\,\mathrm{d}^3\boldsymbol{y}\,\mathrm{d}\tau. \tag{4.14}$$

Alternatively we could rewrite this in terms of an integral over the frequency, because Parseval's theorem gives

$$\int\{\bar{H}T'_{ij} - \bar{H}_0(\rho_0 U_1^2\delta_{i1}\delta_{j1} - c_1^2(\rho_0-\rho_1)\,\delta_{ij})\}\frac{\partial^2 G_1^\dagger}{\partial y_i\,\partial y_j}\,\mathrm{d}^3\boldsymbol{y}\,\mathrm{d}\tau$$
$$= \frac{1}{2\pi}\int T'_{ij}(\boldsymbol{y},-\omega)\frac{\partial^2 G_1}{\partial y_i\,\partial y_j}(\boldsymbol{y},\omega)\,\mathrm{d}^3\boldsymbol{y}\,\mathrm{d}\omega, \tag{4.15}$$

where $T'_{ij}(\boldsymbol{y},\omega)$ is the Fourier transform of $\bar{H}T'_{ij} - \bar{H}_0(\rho_0 U_1^2\delta_{i1}\delta_{j1} - c_1^2(\rho_0-\rho_1)\,\delta_{ij})$ with respect to time, and $G_1(\boldsymbol{y},\omega)$ the transform of $G_1^\dagger(\boldsymbol{y},\tau)$. The far-field density may therefore be written as

$$H\rho'(\boldsymbol{x},t) = \frac{\rho_0}{\rho_1(1-M_r)^2 c_0^2 2\pi}\int T'_{ij}(\boldsymbol{y},-\omega)\frac{\partial^2 G_1}{\partial y_i\,\partial y_j}(\boldsymbol{y},\omega)\,\mathrm{d}^3\boldsymbol{y}\,\mathrm{d}\omega. \tag{4.16}$$

For a compact jet $T'_{ij}(\boldsymbol{y},\omega)$ is zero unless $|\omega|a \ll c_0$ and $G_1(\boldsymbol{y},\omega)$ in this integral can be replaced by $G_1^c(\boldsymbol{y},\omega)$, its low frequency asymptotic form.

The transform of the far-field form of $G_1^+(y,\tau)$ given in (4.11) is

$$G_1(\boldsymbol{y},\omega) = \frac{\rho_1(1-M_r)^2\omega^2}{2\pi^2|\boldsymbol{x}|\mathrm{i}} \sum_{n=-\infty}^{\infty} \frac{J_n(\gamma\sigma)}{F_n(\omega,\,-\omega\cos\theta/c_0)} \exp \mathrm{i}\{-\omega t^* + n(\phi-\Phi-\tfrac{1}{2}\pi)\}, \quad (4.17)$$

and when $\omega a/c_0 \ll 1$ we can use the expansions for Bessel functions of small argument to obtain

$$G_1^c(\boldsymbol{y},\omega) = \frac{1}{|\boldsymbol{x}|}\{a_0(\omega)\,(1-\tfrac{1}{4}(\gamma\sigma)^2+\ldots) - a_1(\omega)\,\mathrm{i}\gamma\sigma\cos(\phi-\Phi) - a_2(\omega)\,\tfrac{1}{4}\gamma^2\sigma^2\cos 2(\phi-\Phi) + O(\epsilon^3)\}\,\mathrm{e}^{-\mathrm{i}\omega t^*} \quad (4.18)$$

where $\epsilon = \omega a/c_0$ and $a_n(\omega)$ is the low frequency expansion of

$$\frac{\rho_1(1-M_r)^2\omega^2}{2\pi^2\mathrm{i}F_n(\omega,\,-\omega\cos\theta/c_0)}.$$

In fact

$$a_n(\omega) = a_{-n}(\omega) = \frac{\rho_1(1-M_r)^2\gamma_0^n}{2\pi\gamma^n\{\rho_0+\rho_1(1-M_r)^2+O(\rho_0\epsilon^2,\rho_1\epsilon^2,\rho_0\epsilon^{2n}\ln\epsilon,\rho_1\epsilon^{2n}\ln\epsilon)\}} \quad \text{for} \quad n \geqslant 1$$

and

$$a_0(\omega) = \frac{\rho_1(1-M_r)^2}{2\pi\{\,2\rho_1(1-M_r)^2+a^2\ln(\gamma_0 a)\,(\rho_0\gamma^2-\rho_1(1-M_r)^2\gamma_0^2)+O(\rho_0\epsilon^2,\rho_1\epsilon^2)\}}. \quad (4.19)$$

If the y-axes are chosen so that $y_2 = \sigma\cos\phi$, $y_3 = \sigma\sin\phi$, then

$$G_1^c(\boldsymbol{y},\omega) = \frac{1}{|\boldsymbol{x}|}\{a_0(\omega)\,(1-\tfrac{1}{4}\gamma^2(y_2^2+y_3^2)\ldots) - \mathrm{i}\gamma a_1(\omega)\,(y_2\cos\Phi+y_3\sin\Phi) - \tfrac{1}{4}\gamma^2 a_2(\omega)\,\big((y_2^2-y_3^2)\cos 2\Phi + 2y_2y_3\sin 2\Phi\big)\}\,\mathrm{e}^{-\mathrm{i}\omega t^*}, \quad (4.20)$$

and the derivatives of $G_1^c(\boldsymbol{y},\omega)$ with respect to $\boldsymbol{y}$ can easily be evaluated;

$$\frac{\partial^2 G_1^c}{\partial y_1^2}(\boldsymbol{y},\omega) = -\frac{\omega^2\cos^2\theta}{|\boldsymbol{x}|c_0^2}\{a_0(\omega)+O(\epsilon)\}\,e^{-i\omega t^*},$$

$$\frac{\partial^2 G_1^c}{\partial y_1\partial y_2}(\boldsymbol{y},\omega) = -\frac{\omega^2\cos\theta}{|\boldsymbol{x}|c_0^2}\{\alpha\cos\Phi a_1(\omega)+O(\epsilon a_0)\}\,e^{-i\omega t^*},$$

$$\frac{\partial^2 G_1^c}{\partial y_2^2}(\boldsymbol{y},\omega) = -\frac{\omega^2}{|\boldsymbol{x}|c_0^2}\{\tfrac{1}{2}\alpha^2(a_0(\omega)+a_2(\omega)\cos 2\Phi)+O(\epsilon^2 a_0,\epsilon a_1)\}\,e^{-i\omega t^*},$$

$$\frac{\partial^2 G_1^c}{\partial y_2\partial y_3}(\boldsymbol{y},\omega) = -\frac{\omega^2}{|\boldsymbol{x}|c_0^2}\{\tfrac{1}{2}\alpha^2\sin 2\Phi a_2(\omega)+O(\epsilon^2 a_0,\epsilon a_1)\}\,e^{-i\omega t^*}, \qquad (4.21)$$

where $\alpha = \{(1-M_r)^2 c_0^2/c_1^2-\cos^2\theta\}^{\frac{1}{2}}$,

so that $\gamma = \omega\alpha/c_0$.

Away from both the mean flow Mach angle and the jet axis we can neglect the second term in the denominator of a_0 in comparison with the first, provided only that the mean jet density is greater than, or of the same order as, the density of the ambient fluid. Then

$$\frac{\partial^2 G_1^c}{\partial y_i\partial y_j}(\boldsymbol{y},\omega) = -\frac{\omega^2 D_{ij}}{4\pi|\boldsymbol{x}|c_0^2}\frac{\rho_1(1-M_r)^2}{\rho_0}\,e^{-i\omega t^*}, \qquad (4.22)$$

where D_{ij} is a directional factor;

$$D_{11} = \frac{\rho_0}{\rho_1(1-M_r)^2}\frac{x_1^2}{|\boldsymbol{x}|^2},$$

$$D_{22} = \left\{\tfrac{1}{2}\alpha^2+\frac{\rho_1(1-M_r)^2}{\rho_0+\rho_1(1-M_r)^2}\frac{(x_2^2-x_3^2)}{|\boldsymbol{x}|^2}\right\}\frac{\rho_0}{\rho_1(1-M_r)^2},$$

$$D_{33} = \left\{\tfrac{1}{2}\alpha^2+\frac{\rho_1(1-M_r)^2}{\rho_0+\rho_1(1-M_r)^2}\frac{(x_3^2-x_2^2)}{|\boldsymbol{x}|^2}\right\}\frac{\rho_0}{\rho_1(1-M_r)^2},$$

$$D_{ij} = \frac{2\rho_0 x_i x_j}{\{\rho_0+\rho_1(1-M_r)^2\}|\boldsymbol{x}|^2} \quad \text{for} \quad i\neq j.$$

These derivatives of $G_1^c(y,\omega)$ can be used in equation (4.16) to estimate the sound field. Alternatively the sound field may be described by (4.14) with $G_1^{\dagger}(y,\tau)$ replaced by its 'compact' form $G_1^c(y,\tau)$, where

$$G_1^c(y,\tau) = \frac{1}{2\pi}\int G_1^c(y,\omega)\, e^{i\omega\tau} d\omega. \tag{4.23}$$

The evaluation of the ω-integral gives

$$\frac{\partial^2 G_1^c}{\partial y_i \partial y_j}(y,\tau) = \frac{D_{ij}}{4\pi|x|c_0^2}\frac{\rho_1(1-M_r)^2}{\rho_0}\frac{\partial^2}{\partial\tau^2}\delta(\tau-t^*). \tag{4.24}$$

We can express these time derivatives at constant y in terms of a Lagrangian time derivative at constant η, since

$$\begin{aligned}\frac{D}{D\tau}\delta(\tau-t^*) &= \left(\frac{\partial}{\partial\tau}+v_i\frac{\partial}{\partial y_i}\right)\delta\left(\tau-t+(|x|-y_1\cos\theta)/c_0\right)\\ &= (1-N_r)\frac{\partial}{\partial\tau}\delta(\tau-t^*),\end{aligned} \tag{4.25}$$

where $D/D\tau$ is the material time derivative, N is the 'Mach number' based on the local fluid velocity and the exterior speed of sound, $N = v/c_0$, and N_r is $v_1 x_1/(c_0|x|)$.

From a repetition of this procedure, we find

$$\frac{\partial^2 G_1^c}{\partial y_i \partial y_j}(y,\tau) = \frac{\rho_1(1-M_r)^2}{\rho_0}\frac{D_{ij}}{4\pi|x|c_0^2(1-N_r)}\frac{D}{D\tau}\left\{\frac{1}{1-N_r}\frac{D}{D\tau}\delta(\tau-t^*)\right\} \tag{4.26}$$

and the representation (4.14) becomes

$$H\rho'(x,t) = \frac{D_{ij}}{4\pi|x|c_0^3}\int d\tau\left\{\int_{V_1}\frac{\rho^* T_{ij}}{\rho(1-N_r)}\frac{D}{D\tau}\left(\frac{1}{(1-N_r)}\frac{D\delta}{D\tau}\right)d^3\eta - \int_{V_1^{(\omega)}}(\rho_0 U_1^2\delta_{i1}\delta_{j1} - c_1^2(\rho_0-\rho_1)\delta_{ij})\frac{\partial^2\delta}{\partial\tau^2}d^3y\right\}. \tag{4.27}$$

The region ν_1 is a constant function of η, and so we may integrate by parts to obtain

$$H\rho'(\boldsymbol{x},t) = \frac{D_{ij}}{4\pi|\boldsymbol{x}|c_0^4}\iint_{\nu_1}\delta(\tau-t^*)\frac{\mathrm{D}}{\mathrm{D}\tau}\left\{\frac{1}{1-N_r}\frac{\mathrm{D}}{\mathrm{D}\tau}\left(\frac{\rho^* T'_{ij}}{\rho(1-N_r)}\right)\right\}\mathrm{d}^3\eta\,\mathrm{d}\tau. \tag{4.28}$$

The τ-integral is now simple to evaluate

$$H\rho'(\boldsymbol{x},t) = \frac{D_{ij}\overline{T}_{ij}}{4\pi|\boldsymbol{x}|c_0^4}, \tag{4.29}$$

where

$$\overline{T}_{ij} = \int_{\nu_1}\left[\frac{\mathrm{D}}{\mathrm{D}\tau}\left\{\frac{1}{1-N_r}\frac{\mathrm{D}}{\mathrm{D}\tau}\left(\frac{\rho^* T'_{ij}}{\rho(1-N_r)}\right)\right\}\frac{\mathrm{d}^3\eta}{|1-N_r|}\right].$$

The square brackets denote that the function they enclose is to be evaluated at a retarded time τ^* satisfying

$$\tau^* = t-\{|\boldsymbol{x}|-\cos\theta y_1(\eta,\tau^*)\}/c_0, \tag{4.30}$$

where $\boldsymbol{y}(\eta,\tau^*) = \eta+\int^{\tau^*}\boldsymbol{v}(\eta,\tau)\,\mathrm{d}\tau$ and the lower limit in this integral is the reference time at which the Lagrangian and Eulerian axes coincide. We differentiate this expression for τ^*, the retarded time, to show

$$\frac{\partial\tau^*}{\partial\eta_i} = \frac{x_1}{|\boldsymbol{x}|c_0}\left\{\delta_{i1}+v_1\frac{\partial\tau^*}{\partial\eta_i}\right\}$$

or

$$\frac{\partial\tau^*}{\partial\eta_i} = \frac{1}{1-N_r}\frac{x_i}{|\boldsymbol{x}|c_0}\delta_{ii}.$$

Hence away from the flow Mach angle the variation in retarded time across the jet may be neglected and (4.29) is a convenient description of the noise produced by turbulence in the vicinity of the jet. $\overline{T}_{ij}$ is the source term found by Ffowcs Williams (1974) to be relevant in shear layer problems and here it is multiplied by a directional factor D_{ij},

which describes the transmission properties of a compact circular cylindrical jet. $D_{11} = \rho_0 x_1^2/\rho_1(1-M_r)^2|x|^2$ and Mani's result that the interaction between a longitudinal quadrupole and the jet flow results in a Doppler amplification of the type $(1-M_r)^{-2}(1-N_r)^{-3}$ is immediate, and even higher powers of the Doppler factor accompany unsteady convection. Goldstein (1975) has shown that a pressure field amplified by five Doppler factors agrees well with Lush's (1971) experimental data. We can use (4.29) to determine the way in which the sound field scales with the various jet parameters.

From the $\rho v_i' v_j'$ term in T_{ij}', we find

$$\overline{\rho'(x,t)\rho'(x,t+\tau)} \sim \rho^2 M^8 a^2/|x|^2, \tag{4.31}$$

where the overbar denotes the time average. This is just Lighthill's scaling law.

The term in T_{ij}' due to the density difference, $c_1^2(\rho-\rho_1)\delta_{ij}$, must be treated more carefully, because although $\Delta\rho = \rho-\rho_1$ may be large near the edge of the jet, $D\rho/D\tau$ is always small, and cannot be scaled as $\Delta\rho U_j/a$. . Instead we expand

$$c_1^2 \frac{D}{D\tau}\left(\frac{\rho^*(\rho-\rho_1)}{\rho(1-N_r)}\right) \quad \text{as} \quad \frac{c_1^2\rho^*\Delta\rho}{\rho(1-N_r)^2}\frac{DN_r}{D\tau} - \frac{c_1^2\rho^*}{(1-N_r)}\frac{D}{D\tau}\left(\frac{\rho_1}{\rho}\right).$$

For small Mach numbers we obtain

$$\overline{\rho'(x,t)\rho'(x,t+\tau)} \sim (\Delta\rho)^2 M^6 a^2/|x|^2. \tag{4.32}$$

Alternatively we could do the scaling in the frequency space and determine the spectral characteristics of the sound. The power spectral density $W(x,s)$ is defined as the Fourier transform of the autocorrelation with respect to a non-dimensional time;

$$W(x,s) = \int \overline{\rho'(x,t)\,\rho'(x,t+\tau)}\, e^{-isU_1\tau/a}\,(U_1/a)\,d\tau, \tag{4.33}$$

or equivalently

$$W(x,s)\,\delta(\omega+\omega') = \overline{\rho'(x,\omega)\,\rho'(x,\omega')}\,U_1/2\pi a, \tag{4.34}$$

where $s = \omega a/U_1$ is the Strouhal number. The total acoustic power is then given by $\int W(x,s)\,ds$.

When the expressions for the derivatives of $G_1^c(y,\omega)$ given in (4.22) are substituted into the representation (4.16) we find

$$H\rho'(x,t) = -\frac{D_{ij}}{8\pi^2|x|c_0^4}\int \omega^2 T'_{ij}(y,-\omega)\exp -i\omega\{t-(|x|-y_1\cos\theta)/c_0\}\,d^3y\,d\omega, \tag{4.35}$$

so that

$$H\rho'(x,\omega) = -\frac{\omega^2 D_{ij}}{4\pi|x|c_0^4}\int T'_{ij}(y,\omega)\exp\{-i\omega(|x|-y_1\cos\theta)/c_0\}d^3y.$$

Rewriting $H\rho'(x,\omega)$ in terms of $T'_{ij}(k^*,\omega)$, the four dimensional Fourier transform of $\bar{H}T'_{ij} - \bar{H}_0(\rho_0 U_1^2\delta_{i1}\delta_{j1} - c_1^2(\rho_0-\rho_1)\,\delta_{ij})$,

$$H\rho'(x,\omega) = -\frac{\omega^2 D_{ij}}{4\pi|x|c_0^4}\,T'_{ij}(k^*,\omega)\exp -i\omega|x|/c_0, \tag{4.36}$$

where $k^* = (-\omega\cos\theta/c_0, 0, 0)$. This form for the transform of the density perturbation can be used in (4.34) to obtain a scaling law for $W(x,s)$. We see that the $\rho v_i' v_j'$ term in T'_{ij} gives

$$W(x,s) \sim \rho^2 M^8 s^3 a^2/|x|^2. \tag{4.37}$$

However if ρ_0 and ρ_1 are not equal, the largest contribution to T'_{ij} at low Mach numbers comes from the density term, $c_1^2(\rho-\rho_1)\,\delta_{ij}$. For low Mach number flows

$$\frac{\partial \rho}{\partial \tau} \approx -v_i \frac{\partial \rho}{\partial y_i} \approx -\frac{\partial}{\partial y_i}(v_i \Delta\rho),$$

so that $\omega\rho(\mathbf{y},\omega) \approx (\omega/c_0)\,(v_i\Delta\rho)\,(\mathbf{y},\omega)$,

and $$W(\mathbf{x},s) \sim (\Delta\rho)^2 M^6 s^3 a^2/|\mathbf{x}|^2. \tag{4.38}$$

This scaling is only valid when $\rho_1(1-M_r)^2 \gg \rho_0(\gamma a)^2 \ln(\gamma_0 a)$, because we have obtained it by neglecting $\rho_0(\gamma a)^2\ln(\gamma_0 a)$ in comparison with $\rho_1(1-M_r)^2$, when they appear in the denominator of $a_0(\omega)$ in (4.19). This is not valid as $\sin\theta \to 0$. Then $\gamma_0 \to 0$, the neglected term grows logarithmically, and from (4.19) $a_n(\omega) = 0$ for all n, which ensures that G_1^c and all its derivatives are zero. No sound is heard on the axis of the jet. Gottlieb (1960) refers to this as the 'Lloyds mirror' effect and explains that the incident and reflected waves cancel in this direction. The form of G_1^c given in (4.24) is also inappropriate at the mean flow Mach angle, $M_r = 1$. In this case the first term in the denominator of $a_0(\omega)$ vanishes and the small second term in the denominator of (4.19) must be retained. G_1^c therefore has a large but finite value and the sound intensity has a local maximum in the direction of the mean flow Mach angle.

In the case of a very light jet the compact limit of the Green function has a different form and different scaling laws are obtained. For a jet which is lighter than it is compact (by that we mean $\rho_1 \ll \rho_0\epsilon^2\ln\epsilon$), the term $\rho_1(1-M_r)^2$ in the expression for $a_0(\omega)$ can be neglected, and

$$a_0(\omega) = \frac{\rho_1(1-M_r)^2}{2\pi\rho_0(\gamma a)^2\ln(|\omega|a/c_0)}\left\{1 + O(\ln\epsilon)^{-1} + O\left(\frac{\rho_1(1-M_r)^2}{\rho_0\epsilon^2\ln\epsilon}\right)\right\},$$

$$a_{-n}(\omega) = a_n(\omega) = \frac{\rho_1(1-M_r)^2}{2\pi\rho_0}\left(\frac{\gamma_0}{\gamma}\right)^n \{1 + O(\epsilon^{2n}\ln\epsilon) + O(\epsilon^n)\} \quad n \geq 1,$$

for x such that $\alpha^2 = (1-M_r)^2 c_0^2/c_1^2 - \cos^2\theta \neq 0$.

Then from (4.21)

$$\frac{\partial^2 G_1^c(y,\omega)}{\partial y_i \partial y_j} = -\frac{\rho_1 (1-M_r)^2}{\rho_0 4\pi |x| a^2} \frac{E_{ij} e^{-i\omega t^*}}{\ln(|\omega| a/c_0)}, \tag{4.39}$$

where $E_{11} = 2\cos^2\theta\alpha^{-2}$, $E_{22} = E_{33} = 1$, $E_{ij} = 0$ for $i \neq j$.

The far-field density may be determined by substituting this form for $G_1^c(y,\omega)$ into equation (4.16);

$$H\rho'(x,t) = -\frac{E_{ij}}{8\pi^2 |x| a^2 c_0^2} \int \frac{T'_{ij}(y,-\omega)}{\ln(|\omega| a/c_0)} \exp[-i\omega\{t - (|x| - y_1\cos\theta)/c_0\}]\, d^3y\, d\omega,$$

$$H\rho'(x,\omega) = -\frac{E_{ij}}{4\pi |x| a^2 c_0^2} \frac{T'_{ij}(k^*,\omega)}{\ln(|\omega| a/c_0)} \exp(-i\omega|x|/c_0). \tag{4.40}$$

We can now use this expression for $\rho'(x,\omega)$ to investigate how $W(x,s)$ depends on the various parameters. The $\rho v'_i v'_j$ term in T'_{ij} is largest near the surface where $\rho \approx \rho_0$ and

$$W(x,s) \sim \frac{\rho_0^2 M^4 a^2}{s \ln^2(sM)\, |x|^2} \qquad \text{for } \rho_1 \ll \rho_0 M^2 s^2 \ln(sM) \text{ and } Ms \ll 1. \tag{4.41}$$

$$\approx \rho_0^2 M^4 a^2/(s|x|^2), \tag{4.42}$$

because for small M the variation of $\ln(sM)$ with M is smaller than algebraic. The Reynolds stress induced waves have an intensity that scales with only the fourth power of the jet velocity rather than Lighthill's eighth power law for free quadrupoles.

However at low Mach numbers the main contribution to the sound field comes from the density term in T'_{ij}, and scaling that term gives

$$W(x,s) \sim \frac{(\Delta\rho)^2 M^{2} a^2}{s \ln^2(sM)\,|x|^2}, \quad \text{for} \quad \rho_1 \ll \rho_0 M^{2} s^2 \ln(sM) \quad \text{and} \quad M s \ll 1, \tag{4.43}$$

$$\approx \frac{(\Delta\rho)^2 M^{2} a^2}{s|x|^2}. \tag{4.44}$$

We see that in general the sound produced by density inhomogeneities within a very light jet scales with the second power of the Mach number. This scaling law predicts that the sound intensity is a factor $(Ms)^{-4}$ larger than the usual scaling law $(\Delta\rho)^2 M^{6} s^3 /|x|^2$.

It is well known that at low Mach numbers the noise of real hot jets is much less sensitive to velocity changes than the U_1^{8} dependence thought to be relevant to the 'pure mixing' noise of a low Mach number jet. Lush & Fisher (1974) show that experimental hot jet data collapses onto a M^4 scaling, although they have no theoretical justification for such a law. Here we demonstrate that the sound produced by a light jet scales as M^4 or even M^2.

The zone of silence (if one exists) is a region of points for which $(1-M_r)^2 c_0^2 - c_1^2 \cos^2\theta$ is negative, and so α is imaginary, and sound which propagates into the far-field of this zone decays exponentially within the jet. On the edge of this region $\alpha = 0$ and the expressions for the derivatives of $G_1^c(y,\omega)$ given in (4.39) are not valid. Even for a light jet the previous form (4.22) should be used, and there is a local peak in the far-field intensity of the noise.

3.5 The slab jet

In §3.4 we found that the Green function describing the sound produced by a compact circular cylindrical jet has quite a different form when the jet is very light (cf. equations (4.22) and (4.39)). We were able to find $G_1^c(y,\omega)$ for a light compact jet, but because of the

complications introduced by the geometry, it was not possible to invert the Fourier transform to find $G_1^c(y,\tau)$ and its derivatives explicitly in this limit. To obtain a clearer understanding of how and why the form of the Green function changes, we now consider a slab jet, a simple shape for which it is possible to evaluate $G_1^c(y,\tau)$ for all density ranges. By a slab jet we mean a jet composed of two plane vortex sheets separated by a distance $2h$, as shown in Figure 3.6.

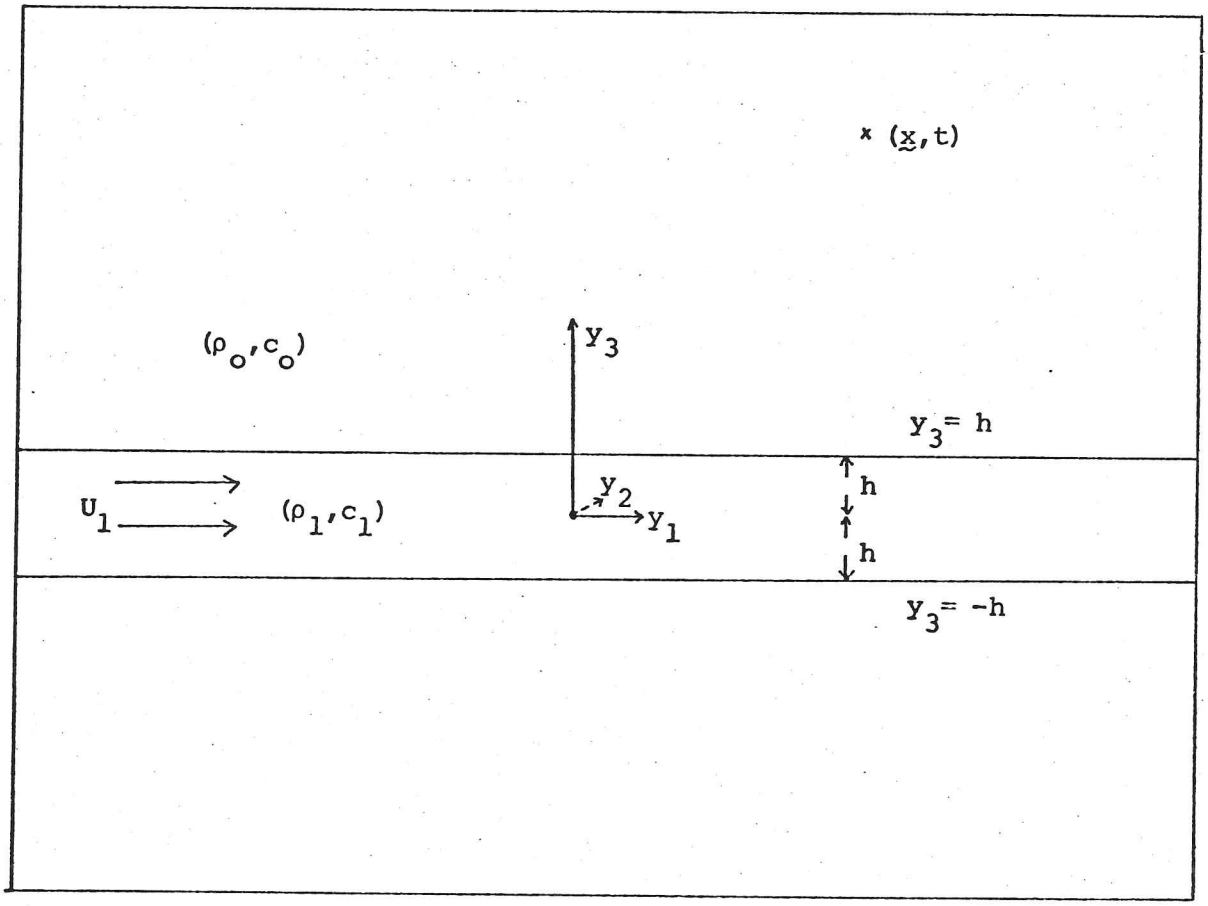

Figure 3.6 A slab jet

The general representation (3.1) has been developed for a jet of finite cross-section. However the theory can be extended to apply to a slab jet if we suppose that the decay rate of the real fluid parameters, at large distances within the jet, is faster than $|y|^{-1}$,

$$p_{ij}, v_i' \sim o(|y|^{-1}) \quad \text{as} \quad |y| \to \infty \text{ in } v_1; \tag{5.1}$$

viscous dissipation in a real jet will ensure that this condition is satisfied. The integral over a bounding surface at infinity then vanishes as required (see Appendix 3.A, equation (A.13) for the exact form of this integral), and the far-field density outside the jet is given by (3.1).

$$c_0^2 H\rho'(x,t) = \frac{\rho_0}{\rho_1(1-M_\tau)^2}\int d\tau\left\{\int_{V_1}\frac{\rho^* T'_{ij}}{\rho}\frac{\partial^2 G_1^\dagger}{\partial y_i\,\partial y_j}\,d^3\eta - \int_{V_1(\tau)}(\rho_0 U_1^2\delta_{i1}\delta_{j1} - c_1^2(\rho_0-\rho_1)\,\delta_{ij})\frac{\partial^2 G_1^\dagger}{\partial y_i\,\partial y_j}\,d^3y\right\}, \tag{5.2}$$

We will later show from this expression that on the jet boundary $\rho' \sim o(|y|^{-1})$, which is consistent with the far-field form (5.1) applied within the jet.

$G^\dagger$ is the instability-free vortex sheet Green function defined by

$$\left\{\frac{\partial^2}{\partial y_i^2} - \frac{1}{c_0^2}\frac{\partial^2}{\partial\tau^2}\right\} G_0^\dagger(y,\tau|x,t) = -\delta(x-y,t-\tau) \qquad \text{for } |y_3| > h$$

$$\left\{\frac{\partial^2}{\partial y_i^2} - \frac{1}{c_1^2}\frac{D_1^2}{D\tau^2}\right\} G_1^\dagger(y,\tau|x,t) = 0, \qquad \text{for } |y_3| < h\ , \tag{5.3}$$

together with the vortex sheet jump conditions

$$G_o^\dagger = G_1^\dagger\ ,\quad \rho_1\frac{D_1^2}{D\tau^2}\frac{\partial G_o^\dagger}{\partial y_3} = \rho_o\frac{\partial^2}{\partial\tau^2}\frac{\partial G_1^\dagger}{\partial y_3} \qquad \text{on} \quad |y_3| = h\ . \tag{5.4}$$

$G^\dagger$ is weakly causal and has incoming wave behaviour in the variables $(\underset{\sim}{y},\tau)$. This system of equations can be solved easily by taking Fourier transforms in y_1, y_2 and τ. On inverting the transform we find $G_1^\dagger$ has the form

$$G_1^\dagger(\underset{\sim}{y},\tau) = -\frac{1}{(2\pi)^3}\int (Ce^{i\gamma y_3} + De^{-i\gamma y_3})\exp i\{k_1(y_1-x_1)+k_2(y_2-x_2)+\omega(\tau-t)+\gamma_o x_3\}dk_1\,dk_2\,d\omega\ , \tag{5.5}$$

where $\gamma_o = (\omega^2/c_o^2 - k_1^2 - k_2^2)^{\frac{1}{2}}$ and $\gamma = \left((\omega+U_1 k_1)^2/c_1^2 - k_1^2 - k_2^2 \right)^{\frac{1}{2}}$.

When the observer at $\underset{\sim}{x}$ is in the far-field, the k_1 and k_2 integrals can be evaluated by the method of stationary phase to give

$$G_1^\dagger(\underset{\sim}{y},\tau) = \frac{i}{4\pi^2|\underset{\sim}{x}|} \int \{Ce^{i\gamma y_3} + De^{-i\gamma y_3}\} \gamma_o e^{i\omega(\tau-t^*)} d\omega \quad , \tag{5.6}$$

where now

$$C = \frac{\rho_1(1-M_r)^2}{i} \frac{P_1 e^{-i\gamma_o h + i\gamma h}}{P_2^2 e^{-2i\gamma h} - P_1^2 e^{2i\gamma h}}$$

$$D = \frac{\rho_1(1-M_r)^2}{i} \frac{P_2 e^{-i\gamma_o h - i\gamma h}}{P_2^2 e^{-2i\gamma h} - P_1^2 e^{2i\gamma h}}$$

$$P_1 = \rho_o\gamma - \rho_1(1-M_r)^2\gamma_o$$

$$P_2 = \rho_o\gamma + \rho_1(1-M_r)^2\gamma_o$$

$$\gamma_o = \omega \sin\theta \sin\phi/c_o$$

$$\gamma = \omega\alpha/c_o \ , \quad \alpha = \{(1-M_r)^2 c_o^2/c_1^2 - \cos^2\theta - \sin^2\theta\cos^2\phi\}^{\frac{1}{2}}$$

with $t^* = t - (|\underset{\sim}{x}| - y_1\cos\theta - y_2\sin\theta\cos\phi)/c_o$,

$$(x_1,x_2,x_3) = |\underset{\sim}{x}| \ (\cos\theta, \sin\theta\cos\phi, \sin\theta\sin\phi) \ .$$

Only the elements of $G_1^\dagger$ with a supersonic phase speed affect the far-field; the components of the Fourier transform of $G_1^\dagger$ that propagate towards the point $\underset{\sim}{x}$ are those whose vector wave number is related to the frequency by $(k_1,k_2) = -(\cos\theta, \sin\theta\cos\phi)\omega/c_o$. The integrand in (5.6) has no poles for real ω , because $P_2^2 e^{-2i\gamma h} - P_1^2 e^{2i\gamma h}$ is always non-zero when ω is real, and again, as in the case of the circular cylindrical jet, we discover that the reciprocal source at a far-field point $\underset{\sim}{x}$ cannot excite a neutrally stable mode of the vortex sheet jet.

An application of Parseval's theorem to the representation (5.2) shows that it may be rewritten in terms of a frequency integral;

$$H\rho'(\underset{\sim}{x},t) = \frac{\rho_o}{2\pi\rho_1(1-M_r)^2c_o^2}\int T'_{ij}(\underset{\sim}{y},-\omega)\,\frac{\partial^2 G_1}{\partial y_i\partial y_j}(\underset{\sim}{y},\omega)\,d\omega \quad , \tag{5.7}$$

where $T'_{ij}(\underset{\sim}{y},\omega)$ is the Fourier transform of $HT'_{ij}-\overline{H}_o\left(\rho_o U_1^2\delta_{i1}\delta_{j1}-c_1^2(\rho_o-\rho_1)\delta_{ij}\right)$ with respect to time, and $G_1(\underset{\sim}{y},\omega)$ is the transform of $G_1^\dagger(\underset{\sim}{y},\tau)$;

$$G_1(\underset{\sim}{y},\omega) = \frac{i\gamma_o}{2\pi|\underset{\sim}{x}|}\{Ce^{i\gamma y_3}+De^{-i\gamma y_3}\}e^{-i\omega t^*} \quad . \tag{5.8}$$

When the observation point is near the sheet, x_3 is small and so $\gamma_o \to 0$ and $G_1(\underset{\sim}{y},\omega)$ vanishes. From (5.7) it is then apparent that the turbulence within the jet produces an acoustic field which is zero on the jet boundary (Dash 1976(a)), and the perturbed flow parameters decay faster than $|\underset{\sim}{x}|^{-1}$ there. This agrees with the far-field conditions described in (5.1).

For a 'compact' slab jet h , the width of the jet, is small in comparison with the acoustic wavelength, and $T'_{ij}(\underset{\sim}{y},\omega)$ is non-zero only when ω is much less than $c_o h^{-1}$, $\omega h/c_o = \varepsilon << 1$. Then we can replace $\partial^2 G_1(\underset{\sim}{y},\omega)/\partial y_i\partial y_j$ in equation (5.7) by its low frequency limit.

The compact form of $G_1(\underset{\sim}{y},\omega)$ is

$$G_1^c(\underset{\sim}{y},\omega) = \frac{i\gamma_o}{2\pi|\underset{\sim}{x}|}\{(C+D)e^{-i\omega t^*}+O(\varepsilon)(C-D)\} \tag{5.9}$$

also

$$\frac{\partial G_1^c(\underset{\sim}{y},\omega)}{\partial y_3} = -\frac{\gamma_o\gamma}{2\pi|\underset{\sim}{x}|}\{(C-D)e^{-i\omega t^*}+O(\varepsilon)(C+D)\} \quad , \tag{5.10}$$

and the other derivatives of $G_1^c(\underset{\sim}{y},\omega)$ can be evaluated similarly.

For small values of ε ,

$$C+D \simeq \frac{1}{2i}\frac{\rho_1(1-M_r)^2}{\rho_1(1-M_r)^2\gamma_o - i\rho_o\gamma^2 h} \tag{5.11}$$

$$C-D \simeq -\frac{1}{2i}\frac{\rho_1(1-M_r)^2}{\rho_o\gamma - i\rho_1(1-M_r)^2\gamma_o\gamma h} \quad . \tag{5.12}$$

There are three distinct limits for the compact jet depending on the relative magnitudes of $\rho_o\alpha$ and $\rho_1(1-M_r)^2\sin\theta\sin\phi$.

First we consider the case when ρ_o and ρ_1 are of the same order. Then away from the jet and the mean flow Mach angle

$$C+D \simeq \frac{1}{2i\gamma_o} \quad , \quad C-D \simeq -\frac{\rho_1(1-M_r)^2}{2i\rho_o\gamma} \tag{5.13}$$

and

$$\frac{\partial^2 G_1^c(\underset{\sim}{y},\omega)}{\partial y_i \partial y_j} = -\frac{\omega^2 D_{ij}}{4\pi|\underset{\sim}{x}|c_o^2}\frac{\rho_1(1-M_r)^2}{\rho_o}e^{-i\omega t^*} \quad , \tag{5.14}$$

where D_{ij} is a directional factor,

$$D_{pq} = \frac{\rho_o}{\rho_1(1-M_r)^2}\frac{x_p x_q}{|\underset{\sim}{x}|^2} \qquad \text{for} \quad p,q = 1 \text{ or } 2$$

$$D_{p3} = D_{3p} = \frac{x_p x_3}{|\underset{\sim}{x}|^2} \qquad \text{for} \quad p = 1 \text{ or } 2$$

$$D_{33} = \frac{\rho_o}{\rho_1(1-M_r)^2}\alpha^2 \quad .$$

We could use $G_1^c(\underset{\sim}{y},\omega)$ in (5.7) to determine $H\rho'$, but instead we return to equation (5.2) and replace $G_1^+(\underset{\sim}{y},\tau)$ by the compact jet Green function $G_1^c(\underset{\sim}{y},\tau)$,

$$G_1^c(\underset{\sim}{y},\tau) = \frac{1}{2\pi}\int G_1^c(\underset{\sim}{y},\omega)e^{i\omega\tau}d\omega \quad . \tag{5.15}$$

The derivatives of $G_1^c(\underset{\sim}{y},\omega)$ are described by (5.14), and when we evaluate the ω-integral we find

$$\frac{\partial^2 G_1^c(\underset{\sim}{y},\tau)}{\partial y_i \partial y_j} = \frac{\rho_1(1-M_r)^2}{\rho_o 4\pi|\underset{\sim}{x}|c_o^2} D_{ij} \frac{\partial^2}{\partial \tau^2} \delta(\tau - t^*) \quad . \tag{5.16}$$

This expression for G_1^c is similar to the form for a jet of circular cross-section given in (4.24). After G_1^c has been substituted into the representation (5.2), we can rearrange it in the way described in §3.4 to obtain the density perturbation at $\underset{\sim}{x}$, when $x_3 \neq 0$, $M_r \neq 1$,

$$H\rho'(\underset{\sim}{x},t) = \frac{D_{ij}}{4\pi|\underset{\sim}{x}|c_o^4} \int_{v_1} \left[\frac{D}{D\tau} \left\{ \frac{1}{1-N_r} \frac{D}{D\tau} \left(\frac{\rho^* T'_{ij}}{\rho(1-N_r)} \right) \right\} \frac{d^3\underset{\sim}{\eta}}{|1-N_r|} \right] , \tag{5.17}$$

where $N_r = \dfrac{v_1 x_1 + v_2 x_2}{c_o|\underset{\sim}{x}|}$.

The intensity of the sound generated by the Reynolds stress term in T'_{ij} scales as $\rho^2 M^8 h^2/|\underset{\sim}{x}|^2$; Lighthill's eighth power law. $D_{pq} = \rho_o x_p x_q/(\rho_1(1-M_r)^2|\underset{\sim}{x}|^2)$ for $p,q = 1,2$ and again as for the circular cylindrical jet the in-plane quadrupoles are modified by a factor $(1-M_r)^{-2}(1-N_r)^{-3}$. If the two densities ρ_o and ρ_1 are not equal, the density inhomogeneity is an additional source term and the noise scales as $(\Delta\rho)^2 M^6 h^2/|\underset{\sim}{x}|^2$.

When the observer is near the jet axis, we have already shown that G_1^c and all its derivatives are zero. At the jet Mach angle $M_r = 1$, C+D has a large but finite value and G_1^c has a local maximum. The sound field therefore peaks in this direction.

These scaling laws are not valid when the density difference is extreme. In the case of a very light jet, and by that we mean that the jet is even lighter than it is compact, so that $\rho_1 \ll \rho_o \varepsilon$, the low frequency limits are

$$C+D \simeq \frac{\rho_1(1-M_r)^2}{2\rho_o \gamma^2 h} \quad , \quad C-D \simeq -\frac{\rho_1(1-M_r)^2}{2i\rho_o \gamma} \quad , \tag{5.18}$$

for $\alpha \neq 0$, and for all values of the sound speeds c_o and c_1 . γh is small, and so C+D is large, and correct to the lowest order in the compactness ratio ε

$$G_1^c(\underset{\sim}{y},\omega) = \frac{\rho_1(1-M_r)^2 ic_o}{\rho_o 4\pi|\underset{\sim}{x}|h\alpha^2\omega} \sin\theta\sin\phi \; e^{-i\omega t^*} , \tag{5.19}$$

$$\frac{\partial^2 G_1^c(\underset{\sim}{y},\omega)}{\partial y_i \partial y_j} = \frac{-i\omega}{4\pi|\underset{\sim}{x}|c_o h} E_{ij} \frac{\rho_1(1-M_r)^2}{\rho_o} e^{-i\omega t^*} , \tag{5.20}$$

where $$E_{pq} = \frac{x_3 x_p x_q}{\alpha^2|\underset{\sim}{x}|^3} \quad \text{for} \quad p,q = 1,2$$

$$E_{33} = \frac{x_3}{|\underset{\sim}{x}|}$$

and $$E_{p3} = E_{3p} = 0 \quad \text{for} \quad p = 1,2 .$$

This leads to a different form for the compact jet Green function;

$$G_1^c(\underset{\sim}{y},\tau) = \frac{\rho_1(1-M_r)^2 c_o}{\rho_o 4\pi|\underset{\sim}{x}|h} \frac{\sin\theta\sin\phi}{\alpha^2} H(t^*-\tau) \tag{5.21}$$

and $$\frac{\partial^2 G_1^c(\underset{\sim}{y},\tau)}{\partial y_i \partial y_j} = - E_{ij} \frac{\rho_1(1-M_r)^2}{\rho_o 4\pi|\underset{\sim}{x}|hc_o} \frac{\partial}{\partial\tau} \delta(\tau-t^*) . \tag{5.22}$$

Hence, when the jet is excited by a monopole source whose frequency lies in the range $c_o\rho_1/(h\rho_o) \ll \omega \ll c_o/h$, it continues to ring. We can understand this by considering a point source within a slab jet. For a light jet the reflexion coefficient for each face of the slab jet is almost unity, and most of the energy is reflected. At each of the multiple reflexions a small amount of energy leaks out. Because the jet is thin, successive reflexions are in phase, and the sound heard outside the jet persists for some time. This arrangement is illustrated in Figure 3.7. The field of a dipole with its axis in the

3-direction is not enhanced in this way because its reflected wave almost cancels the incident wave.

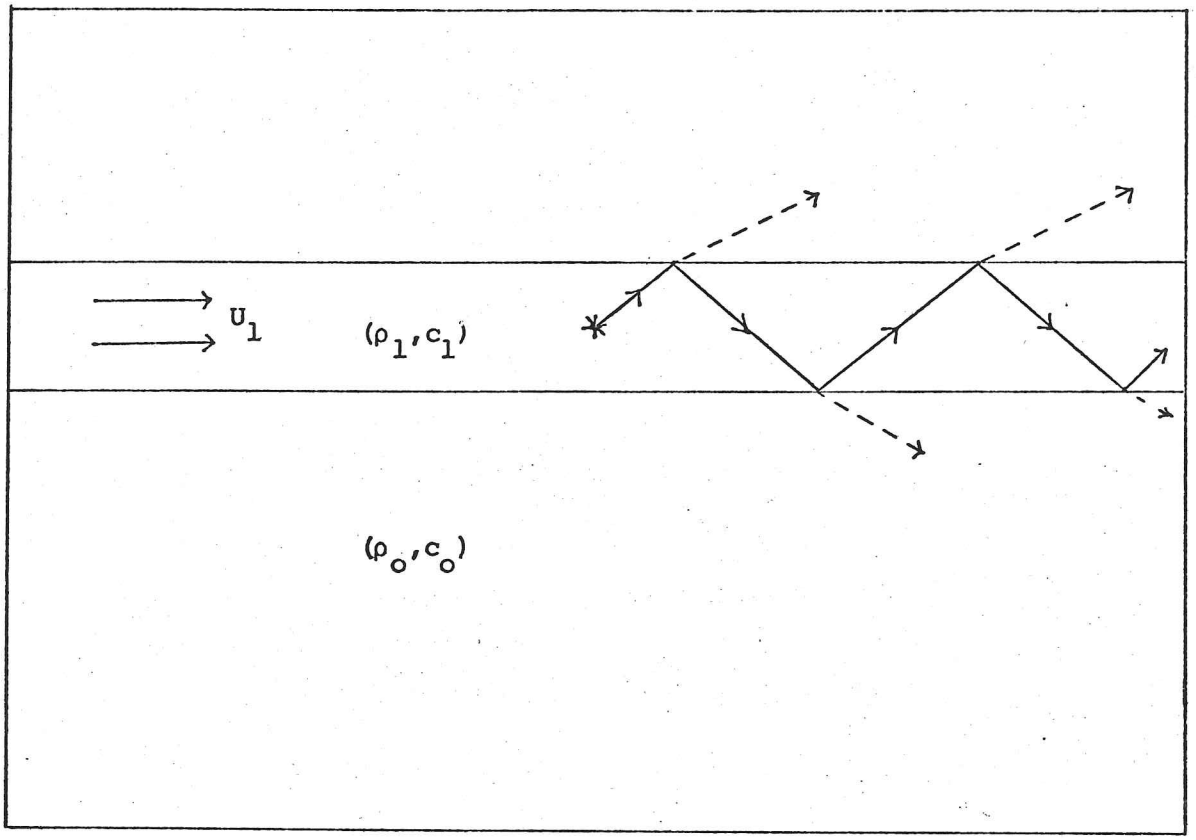

Figure 3.7 Multiple reflexion in a light jet

The far-field density perturbation can be obtained by using the form for the compact Green function in the representation (5.2)

$$H\rho'(\underset{\sim}{x},t) = -\frac{E_{ij}}{4\pi|\underset{\sim}{x}|hc_o^3}\int d\tau \left\{ \int_{\nu_1} \frac{\rho^* T'_{ij}}{\rho} \frac{\partial}{\partial\tau}\delta(\tau-t^*)d^3\underset{\sim}{\eta} \right.$$

$$\left. - \int_{\nu_1(0)} \{\rho_o U_1^2 \delta_{i1}\delta_{j1} - c_1^2(\rho_o-\rho_1)\delta_{ij}\} \frac{\partial}{\partial\tau}\delta(\tau-t^*)d^3\underset{\sim}{y} \right\} . \qquad (5.23)$$

There is only one time derivative acting on the δ-function. $E_{33} = x_3/|\underset{\sim}{x}|$; a 3-3 quadrupole within the jet produces a sound field of the type more usually associated with a dipole normal to the jet, and we would therefore expect the far-field density perturbation to scale on a lower power of the Mach number than Lighthill's eighth power law. To obtain this scaling law explicitly, we rewrite the time derivative,

$$\frac{\partial}{\partial\tau}\,\delta(\tau-t^*) \;=\; \frac{1}{1-N_r}\,\frac{D}{D\tau}\,\delta(\tau-t^*) \quad . \tag{5.24}$$

We substitute this material derivative into (5.23). Then integrate by parts, and evaluate the τ-integral

$$H\rho'(\underset{\sim}{x},t) \;=\; \frac{E_{ij}}{4\pi|\underset{\sim}{x}|hc_o^3}\int_{v_1}\left[\frac{D}{D\tau}\left(\frac{\rho^*T'_{ij}}{\rho(1-N_r)}\right)\frac{d^3\underset{\sim}{\eta}}{|1-N_r|}\right] \quad . \tag{5.25}$$

The intensity of the sound produced by the Reynolds stress term $\rho v'_i v'_j$ scales on $\rho_o^2 M^6 h^2/|\underset{\sim}{x}|^2$ and the noise of the density perturbation term in T'_{ij} scales as $(\Delta\rho)^2 M^4 h^2/|\underset{\sim}{x}|^2$, which means that the sound produced within a light compact jet is less sensitive to changes in the Mach number than the usual Lighthill M^8 law.

For a point $\underset{\sim}{x}$ on the edge of the 'zone of relative silence' where α is zero, i.e. $(1-M_r)^2 c_o^2 = c_1^2\cos^2\theta + c_1^2\sin^2\theta\cos^2\phi$, even for a light jet the expression (5.14) should be used. This Green function leads to the scaling laws $\dfrac{\rho_o^4 M^8 h^2}{\rho_1^2|\underset{\sim}{x}|^2}$, $\dfrac{\rho_o^2\,(\Delta\rho)^2 M^6 h^2}{\rho_1^2|\underset{\sim}{x}|^2}$ and there is a local peak in intensity.

For a compact slab jet, the Green function also has a different form for a heavy jet, although this limit contains no surprises for a jet with a circular cross-section. We will now investigate a very heavy jet which satisfies

$$\alpha\rho_o \;<<\; \rho_1\varepsilon \quad . \tag{5.26}$$

If the sound speeds within the jet, c_1, and the ambient fluid, c_o, are either comparable or c_o is less than c_1, this condition is just

$$\rho_o \;<<\; \rho_1\varepsilon \quad . \tag{5.27}$$

When the two jets have the same specific heat, $\rho_o c_o^2 = \rho_1 c_1^2$, and c_o is

much larger than c_1 . Then,

$$\alpha \simeq (1-M_r)c_o/c_1 = (1-M_r)(\rho_1/\rho_o)^{\frac{1}{2}} , \tag{5.28}$$

and we can write (5.26) as

$$\rho_o^{\frac{1}{2}} << \rho_1^{\frac{1}{2}}\varepsilon ; \tag{5.29}$$

a stronger condition on the density ratio than (5.27). The Green function has a simple form whenever (5.26) is satisfied.

Away from both the jet and the Mach angle

$$C + D \simeq \frac{1}{2i\gamma_o} , \quad C - D \simeq -\frac{1}{2\gamma_o\gamma h} ,$$

and

$$G_1^c(\underset{\sim}{y},\omega) = \frac{(h+y_3)}{4\pi|\underset{\sim}{x}|h} e^{-i\omega t^*} \tag{5.30}$$

$$\frac{\partial G_1^c(\underset{\sim}{y},\omega)}{\partial y_3} = \frac{1}{4\pi|\underset{\sim}{x}|h} e^{-i\omega t^*} , \tag{5.31}$$

or alternatively

$$G_1^c(\underset{\sim}{y},\tau) = \frac{(h+y_3)}{4\pi|\underset{\sim}{x}|h} \delta(\tau-t^*) \tag{5.32}$$

$$\frac{\partial G_1^c(\underset{\sim}{y},\tau)}{\partial y_3} = \frac{1}{4\pi|\underset{\sim}{x}|h} \delta(\tau-t^*) . \tag{5.33}$$

G_1^c varies across the jet on a scale h , and so the spatial derivative across the jet is large, and considerable sound is produced by a dipole with its axis in the 3-direction. It has a radiation field of monopole type.

These results may be easily understood by considering point sources within the jet. In this case of a heavy jet the reflexion coefficient for each face of the jet is -1 . Rays from a dipole with

its axis normal to the jet are reflected many times and the sound field is enhanced.

We can evaluate the second derivatives of $G_1^c(\underset{\sim}{y},\tau)$ and then use them in the representation (5.2) to determine the far-field density perturbation. The (1-3) and (2-3) second derivatives are large; they have a radiation field of the form more usually associated with a dipole with its axis in the 1 and 2 directions respectively;

$$\frac{\partial^2 G_1^c(\underset{\sim}{y},\tau)}{\partial y_p \partial y_3} = -\frac{x_p}{4\pi|\underset{\sim}{x}|^2 hc_o}\frac{\partial\delta(\tau-t^*)}{\partial\tau} + O\left(\frac{1}{|\underset{\sim}{x}|c_o^2}\frac{\partial^2\delta}{\partial\tau^2}\right) \quad \text{for} \quad p = 1,2. \tag{5.34}$$

Although the other second derivatives of $G_1^c(\underset{\sim}{y},\tau)$ are smaller in magnitude, we still need to determine them, because in (5.2) $\nabla^2 G_1^c$ is multiplied by $c_1^2\Delta\rho$ the largest term in the source T'_{ij}.

$$\nabla^2 G_1^c(\underset{\sim}{y},\tau) = \frac{(1-M_r)^2}{4\pi|\underset{\sim}{x}|c_1^2}\frac{h+y_3}{h}\frac{\partial^2\delta(\tau-t^*)}{\partial\tau^2} \quad . \tag{5.35}$$

When only the lowest order terms are retained in (5.2), we find that away from the jet and the Mach angle

$$H\rho'(\underset{\sim}{x},t) = \frac{2\rho_o}{\rho_1(1-M_r)^2}\frac{x_p}{4\pi|\underset{\sim}{x}|^2 hc_o^3}\int_{\nu_1}\left[\frac{D}{D\tau}\left(\frac{\rho^* T'_{p3}}{\rho(1-N_r)}\right)\frac{d^3\underset{\sim}{\eta}}{|1-N_r|}\right]$$

$$+\frac{\rho_o}{\rho_1 4\pi|\underset{\sim}{x}|hc_o^2}\int_{\nu_1}\left[\frac{D}{D\tau}\left\{\frac{1}{1-N_r}\frac{D}{D\tau}\left(\frac{\rho^*(h+y_3)\Delta\rho}{\rho(1-N_r)}\right)\right\}\frac{d^3\underset{\sim}{\eta}}{|1-N_r|}\right] \quad , \tag{5.36}$$

where p is summed over 1 and 2 . The intensity of the sound produced by the first term on the right-hand side scales as $\rho_o M^6 h^2/|\underset{\sim}{x}|^2$ and the second term as $\rho_o^2(\Delta\rho)^2 M^4/(\rho_1^2|\underset{\sim}{x}|^2)$.

By considering a slab jet, we have shown that different scaling laws apply in the case of a compact jet that is either very heavy or

very light. Although stronger conditions at infinity, (5.1), had to be assumed before the general theory could be applied to a slab jet, it was nevertheless still instructive; it helped to clarify the physics behind the somewhat surprising results obtained in §3.4 for a circular cylindrical jet and gives us confidence that the phenomenon is not simply an artifact of the theoretical procedure.

3.6 Conclusions

We have obtained an exact analogy between the sound produced by turbulence within a mean flow, and quadrupoles within a vortex sheet. This theory shows that the jet noise problem may be modelled by particle attached quadrupoles convected with the velocity of the actual fluid particles but positioned within a hypothetical instability-free vortex sheet. The strength of each quadrupole is Lighthill's stress tensor per unit mass. Equation (2.34) expresses our main result. Mani's (1976) work has shown that this type of model agrees well with experiment and our theory justifies Mani's general procedure while establishing the source characteristics needed for an exact result. They differ from and are simpler than those used by Mani which contain spurious monopoles and dipoles due to density gradient terms. The effect of density variation on the source is shown to vanish unless the density or the velocity of a material particle changes.

The deliberate emphasis on 'finiteness' rather than 'causality' in our analogy results in the shear layer's instability waves, that grow into turbulence, being heard as sound that builds up as a precursor of the main turbulence driven field.

Some jet flows will also support neutrally stable free waves that travel without decay along the jet at constant speed. These might provide a means by which distant irrelevant details of the jet's history

are retained as a source of sound, but we have shown that the effect of these vortex sheet resonances is to ensure that the equivalent sources vanish at infinity. Moreover for jets with particular geometries, a round or a slab jet, we were able to show that these resonances cannot propagate into the distant sound field; the sound field is totally uncoupled from any free modes of the basic flow.

We have examined a compact circular jet in some detail, and in addition to some previously known features of the mean flow acoustic interaction, for example that negligible sound is heard on the jet axis (Dash 1976b), and that the density perturbation produced by the longitudinal quadrupoles is modified by five Doppler factors (Mani 1976), we have uncovered an interesting new aspect of the problem. Whenever the jet is very light, it can provide a wave guide in which the effects of source activity persist for some time but eventually leak out as sound. This interaction drastically distorts the far-field characteristics of the turbulent sources and in fact results in the Reynolds stress induced waves having an intensity which scales with only the fourth power of jet velocity rather than Lighthill's eighth power law for free quadrupoles. The source terms associated with density inhomogeneities have an even lower sensitivity to jet speed variation, the intensity of their sound scaling on the square of the jet speed. We also considered a compact slab jet of very light fluid and showed that the sound produced scales on the fourth power of the Mach number. We do not think that these results are a spurious artifact of the model, but believe that they may have some bearing on the so-called 'excess noise' problem. There, the noise of real hot jets is known to be much less sensitive to velocity changes than the U^8 dependence thought to be relevant to the 'pure mixing' noise of a low Mach number jet.

Our exact extension of the Lighthill theory includes mean flow acoustic interaction in a way that is analytically tractable, and which

may be useful in describing the sound produced by real turbulent flows. We believe that in many applications our modelling will be representative of the real thing; the success of Mani's calculations supports this belief.

The work described in this chapter has been published as a joint paper with both Professor Ffowcs Williams and Dr. Goldstein (Dowling, Ffowcs Williams & Goldstein, 1978 Phil.Trans.Roy.Soc. A288, 321-349). The theory is based on an initial idea of Dr. Goldstein. He used a Green function, which satisfied the convected wave equation within the jet and the non-convected form outside, to describe the sound produced by a jet. But he took a fixed dividing surface and his results had no obvious physical meaning and were in fact initially incorrect in some respects. Professor Ffowcs Williams then showed that the vortex sheet Green function emerged naturally if the Leibnitz terms in Dr. Goldstein's analysis were modified to describe a moving surface, but his arguments were not at that time watertight. I expanded on his arguments and added some rigour. In doing so, certain fundamental questions concerning resonances and instabilities were thrown into sharp perspective. To analyse the problem more thoroughly I recast the theory in terms of generalized functions and investigated the effect of those resonances; although the more complex points were only resolved after many helpful discussions with Professor Ffowcs Williams. The new results on the singular nature of the 'light jet' Green function and the prediction of the anomalously low velocity index in that case were entirely mine.

CHAPTER 4

THE SOUND OF A SUDDENLY TENSIONED MEMBRANE

4.1 Introduction

A significant part of the noise of a modern rotary press is thought to be associated with the vibration of the web of paper that moves under variable tension between high speed rollers (Ffowcs Williams 1976b). In this chapter we attempt to model this process. Printers have noticed that the noise of a press alters when it is run with different types of paper, and we try to determine what parameters control the membrane noise and the sensitivity of the sound field to changes in these variables. The practical problem is extremely complex, and our model is necessarily highly idealized.

We consider a semi-infinite elastic sheet initially at rest with a small prescribed displacement. The sound field produced by suddenly tugging one end is investigated in the case where the sheet parameters are chosen to resemble typical paper. When a sheet is tugged in this way it produces a loud cracking sound. Bernstein et al. (1958) studied a related impulsive problem. They discovered that the distinctive cracking of a whip occurs when the tip of the whip moves supersonically and they produced very clear photographs of the Mach waves induced by that motion.

We first determine the displacement of the sheet by solving the elastic equations of motion within the membrane, in the limit where the fluid loading has a negligible effect on the web response. It is found that a tension wave propagates supersonically through the sheet and triggers off a transverse vibration. The sheet is stationary ahead of the tension front and behind it the sheet is uniformly tensioned and supports the waves associated with a tensioned elastic membrane. This transverse wave is composed of elements propagating in both directions with a constant,

usually subsonic, speed and may be expressed in terms of the prescribed initial displacement.

Once the normal displacement of the sheet has been determined for all time we can write down an expression for the sound produced. It is found that the motion of the sheet is silent except at the tugged end and at the tension front. Transverse waves are reflected noisily from the tugged end and the sudden switch-on of normal velocity at the tension front is like a supersonically moving sound source. Sound is only heard within a two-dimensional Mach wedge, with the Mach number being based on the speed of the tension waves. The far-field density perturbation has all the characteristic features of a two-dimensional sound field; it decays as the inverse square-root of distance from the source, and involves half-derivatives and Doppler factors. When the tension is applied instantaneously there is a 'sonic boom' that travels in an unattenuated beam on the Mach wedge, but whenever the tension is applied over a small non-zero time the strength of the density perturbation on the Mach wedge in the far-field does decay with the inverse square-root of the distance of the observer from the source.

The parameters that control the noise produced are α/c , β/c , $\bar{h}$ and ℓ , where α is the speed of the tension front, β the speed of the transverse waves in the membrane and c is the speed of sound in the fluid. $\bar{h}$ is a typical height of the initial displacement of the sheet, and ℓ is the length over which this displacement varies. The intensity of the noise from the tugged end scales as $\rho_o \beta^3 \bar{h}^2/(\ell r)$, with ρ_o the density of the fluid and r the distance of the observer from the source; the frequency of this sound varies with $\beta \ell^{-1}(1+\beta/\alpha)^{-1}$. Within the Mach wedge the intensity of the sound produced at the tension front scales as $\rho_o \alpha \beta^4 \bar{h}^2/\{c^2 \ell r(1-\alpha \cos\phi/c)\}$, where ϕ is the angle between the observer and the direction of motion of the tension front. The frequency of this

sound undergoes a Doppler shift because the source is moving; it is proportional to $\alpha l^{-1}|1-\alpha\cos\phi/c|^{-1}$. These scaling laws do not describe the sound field on the Mach wedge, there the mean intensity is proportional to $\rho_o\beta^{4-2}h^2/\{cl^2(\alpha^2/c^2-1)\}$ and the frequency to $\alpha l^{-1}(\alpha^2/c^2-1)^{-1}$, when the tension is applied instantaneously.

The effect of fluid loading is also investigated. It is found to be important when the sheet is very thin. The surrounding fluid then dampens the motion of the membrane, because the sheet loses energy which propagates into the far-field. Sound is radiated from all points behind the tension front. However when the fluid is much less dense than the membrane the strongest sound sources are still at the tugged end and at the tension front.

4.2 The sound of a suddenly tensioned membrane

We consider an elastic sheet of uniform thickness d , which when undeformed lies in the 1,2-plane and occupies the region $y_1 \geq 0$, $\infty \geq y_2 \geq -\infty$. Initially the membrane is at rest with a prescribed vertical displacement, $h(y_1)$, and then the end at $y_1 = 0$ is tugged. We investigate the sound waves propagated into the surrounding fluid; a problem which is independent of the y_2-coordinate. This situation is illustrated in Figure 4.1. The vertical displacement of the membrane from $y_3 = 0$ at a point y_1 and time τ is denoted by $\xi(y_1,\tau)$, and the in-plane displacement in the 1-direction by $u_1(y_1,\tau)$. We consider the plate to be thin compared with the deflections, $|\xi| >> d$; then the resistance of the sheet to bending is small. However the deflections themselves are small in comparison with l , a typical length over which $h(y_1)$ varies, so that the stress set up in the membrane may be related to the strain by the linear elastic constitutive relations. The elastic equations of motion are derived in Appendix 4.A by a simple extension of

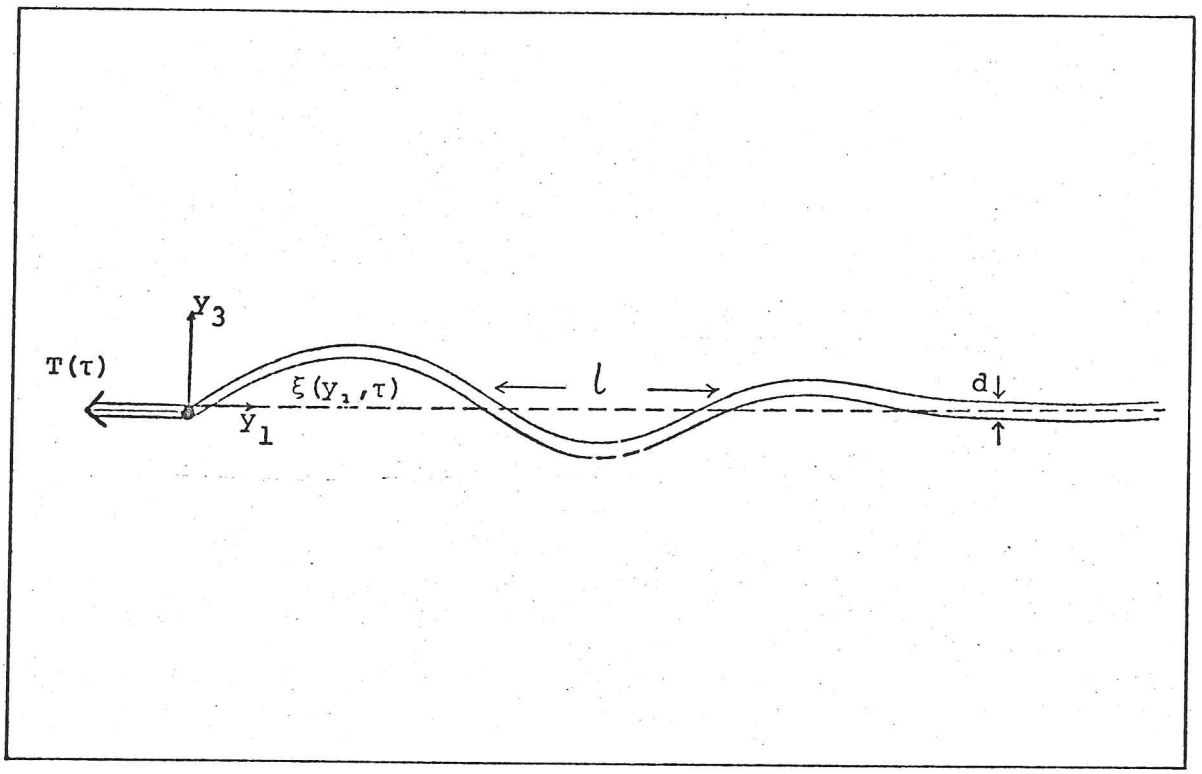

Figure 4.1 The initial position of the membrane

the procedure described by Landau and Lifshitz (1959, II §14), and they are shown to be

$$\rho_M \frac{\partial^2 u_1}{\partial \tau^2} - \frac{E}{1-\nu^2} \frac{\partial^2 u_1}{\partial y_1^2} = 0 \qquad (2.1)$$

$$d \left\{ \rho_M \frac{\partial^2 \xi}{\partial \tau^2} - \frac{\partial}{\partial y_1} \left(\sigma_{11} \frac{\partial \xi}{\partial y_1} \right) \right\} = P \ , \qquad (2.2)$$

where ρ_M is the density, E Young's modulus and ν Poisson's ratio for the material in the sheet. $\sigma_{11}(y_1,\tau)$ is the 1-1 component of the stress tensor and is related to the in-plane deformation by linear elasticity ,

$$\sigma_{11} = \frac{E}{1-\nu^2} \frac{\partial u_1}{\partial y_1} \ . \qquad (2.3)$$

P is the external force per unit area applied to the sheet in

the y_3-direction, and since the membrane is surrounded by fluid P is just the difference in pressure on either side of the sheet. If we assume the density of the material in the sheet to be much greater than that of the fluid, we may neglect the fluid loading P . The effect of including this term is described later. The bending stiffness has been neglected in equation (2.2), because it is of order d^2/ℓ^2 smaller than the terms retained.

We now want to solve these equations for u_1 and ξ subject to the prescribed initial and boundary conditions. Initially the membrane is at rest with a vertical displacement $h(y_1)$ $(h(0) = 0)$, and there is no in-plane deformation;

$$\xi(y_1,0) = h(y_1) \quad , \quad \frac{\partial \xi}{\partial \tau}(y_1,0) = 0 \quad , \quad u_1(y_1,0) = 0 \quad \text{for} \quad y_1 \geq 0 \quad . \tag{2.4}$$

When the end of the sheet is tugged the normal component of stress in the membrane must be equal to the applied tension, which we denote by $T(\tau)$, and there can be no vertical displacement. The boundary conditions are therefore

$$\xi(0,\tau) = 0 \qquad \text{and} \qquad \sigma_{11}(0,\tau) = \frac{E}{1-\nu^2}\frac{\partial u_1}{\partial y_1}(0,\tau) = T(\tau) \quad . \tag{2.5}$$

The problem for $u_1(y_1,\tau)$ can now easily be solved to obtain

$$u_1(y_1,\tau) = -\frac{\alpha(1-\nu^2)}{E}\int_0^{\tau - y_1/\alpha} T(\tilde{\tau})\,d\tilde{\tau} \quad , \tag{2.6}$$

where $\alpha = \left(\frac{E}{\rho_M(1-\nu^2)}\right)^{\frac{1}{2}}$ is the speed of longitudinal waves in an elastic plate. Then using (2.3) we find that

$$\sigma_{11}(y_1,\tau) = T(\tau - y_1/\alpha) \quad ; \tag{2.7}$$

a tension front propagates along the sheet with speed α .

When the tension is applied instantaneously, $T(\tau) = T_o H(\tau)$, where T_o is a constant and H is a Heaviside function. We can use equation (2.6) to investigate the effect of this applied tension on the in-plane displacement

$$\frac{\partial u_1}{\partial \tau} = \begin{cases} 0 & \text{at } y_1 = 0 \text{ for } \tau < 0 \\ -T_o/(\alpha \rho_M) & \text{at } y_1 = 0 \text{ for } \tau > 0 \end{cases} ; \tag{2.8}$$

when the sheet is pulled with a uniform tension the end has a uniform velocity and our solution for a membrane tugged with a uniform tension also solves the problem of a sheet pulled at a constant rate.

In the limit where the surrounding fluid has a negligible effect on the membrane, the problem for ξ reduces to the simpler form

$$\frac{\partial^2 \xi}{\partial \tau^2} - \beta^2 \frac{\partial}{\partial y_1}\left(H(\tau - y_1/\alpha) \frac{\partial \xi}{\partial y_1} \right) = 0 , \tag{2.9}$$

where $\beta = (T_o/\rho_M)^{\frac{1}{2}}$ is the speed of transverse waves in a tensioned membrane. This equation, subject to the initial conditions (2.4), has a solution of the form

$$\xi(y_1, \tau) = \begin{cases} h(y_1) & \text{for } \tau < y_1/\alpha \\ f_1(y_1 + \beta\tau) + f_2(y_1 - \beta\tau) & \text{for } \tau > y_1/\alpha \end{cases} . \tag{2.10}$$

The functions f_1 and f_2 represent propagating waves in the membrane behind the tension front. They can be determined by the conditions at $y_1 = \alpha\tau$ and $y_1 = 0$. Obviously the displacement ξ must be continuous at $y_1 = \alpha\tau$. We can obtain a second condition by integrating equation (2.9) across the tension front from $y_1 = \alpha\tau - \varepsilon$ to $y_1 = \alpha\tau + \varepsilon$, where ε is a small parameter.

$$\int_{\alpha\tau-\varepsilon}^{\alpha\tau+\varepsilon} \frac{\partial^2 \xi}{\partial \tau^2} \, dy_1 = \beta^2 \left[H(\tau - y_1/\alpha) \frac{\partial \xi}{\partial y_1} \right]_{\alpha\tau-\varepsilon}^{\alpha\tau+\varepsilon} . \tag{2.11}$$

But

$$\int_{\alpha\tau-\varepsilon}^{\alpha\tau+\varepsilon} \frac{\partial^2\xi}{\partial\tau^2}\, dy_1 = \frac{\partial^2}{\partial\tau^2}\int_{\alpha\tau-\varepsilon}^{\alpha\tau+\varepsilon} \xi\, dy_1 - \left[\alpha\frac{\partial\xi}{\partial\tau}\right]_{\alpha\tau-\varepsilon}^{\alpha\tau+\varepsilon} - \frac{\partial}{\partial\tau}\left[\alpha\xi\right]_{\alpha\tau-\varepsilon}^{\alpha\tau+\varepsilon}$$

$$= \left[-\alpha\frac{\partial\xi}{\partial\tau}\right]_{\alpha\tau-\varepsilon}^{\alpha\tau+\varepsilon}, \qquad (2.12)$$

because ξ is continuous at $y_1 = \alpha\tau$ and ε is infinitesimal. A second jump condition for ξ may be found by substituting equation (2.12) into (2.11). These two conditions give f_1 and f_2 up until a time $\tau = y_1/\alpha$.

$$\xi(y_1,\tau) = \tfrac{1}{2}h\left(\frac{y_1+\beta\tau}{1+\beta/\alpha}\right) + \tfrac{1}{2}h\left(\frac{y_1-\beta\tau}{1-\beta/\alpha}\right) \quad \text{for} \quad y_1/\beta \geq \tau \geq y_1/\alpha . \qquad (2.13)$$

After $\tau = y_1/\beta$ the wave reflected from the fixed end arrives at y_1. This wave may be determined by applying the end condition, $\xi(0,\tau) = 0$, and two jump conditions across $y_1 = \beta\tau$. ξ must be continuous at $y_1 = \beta\tau$ and a second condition may be derived exactly as before by integrating equation (2.9) across the reflected wave front, from $y_1 = \beta\tau-\varepsilon$ to $y_1 = \beta\tau+\varepsilon$. We find

$$\xi(y_1,\tau) = \tfrac{1}{2}h\left(\frac{y_1+\beta\tau}{1+\beta/\alpha}\right) - \tfrac{1}{2}h\left(\frac{\beta\tau-y_1}{1+\beta/\alpha}\right) \quad \text{for} \quad \tau \geq y_1/\beta . \qquad (2.14)$$

Then if we linearize in ξ, the normal fluid velocity on the surface $y_3 = 0$, $v(y_1,\tau)$, is just the time derivative of ξ and is given by

$$v(y_1,\tau) = \begin{cases} g_1(y_1+\beta\tau) + g_2(y_1-\beta\tau) & \text{for} \quad \alpha\tau > y_1 > 0 \\ 0 & \text{for} \quad y_1 > \alpha\tau \end{cases} \qquad (2.15)$$

where

$$g_1(\eta_1) = \tfrac{1}{2}\frac{\beta}{1+\beta/\alpha}\, h'\left(\frac{\eta_1}{1+\beta/\alpha}\right),$$

$$g_2(\eta_1) = -\tfrac{1}{2}\left\{\frac{\beta}{1-\beta/\alpha}\, H(\eta_1)h'\left(\frac{\eta_1}{1-\beta/\alpha}\right) + \frac{\beta}{1+\beta/\alpha}\, H(-\eta_1)h'\left(-\frac{\eta_1}{1+\beta/\alpha}\right)\right\}, \qquad (2.16)$$

and the prime denotes differentiation with respect to the argument.

If we suppose that the elastic membrane is tugged by a plane rigid sheet which lies on $y_3 = 0$ in $y_1 \lesseqgtr 0$, as illustrated in Figure 4.2,

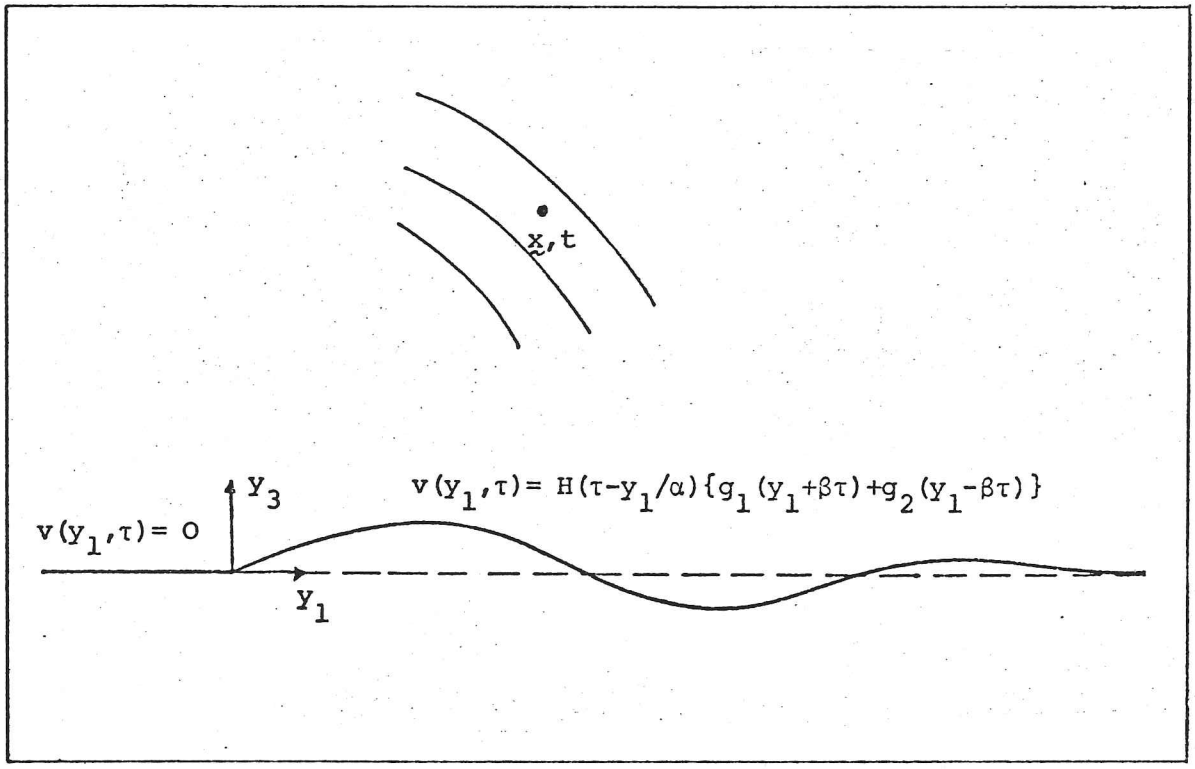

Figure 4.2 The boundary conditions determining the sound field

we also know the normal velocity for negative y_1 ;

$$\text{on} \quad y_3 = 0 \quad , \quad v(y_1,\tau) = 0 \qquad \text{for} \quad y_1 \lesseqgtr 0 \ , \ -\infty \lesseqgtr y_2 \lesseqgtr \infty \quad . \tag{2.17}$$

In the region $y_3 > 0$, the compressible fluid is only linearly disturbed and therefore the flow satisfies the homogeneous wave equation. We can express the perturbation density at a point $(\underset{\sim}{x},t)$ in terms of the fluid motion on the surface $y_3 = 0$ by using the exact Green function for the half-space;

$$(\rho-\rho_o)(\underset{\sim}{x},t) = \frac{\rho_o}{2\pi c^2}\frac{\partial}{\partial t}\int\left[\frac{v(y_1,\tau)}{|\underset{\sim}{x}-\underset{\sim}{y}|}\right]dy_1dy_2 \quad ; \tag{2.18}$$

ρ is the actual fluid density, ρ_o and c are the unperturbed values of density and sound speed in the fluid, and the square brackets denote that the function they enclose is to be evaluated at a retarded time $\tau = t-|\underset{\sim}{x}-\underset{\sim}{y}|/c$.

When we substitute v from equations (2.15) and (2.17) into this expression we find

$$(\rho-\rho_o)(\underset{\sim}{x},t) = \frac{\rho_o}{2\pi c^2}\frac{\partial}{\partial t}\int_{y_2=-\infty}^{\infty}\int_{y_1=0}^{\infty}\left[\frac{H(\tau-y_1/\alpha)\{g_1(y_1+\beta\tau)+g_2(y_1-\beta\tau)\}}{|\underset{\sim}{x}-\underset{\sim}{y}|}\right] dy_1 dy_2. \tag{2.19}$$

The speed, α , of the tension front in a sheet of paper has been measured by various experimenters (Horio & Onogi 1951, Craver & Taylor 1965). They have found that it varies with the stiffness and moisture content of the paper but that typically it is between 1,000 and 2,000 m/sec . It is therefore certainly greater than c , the speed of sound waves in air. We will consider the case when the speed of the transverse waves β is subsonic, which means that the applied tension T_o is less than $c^2\rho_M$.

Equation (2.19) represents the sound produced by sources g_1 and g_2 convected with a constant speed β , which switch on at $y_1 = 0$ and off at $y_1 = \alpha\tau$. It is well known that a non-evolving source moving with a constant subsonic velocity produces no sound. We would therefore expect g_1 and g_2 to be silent except at their end-points. The integral in (2.19) can be rearranged to show this explicitly; the details are given in Appendix 4.B. We find for $\underset{\sim}{x}$ in the far-field

$$(\rho-\rho_o)(\underset{\sim}{x},t) = J_1 + J_2 + O(\ell/R) \tag{2.20}$$

where

$$J_1 = -\frac{\rho_o\beta^2 H(t-R/c)}{\pi c(1+\beta/\alpha)}\int_{\tau=o}^{t-R/c}\frac{h'(\beta\tau\{1+\beta/\alpha\}^{-1})\,d\tau}{\{c^2(t-\tau)^2-R^2\}^{\frac{1}{2}}(1-\beta^2\cos^2\theta/c^2)} \tag{2.21}$$

and

$$J_2 = -\frac{\rho_o \beta^2 \alpha}{\pi c^2} \int_{\tau=0}^{\infty} \frac{H\left(t-\tau-\{(x_1-\alpha\tau)^2+x_3^2\}^{\frac{1}{2}}/c\right)h'(\alpha\tau)\cos\phi\, d\tau}{\left\{c^2(t-\tau)^2-(x_1-\alpha\tau)^2-x_3^2\right\}^{\frac{1}{2}}(1-\beta^2\cos^2\phi/c^2)} \tag{2.22}$$

with

$$R = (x_1^2+x_3^2)^{\frac{1}{2}} \quad , \quad \cos\theta = \frac{x_1}{c(t-\tau)} \quad , \quad \cos\phi = \frac{x_1-\alpha\tau}{c(t-\tau)} \quad ,$$

and we have neglected terms in (2.20) which are of order ℓ/R smaller than those retained.

The integral J_1 represents the sound field produced by a line source at $y_1 = 0$ of varying strength h. We see that the sound at the field point $\underset{\sim}{x}$ does not only depend on the source at a time R/c earlier but on all previous times as well. The source at each time is weighted differently by the square-root factor, and since the denominator is singular at $\tau = t-R/c$ the main contribution to the sound in the far-field comes from that region.

A Taylor expansion shows that

$$\frac{1}{\{c(t-\tau)+R\}^{\frac{1}{2}}(1-\beta^2\cos^2\theta/c^2)} = \frac{1}{(2R)^{\frac{1}{2}}(1-\beta^2\cos^2\theta_o/c^2)} + \{c(t-\tau)-R\} \times O\left(\frac{1}{R^{3/2}}\right) \tag{2.23}$$

where $\cos\theta_o = x_1/R$.

When we use this to rewrite the denominator in J_1, we obtain

$$J_1 = -\frac{\rho_o \beta^2 H(t-R/c)}{(2R)^{\frac{1}{2}}\pi c(1+\beta/\alpha)(1-\beta^2\cos^2\theta_o/c^2)} \int_o^{t-R/c} \frac{h'(\beta\tau\{1+\beta/\alpha\}^{-1})\,d\tau}{\{c(t-\tau)-R\}^{\frac{1}{2}}}$$

$$+ O(R^{-3/2})H(t-R/c) \int_o^{t-R/c} \{c(t-\tau)-R\}^{\frac{1}{2}} h'(\beta\tau\{1+\beta/\alpha\}^{-1})\,d\tau \quad . \tag{2.24}$$

An integration by parts shows that the second term on the right-hand side is $O(\ell/R)$ smaller than the first and so is negligible for $\underset{\sim}{x}$ in

the far-field. Therefore

$$J_1 = -\left(\frac{\beta^3}{2Rc^3(1+\beta/\alpha)}\right)^{\frac{1}{2}} \frac{\rho_o H(t-R/c)}{\pi(1-\beta^2\cos^2\theta_o/c^2)} F\left(\frac{\beta(t-R/c)}{1+\beta/\alpha}\right) , \qquad (2.25)$$

where

$$F(z) = \int_o^z \frac{h'(s)}{(z-s)^{\frac{1}{2}}} ds .$$

We have shown that the contribution to the sound field from the tugged end has all the usual properties of a line source. In the far-field the density perturbation decays with the inverse square-root of the distance from the source. It is modified by Doppler factors based on the speed of the tension waves and involves a half-derivative of h. The relation between F and h is the definition of a half-derivative, since two applications of this operator give the derivative of h (see Oldham & Spanier 1974).

The second integral J_2 describes the sound field of a moving line source of variable strength at $y_1 = \alpha\tau$. The integrand is multiplied by $H\left(t-\tau-\{(x_1-\alpha\tau)^2+x_3^2\}^{\frac{1}{2}}/c\right)$. For $(\underset{\sim}{x},t)$ outside the Mach wedge, i.e. for $(\underset{\sim}{x},t)$ such that $c^2(x_1-\alpha t)^2 \leq x_3^2(\alpha^2-c^2)$, this Heaviside function is zero for all τ. When the field point is within the Mach wedge the Heaviside function is non-zero for values of τ between τ_1 and τ_2, where τ_1 and τ_2 are the two solutions of

$$c(t-\tau) = \{(x_1-\alpha\tau)^2+x_3^2\}^{\frac{1}{2}} \qquad (2.26)$$

which means

$$\tau_1 = \frac{\alpha x_1 - c^2 t + \sqrt{c^2(x_1-\alpha t)^2 - x_3^2(\alpha^2-c^2)}}{\alpha^2 - c^2} \qquad (2.27)$$

and

$$\tau_2 = \frac{\alpha x_1 - c^2 t - \sqrt{c^2(x_1-\alpha t)^2 - x_3^2(\alpha^2-c^2)}}{\alpha^2 - c^2} . \qquad (2.28)$$

the far-field. Therefore

$$J_1 = -\left(\frac{\beta^3}{2Rc^3(1+\beta/\alpha)}\right)^{\frac{1}{2}} \frac{\rho_o H(t-R/c)}{\pi(1-\beta^2\cos^2\theta_o/c^2)} F\left(\frac{\beta(t-R/c)}{1+\beta/\alpha}\right) , \qquad (2.25)$$

where

$$F(z) = \int_o^z \frac{h'(s)}{(z-s)^{\frac{1}{2}}} ds .$$

We have shown that the contribution to the sound field from the tugged end has all the usual properties of a line source. In the far-field the density perturbation decays with the inverse square-root of the distance from the source. It is modified by Doppler factors based on the speed of the tension waves and involves a half-derivative of h. The relation between F and h is the definition of a half-derivative, since two applications of this operator give the derivative of h (see Oldham & Spanier 1974).

The second integral J_2 describes the sound field of a moving line source of variable strength at $y_1 = \alpha\tau$. The integrand is multiplied by $H\left(t-\tau-\{(x_1-\alpha\tau)^2+x_3^2\}^{\frac{1}{2}}/c\right)$. For $(\underset{\sim}{x},t)$ outside the Mach wedge, i.e. for $(\underset{\sim}{x},t)$ such that $c^2(x_1-\alpha t)^2 \leq x_3^2(\alpha^2-c^2)$, this Heaviside function is zero for all τ. When the field point is within the Mach wedge the Heaviside function is non-zero for values of τ between τ_1 and τ_2, where τ_1 and τ_2 are the two solutions of

$$c(t-\tau) = \{(x_1-\alpha\tau)^2+x_3^2\}^{\frac{1}{2}} \qquad (2.26)$$

which means

$$\tau_1 = \frac{\alpha x_1 - c^2 t + \sqrt{c^2(x_1-\alpha t)^2 - x_3^2(\alpha^2-c^2)}}{\alpha^2 - c^2} \qquad (2.27)$$

and

$$\tau_2 = \frac{\alpha x_1 - c^2 t - \sqrt{c^2(x_1-\alpha t)^2 - x_3^2(\alpha^2-c^2)}}{\alpha^2 - c^2} . \qquad (2.28)$$

the far-field. Therefore

$$J_1 = -\left(\frac{\beta^3}{2Rc^3(1+\beta/\alpha)}\right)^{\frac{1}{2}} \frac{\rho_o H(t-R/c)}{\pi(1-\beta^2\cos^2\theta_o/c^2)} F\left(\frac{\beta(t-R/c)}{1+\beta/\alpha}\right) , \qquad (2.25)$$

where

$$F(z) = \int_o^z \frac{h'(s)}{(z-s)^{\frac{1}{2}}} ds .$$

We have shown that the contribution to the sound field from the tugged end has all the usual properties of a line source. In the far-field the density perturbation decays with the inverse square-root of the distance from the source. It is modified by Doppler factors based on the speed of the tension waves and involves a half-derivative of h. The relation between F and h is the definition of a half-derivative, since two applications of this operator give the derivative of h (see Oldham & Spanier 1974).

The second integral J_2 describes the sound field of a moving line source of variable strength at $y_1 = \alpha\tau$. The integrand is multiplied by $H\left(t-\tau-\{(x_1-\alpha\tau)^2+x_3^2\}^{\frac{1}{2}}/c\right)$. For $(\underset{\sim}{x},t)$ outside the Mach wedge, i.e. for $(\underset{\sim}{x},t)$ such that $c^2(x_1-\alpha t)^2 \leq x_3^2(\alpha^2-c^2)$, this Heaviside function is zero for all τ. When the field point is within the Mach wedge the Heaviside function is non-zero for values of τ between τ_1 and τ_2, where τ_1 and τ_2 are the two solutions of

$$c(t-\tau) = \{(x_1-\alpha\tau)^2+x_3^2\}^{\frac{1}{2}} \qquad (2.26)$$

which means

$$\tau_1 = \frac{\alpha x_1 - c^2 t + \sqrt{c^2(x_1-\alpha t)^2 - x_3^2(\alpha^2-c^2)}}{\alpha^2 - c^2} \qquad (2.27)$$

and

$$\tau_2 = \frac{\alpha x_1 - c^2 t - \sqrt{c^2(x_1-\alpha t)^2 - x_3^2(\alpha^2-c^2)}}{\alpha^2 - c^2} . \qquad (2.28)$$

Hence no sound is heard at a point $(\underset{\sim}{x},t)$ outside the Mach wedge. Within this wedge the density at the field point depends on the source between the times τ_1 and τ_2. The source strength is zero at negative times before the sheet has been tugged, and therefore the sound field is only non-zero if $\tau_1 > 0$, which means sound is only heard in the region shaded in Figure 4.3. This diagram also shows where τ_2 is positive.

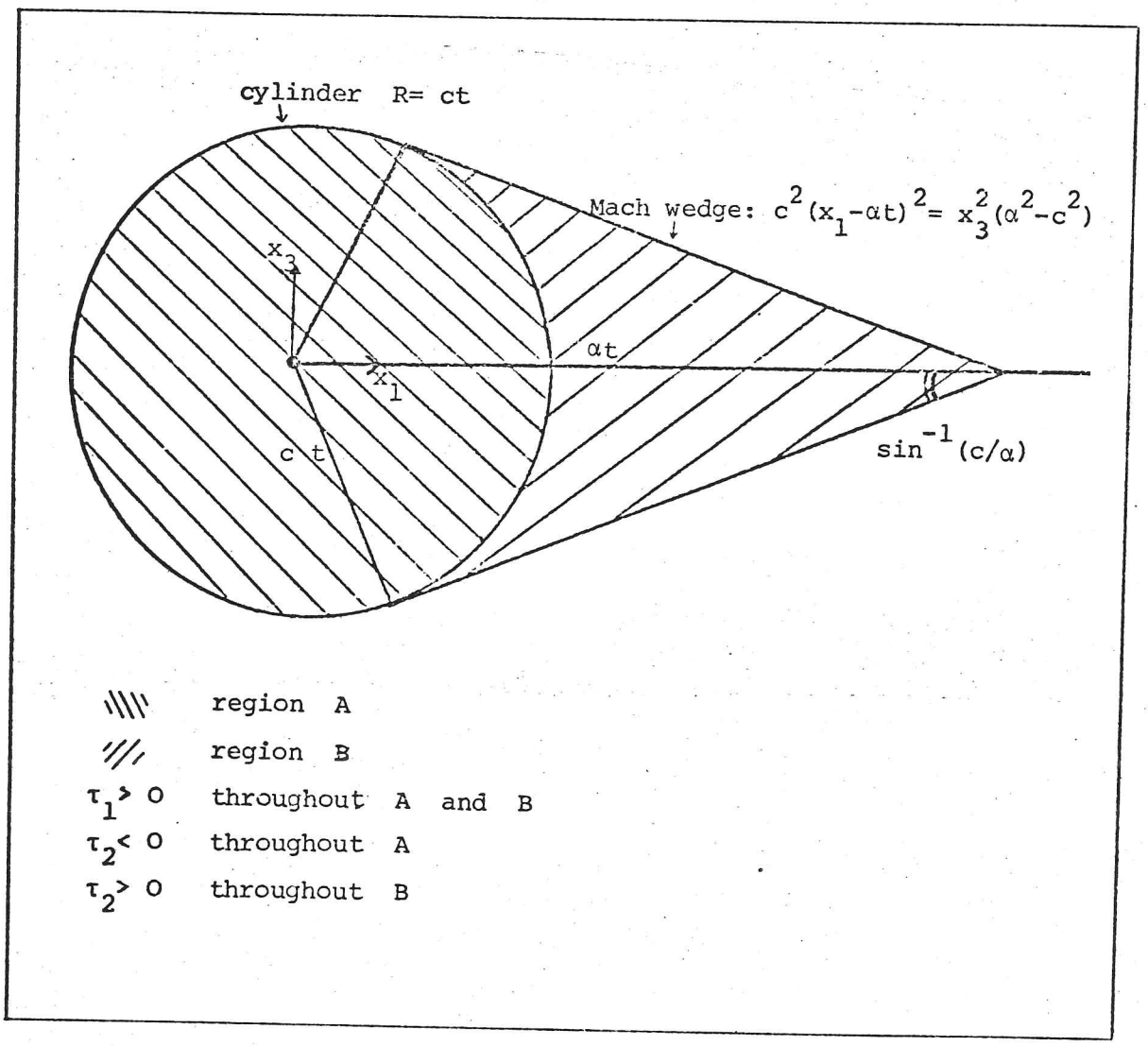

Figure 4.3 The Mach wedge

We can factorize the denominator of the integrand in J_2 by writing

$$c^2(t-\tau)^2 - (x_1-\alpha\tau)^2 - x_3^2 = (\alpha^2-c^2)(\tau_1-\tau)(\tau-\tau_2) \quad ,$$

so that within the region where sound is heard

$$J_2 = -\frac{\rho_o \beta^2 \alpha}{c^2 \pi (\alpha^2-c^2)^{\frac{1}{2}}} \int_{\text{maximum of } 0 \text{ and } \tau_2}^{\tau_1} \frac{h'(\alpha\tau)\cos\phi \, d\tau}{(\tau_1-\tau)^{\frac{1}{2}}(\tau-\tau_2)^{\frac{1}{2}}(1-\beta^2\cos^2\phi/c^2)} \quad . \qquad (2.29)$$

Again the effect of the sources is weighted by the square-root factor and we might expect a greater contribution to come from the region where this factor is singular. When $R < ct$ that is in region A in Figure 4.3, τ_2 is negative and the denominator has only one zero in the range of integration. We expand about it as before to find

$$J_2 = -\frac{\rho_o \beta^2 \alpha \cos\phi_1}{\pi c^2 (\alpha^2-c^2)^{\frac{1}{2}}(\tau_1-\tau_2)^{\frac{1}{2}}(1-\beta^2\cos^2\phi_1/c^2)} \int_o^{\tau_1} \frac{h'(\alpha\tau)d\tau}{(\tau_1-\tau)^{\frac{1}{2}}} \left\{1 + O\left(\frac{L}{\alpha(\tau_1-\tau_2)}\right)\right\} , \qquad (2.30)$$

where

$$\cos\phi_1 = \frac{x_1-\alpha\tau_1}{c(t-\tau_1)} \quad .$$

This form for the sound field is more conveniently expressed in terms of r_1, the shortest distance from the observer to the position of the line source at a time τ_1;

$$r_1 = \{(x_1-\alpha\tau_1)^2+x_3^2\}^{\frac{1}{2}}$$

or from (2.26)

$$r_1 = c(t-\tau_1) \quad .$$

Then $\cos\phi_1 = (x_1-\alpha\tau_1)/r_1$; ϕ_1 is the angle between the observer and the 1-axis measured from the source position at time τ_1, as illustrated in Figure 4.4. Also

$$\tau_1 - \tau_2 = \frac{2cr_1}{\alpha^2-c^2}(1-\alpha\cos\phi_1/c) \quad , \qquad (2.31)$$

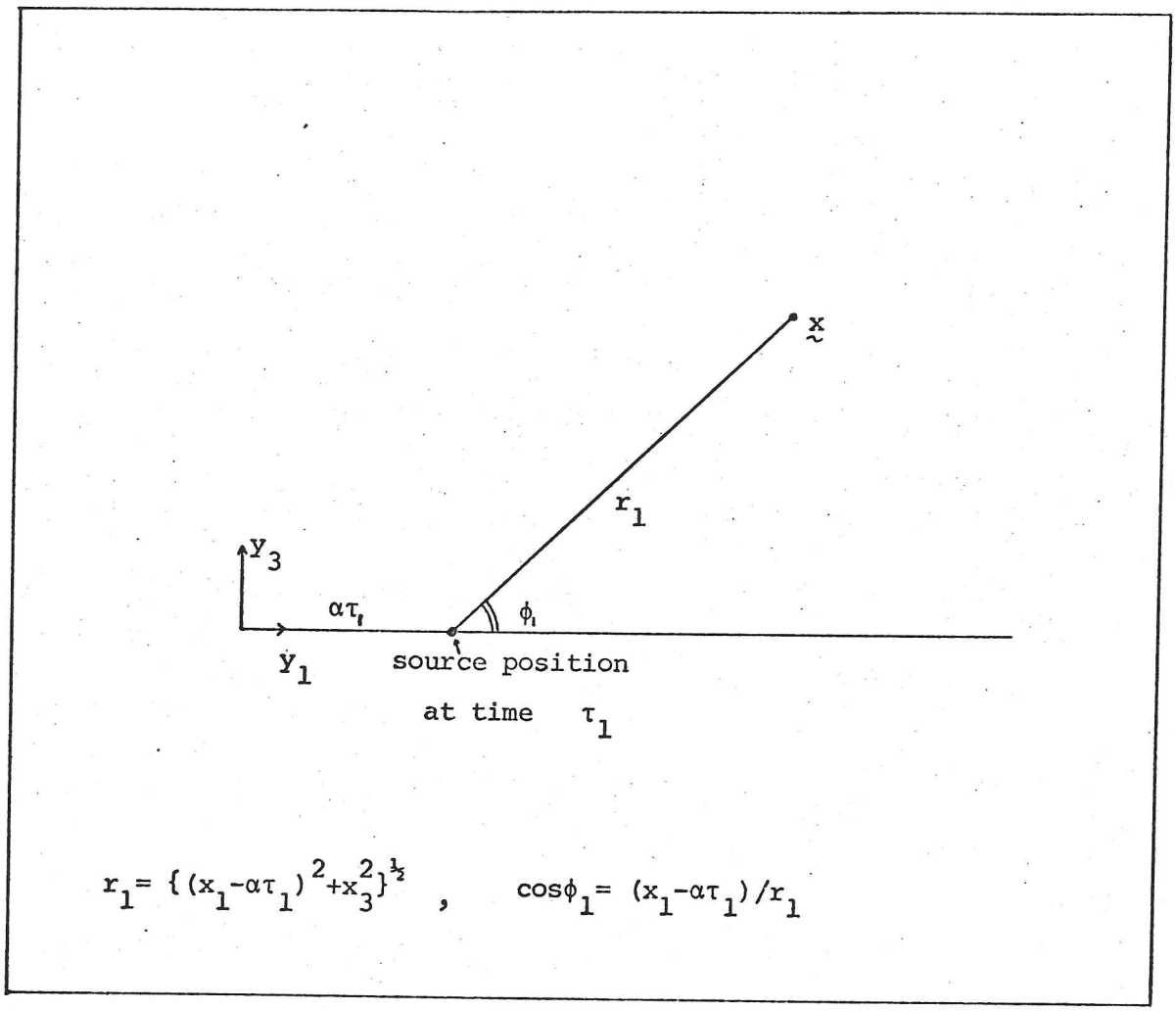

Figure 4.4 The definition of r_1 and ϕ_1

and then

$$J_2 = -\left(\frac{\alpha}{2r_1c^5(1-\alpha\cos\phi_1/c)}\right)^{\frac{1}{2}} \frac{\rho_o\beta^2\cos\phi_1}{\pi(1-\beta^2\cos^2\phi_1/c^2)} F(\alpha\{t-r_1/c\}) \qquad (2.32)$$

where, as in (2.25),

$$F(z) = \int_0^z \frac{h'(s)ds}{(z-s)^{\frac{1}{2}}} .$$

Here terms of order $r_1^{-1}(1-\alpha\cos\phi_1/c)^{-1}$ smaller than those retained have been neglected.

Within the region B in Figure 4.3 τ_2 is positive and the denominator in J_2 appears to have two singularities for positive τ .

Initially only a finite length, L , of the elastic sheet is displaced and

$$h'(y_1) = 0 \qquad \text{for} \quad y_1 > L \ .$$

Hence for $\underset{\sim}{x}$ in the far-field, h' will be zero at τ_1 , when $\tau_2 > 0$, and only the lower singularity at $\tau = \tau_2$ matters. We can obtain an expression for the sound field by expanding the integrand about τ_2 and we find

$$J_2 = -\left(\frac{\alpha}{2r_2c^5(\alpha\cos\phi_2/c-1)}\right)^{\frac{1}{2}} \frac{\rho_o\beta^2\cos\phi_2}{\pi(1-\beta^2\cos^2\phi_2/c^2)} \int_{\alpha(t-r_2/c)}^{L} \frac{h'(s)ds}{(s-\alpha t+r_2\alpha/c)^{\frac{1}{2}}}$$

$$\times \left\{1 + O\left(\frac{l}{r_2(\alpha\cos\phi_2/c-1)}\right)\right\} , \qquad (2.33)$$

where r_2 is the shortest distance from the observer at $(\underset{\sim}{x},t)$ to the position of the moving line source at $\tau = \tau_2$, and ϕ_2 is the angle between the observer and the 1-direction.

We have obtained a far-field expression for the density perturbation produced by the tension front propagating through the sheet. The field decays with the inverse square-root of the distance from the source, and involves Doppler factors based on β and α , the speed of the transverse waves and the tension front.

On the Mach wedge where $\cos\phi_1$ and $\cos\phi_2$ are equal to c/α , the expressions (2.32) and (2.33) are no longer a valid description of the sound field, because then $l r_1^{-1}(1-\alpha\cos\phi_1/c)^{-1}$ is large, and the terms we have neglected are important.

From (2.31) when $\alpha\cos\phi_1/c-1$ is small τ_1 and τ_2 are nearly equal and we will write

$$\tau_1 = \tau_o + \gamma$$

$$\tau_2 = \tau_o - \gamma$$

where from (2.27) and (2.28)

$$\tau_o = \frac{\alpha x_1 - c^2 t}{\alpha^2 - c^2} \quad \text{and} \quad \gamma = \frac{\sqrt{c^2(x_1-\alpha t)^2 - x_3^2(\alpha^2-c^2)}}{\alpha^2-c^2} \ .$$

γ is a small parameter for points $(\underset{\sim}{x},t)$ near the Mach cone.

When we change the integration variable in (2.29) to $s = \tau - \tau_o$

$$J_2 = -\frac{\rho_o \beta^2 \alpha}{\pi c^2 (\alpha^2-c^2)^{\frac{1}{2}}} \int_{-\gamma}^{\gamma} \frac{h'(\alpha\tau_o+\alpha s)\cos\phi \, ds}{(\gamma^2-s^2)^{\frac{1}{2}}(1-\beta^2\cos^2\phi/c^2)} \ . \qquad (2.34)$$

If we retain only the lowest order in γ/ℓ we find

$$J_2 = -\frac{\rho_o \beta^2 \alpha \, h'(\alpha\tau_o)\cos\phi_o}{\pi c^2 (\alpha^2-c^2)^{\frac{1}{2}}(1-\beta^2\cos^2\phi_o/c^2)} \int_{-\gamma}^{\gamma} \frac{ds}{(\gamma^2-s^2)^{\frac{1}{2}}} \ , \qquad (2.35)$$

where

$$\cos\phi_o = \frac{x_1-\alpha\tau_o}{c(t-\tau_o)} = \frac{c}{\alpha} \ .$$

Hence near the Mach wedge, where $r_1|1-\alpha\cos\phi_1/c| \ll \ell$,

$$J_2 = -\frac{\rho_o \beta^2}{c(\alpha^2-c^2)^{\frac{1}{2}}(1-\beta^2/\alpha^2)} h'\left(\frac{\alpha^2 x_1 - \alpha c^2 t}{\alpha^2-c^2}\right) \ . \qquad (2.36)$$

We have shown that on the Mach wedge there is no decay of the sound with distance from the source. This sound field is characteristic of a supersonically moving line source, with zero length scale in the direction of motion. The source in this problem has zero size because we have assumed that the tension is applied instantaneously. In practice the tension is applied over some small time and then the source at $y_1 = \alpha\tau$ has a small non-zero length scale, which we denote by δ ; the analysis described above is for $\delta = 0$.

Ffowcs Williams & Hawkings (1969) have shown that the value of

the factor δRL^{-2} determines the form of the Mach wave field. The result (2.36) is valid in the limit $\delta R \ll L^2$ and it shows there is no decay on the Mach wedge with increasing distance. For $\delta R \gg L^2$ the expressions (2.32) and (2.33) still describe the flow within the wedge but (2.36) is no longer a valid description of the Mach wedge behaviour. In fact then the sound field everywhere decays with the inverse square-root of the distance from the source.

We have therefore determined the sound field for $l \ll R \ll L^2/\delta$. The details of this field are summarized below.

For $R < ct$, within the region A in Figure 4.3, sound is heard from both the tugged end and the tension front. When we substitute the expressions (2.25) and (2.32) for J_1 and J_2 into (2.20), we find

$$(\rho-\rho_o)(\underset{\sim}{x},t) = -\left(\frac{\beta^3}{2Rc^3(1+\beta/\alpha)}\right)^{\frac{1}{2}} \frac{\rho_o}{\pi(1-\beta^2\cos^2\theta_o/c^2)} F\left(\frac{\beta(t-R/c)}{1+\beta/\alpha}\right)$$

$$-\left(\frac{\alpha}{2r_1c^5(1-\alpha\cos\phi_1/c)}\right)^{\frac{1}{2}} \frac{\rho_o\beta^2\cos\phi_1}{\pi(1-\beta^2\cos^2\phi_1/c^2)} F\left(\alpha(t-r_1/c)\right)$$

$$\text{for} \quad R < ct, \quad r_1(1-\alpha\cos\phi_1/c) \gg l \quad ; \qquad (2.37)$$

where $$F(z) = \int_o^z \frac{h'(s)ds}{(z-s)^{\frac{1}{2}}} \quad .$$

The first term describes the sound from the end $y_1 = 0$. R is the distance of the observer from this source position. The Doppler factors $(1-\beta\cos\theta_o/c)$ and $(1+\beta\cos\theta_o/c)$ appear because elements of the transverse waves are convected in both directions with a speed β. The second term describes the sound produced at $y_1 = \alpha\tau$. Since this source is moving there is an extra Doppler factor $(1-\alpha\cos\phi_1/c)^{\frac{1}{2}}$.

Equation (2.25) shows that no sound from the tugged end propagates outside the cylinder $R = ct$. So that within the region B

in Figure 4.3, only sound from the tension front is heard and from (2.33) the density perturbation is given by:

$$(\rho-\rho_o)(\underset{\sim}{x},t) = -\left(\frac{\alpha}{2r_2c^5(\alpha\cos\phi_2/c-1)}\right)^{\frac{1}{2}} \frac{\rho_o\beta^2\cos\phi_2}{\pi(1-\beta^2\cos^2\phi_2/c^2)} \int_{\alpha(t-r_2/c)}^{L} \frac{h'(s)ds}{(s-\alpha t+r_2\alpha/c)^{\frac{1}{2}}}$$

$$\text{for} \quad r_2(\alpha\cos\phi_2/c-1) \gg l \quad . \tag{2.38}$$

When $(\underset{\sim}{x},t)$ is outside the two regions A and B no sound can be heard;

$$(\rho-\rho_o)(\underset{\sim}{x},t) = 0 \quad . \tag{2.39}$$

Near the Mach cone, where $\alpha\cos\phi_1-c$ and $\alpha\cos\phi_2-c$ are both small, we see from equation (2.36)

$$(\rho-\rho_o)(\underset{\sim}{x},t) = -\frac{\rho_o\beta^2}{c(\alpha^2-c^2)^{\frac{1}{2}}(1-\beta^2/\alpha^2)} h'\left(\frac{\alpha^2x_1-\alpha c^2t}{\alpha^2-c^2}\right) ,$$

$$\text{for} \quad r_1(1-\alpha\cos\phi_1/c) \ll l \quad ; \tag{2.40}$$

the sound field does not decay with distance from the source, and there is a 'sonic boom'. Similar shock waves are produced in the related problem of the cracking of a whip, and have been photographed by Bernstein et al. (1958). However in their analysis they investigate a different mechanism of generation. They concentrate on showing that there are particular motions of the whip in which the tip can move very fast, and produce Mach waves. In our case a supersonically moving source is generated far more easily. The membrane does not need to flap rapidly; the tension front propagates through the sheet supersonically, and since the derivatives of the displacement are discontinuous at this moving point a supersonic source is obtained.

When we evaluate the time average of the square of expression (2.37), the answer we obtain is just proportional to the sum of the square

of the amplitudes of the two terms; the cross product averages to zero because the two components of the sound field have different frequencies. A dimensional analysis of this expression shows us how the sound field depends on the various parameters in the problem.

The mean intensity of the sound produced by the source at the tugged end scales as

$$\rho_o \beta^3 \frac{\bar{h}^2}{\ell R} (1+\beta/\alpha)^{-1} (1-\beta^2 \cos^2\theta_o/c^2)^{-2} \qquad (2.41)$$

where $\bar{h}$ is a typical amplitude of the initial displacement h, and ℓ is the length over which h varies. $\beta = (T_o/\rho_M)^{\frac{1}{2}}$ and we have determined how the sound intensity varies when the applied tension is increased, or the sheet density changed. The frequency of this part of the sound field scales as $\beta \ell^{-1} (1+\beta/\alpha)^{-1}$.

Similarly away from the Mach wedge the intensity of the sound produced at the tension front is proportional to

$$\rho_o \frac{\alpha \beta^4}{c^2} \frac{\bar{h}^2}{\ell r} \cos^2\phi (1-\beta^2 \cos^2\phi/c^2)^{-2} |1-\alpha\cos\phi/c|^{-1} \quad ; \qquad (2.42)$$

r is the distance of the observer from the source, and ϕ is the angle between the observer and the 1-axis. This sound field is obviously maximal near $\cos\phi = c/\alpha$. The motion of the source at the tension front causes the frequency of the sound field to be Doppler shifted; in fact the frequency varies as $\alpha \ell^{-1} |1-\alpha\cos\phi/c|^{-1}$.

For points $(\underset{\sim}{x},t)$ on the Mach wedge the mean intensity is proportional to

$$\rho_o \frac{\beta^4}{c} \frac{\bar{h}^2}{\ell^2} (\alpha^2/c^2-1)^{-1} (1-\beta^2/\alpha^2)^{-2} \qquad (2.43)$$

and the frequency to $\alpha \ell^{-1} (\alpha^2/c^2-1)^{-1}$.

4.3 Fluid loading has a dampening effect

We now investigate the effect of including the fluid loading. In §4.2 the influence of the surrounding fluid on the membrane was neglected. This is a reasonable approximation whenever the density of the fluid is very much less than that of the sheet, but in general, when the fluid density is not negligible, the waves in the membrane will lose energy in the form of radiation into the surrounding fluid (Brekhovshikh 1960).

The vertical displacement ξ satisfies equation (2.2); when the membrane is suddenly tensioned, and $\sigma_{11} = T_o H(\tau - y_1/\alpha)$, this becomes

$$\rho_M d\left\{\frac{\partial^2 \xi}{\partial \tau^2} - \beta^2 \frac{\partial}{\partial y_1}\left(H(\tau - y_1/\alpha)\frac{\partial \xi}{\partial y_1}\right)\right\} = P \qquad (3.1)$$

where $\beta = (T_o/\rho_M)^{\frac{1}{2}}$ and the fluid loading term P is the difference in pressure on either side of the membrane

$$P = -\Big[\, p(y_1, y_3, \tau) \,\Big]_{y_3=0^-}^{y_3=0^+} . \qquad (3.2)$$

This pressure difference can be related to the surface velocity through the equations of linear compressible motion in the fluid. For an impulsive problem this exact relationship is very complicated, but we will simplify it by recognizing that the flow parameters have large gradients across the impulse front. This front moves along the sheet with speed α, and through the fluid with a speed c. It therefore makes an angle ψ with the 1-axis, where $\sin\psi = c/\alpha$ as shown in Figure 4.5. The surface velocity is discontinuous at the tension front, so that spatial derivatives across the front are much larger than those parallel to it and the wave equation reduces to

$$\frac{\partial p}{\partial n} = -\frac{1}{c}\frac{\partial p}{\partial \tau} , \qquad (3.3)$$

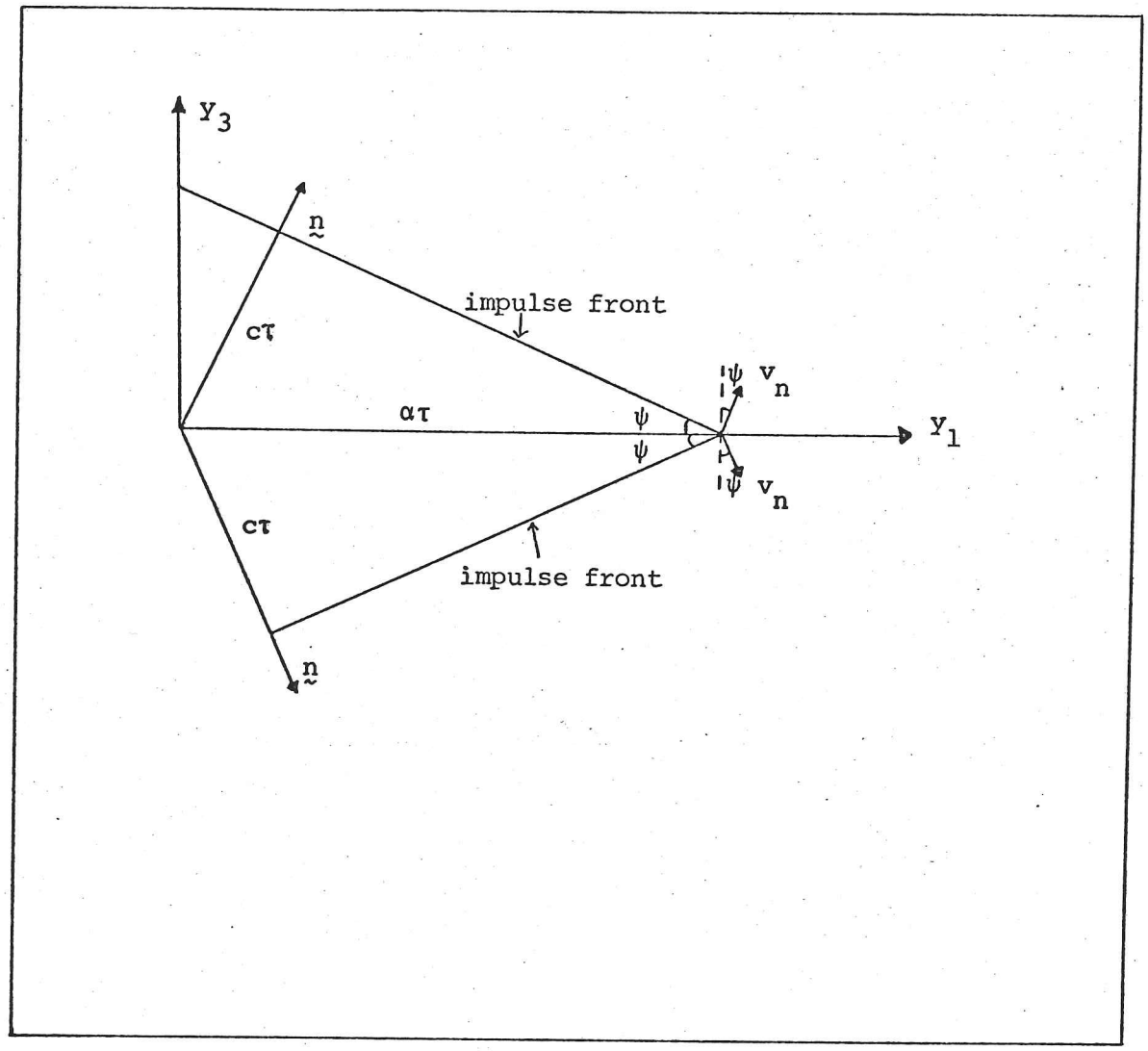

Figure 4.5 The position of the wave front

where $\underset{\sim}{n}$ is the normal illustrated in Figure 4.5. The linearized momentum equation, $\rho_o \partial \underset{\sim}{v}/\partial\tau = -\nabla p$, can be simplified and we find that the pressure perturbation, $p-p_o$, and the fluid velocity $\underset{\sim}{v}$ satisfy the plane wave relationship

$$p-p_o = \rho_o c v_n \quad ; \tag{3.4}$$

v_n is the velocity normal to the wave front. This relationship is exact on the impulse front, elsewhere it is an approximation.

Ffowcs Williams & Lovely (1977) have tested the usefulness of this ray theory approximation outside its strict range of validity and they have shown that in several model problems involving impulsive motion it agrees well with the exact solution.

We see from Figure 4.5

$$\cos\psi\, v_n(y_1,y_3,\tau) = \frac{\partial\xi}{\partial\tau} \qquad \text{on} \quad y_3 = 0^+ ,$$

so that

$$v_n(y_1,y_3,\tau) = \frac{\alpha}{(\alpha^2-c^2)^{\frac{1}{2}}}\frac{\partial\xi}{\partial\tau} \qquad \text{for} \quad y_3 = 0^+ .$$

Similarly

$$v_n(y_1,y_3,\tau) = -\frac{\alpha}{(\alpha^2-c^2)^{\frac{1}{2}}}\frac{\partial\xi}{\partial\tau} \qquad \text{for} \quad y_3 = 0^- ,$$

the sign is different because the direction of the normal is reversed.

We can determine the ray theory approximation to the pressure from equation (3.4);

$$(p-p_o)(y_1,y_3,\tau) = \begin{cases} \dfrac{\rho_o c\alpha}{(\alpha^2-c^2)^{\frac{1}{2}}}\dfrac{\partial\xi}{\partial\tau} & \text{on} \quad y_3 = 0^+ \\ \dfrac{-\rho_o c\alpha}{(\alpha^2-c^2)^{\frac{1}{2}}}\dfrac{\partial\xi}{\partial\tau} & \text{on} \quad y_3 = 0^- \end{cases} \tag{3.5}$$

and

$$P = -2K\rho_M d\, \partial\xi/\partial\tau , \tag{3.6}$$

where K is a positive constant,

$$K = \frac{\rho_o c\alpha}{\rho_M d(\alpha^2-c^2)^{\frac{1}{2}}} . \tag{3.7}$$

Equation (3.1) becomes

$$\frac{\partial^2\xi}{\partial\tau^2} + 2K\frac{\partial\xi}{\partial\tau} - \beta^2\frac{\partial}{\partial y_1}\left(H(\tau-y_1/\alpha)\frac{\partial\xi}{\partial y_1}\right) = 0 \qquad \text{for} \quad y_1 \geq 0 . \tag{3.8}$$

The fluid loading has a dampening effect on the motion of the membrane because the membrane excites the fluid and energy is propagated into the far-field. The effect of the damping is small if $\rho_o \ell \ll \rho_M d$, but for a very thin sheet K can be comparable with $\beta \ell^{-1}$, the frequency of the transverse vibration. For example, typical values of the parameters are $\rho_M = 10^3$ kg/m^3, $\rho_o = 1.22$ kg/m^3 and for a very thin sheet $d = .1$ mm. Then $K\ell/c > 1$ if ℓ is greater than 10 cm, and the surrounding fluid has a considerable effect on the displacement of the membrane. For a thicker sheet ($d = 1$ mm), $K\ell/c \simeq .1$ for $\ell = 10$ cm, and fluid loading is less important.

We now solve this equation for ξ subject to the initial conditions (2.4) and the boundary conditions (2.5).

For $\tau < y_1/\alpha$ the solution to (3.8) is

$$\xi(y_1,\tau) = h(y_1) \qquad \text{for} \quad y_1 > 0 \ . \tag{3.9}$$

ξ must be continuous across the tension front so that

$$\xi(y_1,\tau) = h(y_1) \tag{3.10}$$

when $\tau = y_1/\alpha + \varepsilon$ and ε is a small parameter. A second jump condition can be obtained exactly as before by integrating equation (3.8) across the front from $y_1 = \alpha\tau - \varepsilon$ to $y_1 = \alpha\tau + \varepsilon$. We find

$$\left(\frac{\partial}{\partial\tau} + \frac{\beta^2}{\alpha}\frac{\partial}{\partial y_1}\right)\xi(y_1,\tau) = 0 \qquad \text{at} \quad \tau = y_1/\alpha + \varepsilon \ . \tag{3.11}$$

We will now derive the solution for $\tau > y_1/\alpha$. The expressions (3.10) and (3.11) give us two 'boundary conditions' on the edge of this range, and when $\tau > y_1/\alpha$ (3.8) reduces to

$$\frac{\partial^2\xi}{\partial\tau^2} + 2K\frac{\partial\xi}{\partial\tau} - \beta^2\frac{\partial^2\xi}{\partial y_1^2} = 0 \qquad \text{for} \quad y_1 > 0 \ . \tag{3.12}$$

This can be converted into an equation valid throughout $y_1 > 0$ by multiplying by $H(\tau-y_1/\alpha)$;

$$H(\tau-y_1/\alpha)\left\{\frac{\partial^2\xi}{\partial\tau^2} + 2K\frac{\partial\xi}{\partial\tau} - \beta^2\frac{\partial^2\xi}{\partial y_1^2}\right\} = 0 \quad . \tag{3.13}$$

After an integration by parts this becomes

$$\frac{\partial^2\bar{\xi}}{\partial\tau^2} + 2K\frac{\partial\bar{\xi}}{\partial\tau} - \beta^2\frac{\partial^2\bar{\xi}}{\partial y_1^2} = \delta(\tau-y_1/\alpha)\left\{\frac{\partial\xi}{\partial\tau} + \frac{\beta^2}{\alpha}\frac{\partial\xi}{\partial y_1} + 2K\xi\right\}$$
$$+ \left(\frac{\partial}{\partial\tau} + \frac{\beta^2}{\alpha}\frac{\partial}{\partial y_1}\right)\left(\delta(\tau-y_1/\alpha)\xi\right) \qquad \text{for } y_1 > 0 , \tag{3.14}$$

where

$$\bar{\xi}(y_1,\tau) = H(\tau-y_1/\alpha)\xi(y_1,\tau) \quad .$$

We introduce a Green function $G(y_1,\tau|z_1,s)$ which satisfies the adjoint equation in $y_1 > 0$;

$$\frac{\partial^2 G}{\partial\tau^2} - 2K\frac{\partial G}{\partial\tau} - \beta^2\frac{\partial^2 G}{\partial y_1^2} = \delta(y_1-z_1)\delta(\tau-s) \quad , \tag{3.15}$$

with the boundary condition

$$G(0,\tau|z_1,s) = 0 \quad . \tag{3.16}$$

G can be determined by taking a Fourier transform of equation (3.15) and inverting the resulting expression,

$$G(y_1,\tau|z_1,s) = \frac{e^{-K(s-\tau)}}{2\beta}\left\{H(\beta(s-\tau)-|z_1-y_1|)I_o\left(K\{(s-\tau)^2-(z_1-y_1)^2/\beta^2\}^{\frac{1}{2}}\right)\right.$$
$$\left. -H(\beta(s-\tau)-|z_1+y_1|)I_o\left(K\{(s-\tau)^2-(z_1+y_1)^2/\beta^2\}^{\frac{1}{2}}\right)\right\}, \tag{3.17}$$

where I_o is the modified Bessel function of order zero. It is easy to verify that this G does in fact satisfy equation (3.15) and the boundary condition (3.16).

It is now simple to solve the equation for $\bar{\xi}$ in terms of G .

$$\bar{\xi}(z_1,s) = \int_{y_1=0}^{\infty} \int_{\tau=-\infty}^{\infty} \bar{\xi}(y_1,\tau)\delta(y_1-z_1)\delta(\tau-s)\,dy_1 d\tau \quad , \qquad \text{for} \quad z_1 > 0 \quad ; \tag{3.18}$$

this follows from the definition of the δ-function. We write the δ-function in terms of G from equation (3.15);

$$\bar{\xi}(z_1,s) = \int_{y_1=0}^{\infty} \int_{\tau=-\infty}^{\infty} \bar{\xi}(y_1,\tau)\left\{\frac{\partial^2 G}{\partial \tau^2} - 2K\frac{\partial G}{\partial \tau} - \beta^2 \frac{\partial^2 G}{\partial y_1^2}\right\} dy_1 d\tau \quad . \tag{3.19}$$

Then we rearrange this by partial integration

$$\bar{\xi}(z_1,s) = \int_{y_1=0}^{\infty} \int_{\tau=-\infty}^{\infty} G\left\{\frac{\partial^2 \bar{\xi}}{\partial \tau^2} + 2K\frac{\partial \bar{\xi}}{\partial \tau} - \beta^2 \frac{\partial^2 \bar{\xi}}{\partial y_1^2}\right\} dy_1 d\tau \quad . \tag{3.20}$$

The integrated terms vanish because G and $\bar{\xi}$ are both zero at $y_1 = 0$, $\bar{\xi}$ is zero at $\tau = -\infty$, and $\bar{\xi}G$ and its derivatives are zero when τ or y_1 is large and positive.

When we substitute (3.14) into this expression and integrate by parts again, we find

$$\bar{\xi}(z_1,s) = \int_{y_1=0}^{\infty} \int_{\tau=-\infty}^{\infty} \delta(\tau-y_1/\alpha)\left\{ G\left(\frac{\partial \xi}{\partial \tau} + \frac{\beta^2}{\alpha}\frac{\partial \xi}{\partial y_1} + 2K\xi\right) - \xi\left(\frac{\partial G}{\partial \tau} + \frac{\beta^2}{\alpha}\frac{\partial G}{\partial y_1}\right)\right\} dy_1 d\tau \quad . \tag{3.21}$$

The τ-integral may be evaluated immediately. The jump conditions (3.10) and (3.11) then show

$$\bar{\xi}(z_1,s) = \int_{y_1=0}^{\infty} h(y_1)\left\{2KG - \frac{\partial G}{\partial \tau} - \frac{\beta^2}{\alpha}\frac{\partial G}{\partial y_1}\right\} dy_1 \quad . \tag{3.22}$$

G in this integral is to be evaluated at $\tau = y_1/\alpha$.

We have now obtained the displacement along the sheet. It is easy to see from the asymptotic form of I_o that the exponential in G decays fast enough to ensure that the displacement is damped and that the sheet eventually comes to rest.

The velocity normal to the sheet is just the time derivative of ξ, and from (2.17)

$$v(z_1,s) = 0 \qquad \text{for} \quad z_1 \lesssim 0 \ .$$

Differentiation of (3.9) gives

$$v(z_1,s) = 0 \qquad \text{for} \quad \alpha s \lesssim z_1 \ .$$

When we substitute for G from equation (3.17) into (3.22) and evaluate its derivative we obtain a complicated expression for the velocity

$$v(z_1,s) = \frac{\frac{1}{2}\beta}{1+\beta/\alpha}\, h'\left(\frac{z_1+\beta s}{1+\beta/\alpha}\right) \exp\left(-K\,\frac{s-z_1/\alpha}{1+\beta/\alpha}\right) + \ldots \qquad \text{for} \quad z_1 < \alpha s \qquad (3.23)$$

The complete expression for v is very long. The term written above is representative of the others which arise in the full expression for v. The corresponding term when there is no fluid loading can be obtained by putting $K = 0$ in (3.23) or from equations (2.15) and (2.16) and is just

$$v(z_1,s) = \frac{\frac{1}{2}\beta}{1+\beta/\alpha}\, h'\left(\frac{z_1+\beta s}{1+\beta/\alpha}\right) + \ldots \qquad \text{for} \quad z_1 < \alpha s \ . \qquad (3.24)$$

From a comparison of (3.23) and (3.24) we see that when the fluid loading is taken into account v is no longer just made up of waves travelling with a constant speed, it is also damped. Sound is therefore produced from all parts of the membrane behind the tension front. An inspection of the time derivative of v at constant $z_1+\beta s$, shows that the sound produced in the middle of the sheet is $O(K\ell/\beta)$ smaller than that from $z_1 = 0$ and $z_1 = \alpha s$. So that when the density of the fluid is much smaller than that of the sheet and $K\ell \ll \beta$, the tugged end and the supersonically moving tension front are still the main noise sources.

4.4 Conclusions

When a membrane with an initial displacement is suddenly tugged,

a tension wave propagates supersonically through the sheet. There is no motion ahead of this front but behind it the tensioned sheet supports a transverse vibration. In the limit where fluid loading may be neglected, the motion of the sheet is silent except at the tugged end and at the tension front. The far-field density perturbation has the characteristic features of a two-dimensional sound field produced by a stationary line source at the tugged end and a supersonically moving line source at the tension front. When the tension is impulsively applied there is a sonic boom that travels in an unattenuated beam on the Mach wedge, where the relevant Mach number is the ratio of the speed of the tension wave to the speed of sound in the surrounding fluid. The sound field is determined by the value of the parameters α/c , β/c , $\bar{h}$ and ℓ . The intensity of the sound from the tugged end scales as $\rho_o \beta^3 \bar{h}^2/(\ell r)$, where r is the distance of the observer from the source; its frequency varies with $\beta \ell^{-1}(1+\beta/\alpha)^{-1}$. Away from the Mach wedge, the intensity of the sound from the tension front scales with $\rho_o \alpha \beta^4 \bar{h}^2/(c^2 \ell r(1-\alpha\cos\phi/c))$, and its frequency is Doppler shifted and is proportional to $\alpha \ell^{-1}|1-\alpha\cos\phi/c|^{-1}$. When the tension is applied instantaneously there is a sound beam on the Mach wedge the intensity of which is proportional to $\rho_o \beta^4 \bar{h}^2/\{c \ell^2(\alpha^2/c^2-1)\}$; but when the tension is applied over a small but non-zero interval the intensity everywhere is always of order r^{-1} .

Fluid loading has a dampening effect on the motion of the sheet. Sound is then produced at all parts of the membrane behind the tension front, but, when the paper is heavy or thick, the main sources are still at the tugged end and at the tension front.

CHAPTER 5

CONCLUSIONS

The way in which the radiation from an acoustic source is changed by motion depends crucially on the form of the source.

In Chapter 2 we investigated two simple real moving sources, a pulsating and a vibrating body. These sources are often thought to be physical models for monopoles and dipoles. But we found that the sound field of a moving pulsatile body is very different from that of a moving monopole. This is because a moving pulsating body, producing a mass flux, necessarily has a momentum flux associated with it. Hence the sound field is that of a monopole and a coupled dipole. Moreover, the strength of the dipole is only of the order of the Mach number smaller than the monopole and so affects the Doppler amplification factor. The far-field form of the pressure field produced by a moving pulsating body of arbitrary shape is modified from its value at rest by a factor $(1+\hat{r}_i\alpha_{il}M)(1-M\cos\theta)^{-3}$, where α_{ij} is the virtual mass tensor. When the velocity is along an eigenvector of the symmetric tensor α_{ij}, the amplifying factor is $(1-M\cos\theta)^{-3-\alpha}$, where α is the corresponding eigenvalue. However in general the far-field may be amplified even for points which lie in a plane perpendicular to the direction of motion. We also found that the acoustic field produced by the vibration of a moving compact sphere is not that of a moving dipole. It cannot be completely described in terms of Doppler factors, for there is an additional omnidirectional term.

Lighthill (1952) has shown that the noise produced by a jet may be modelled by quadrupoles. The mean fluid motion within the jet influences the sound field in two ways; the sources are convected with the stream and the sound rays are refracted by it. Lighthill's theory

takes account of the convection quite explicitly but not the refraction. In Chapter 3 we describe an extension to Lighthill's acoustic analogy that enables the interaction between the sound field and the mean flow to be made explicit in an analytically tractable way. We have shown that there is an exact analogy between the sound of a real jet and sources within a model flow with a 'top-hat' velocity profile. The equivalent sources are quadrupoles convected with the material particles; their strength is given by Lighthill's stress tensor measured relative to the mean jet flow. The analogy does not allow the model flow's instability waves to be excited and as a result there is a precursor ahead of the main turbulence driven field.

Some model flows will have neutrally stable waves that can propagate along the jet without decay. These modes might provide a mechanism whereby distant irrelevant details of the jet's history could be retained as a source of sound, but in fact their only effect is to ensure that the equivalent sources vanish at infinity. Moreover, when we evaluated the Green function explicitly for two different geometries, a circular cylindrical jet and a slab jet, we were able to show that these resonances decay outside the jet and cannot influence the distant sound field.

Our exact extension of the Lighthill theory provides a way of including the effect of the mean flow acoustic interactions in an estimate of jet noise. We believe that in many applications our vortex sheet analogy will accurately describe jet noise; the success of Mani's (1976) calculations supports this belief.

In our vortex sheet model the role of the instability waves is clarified, and it is easy to imagine that the procedure advocated by Lilley (1974) could be justified by other analogies based on different 'mean' velocity profiles. However, we suspect that our analogy will

prove to be the easiest to handle as it is based on the simplest possible 'mean' velocity profile.

We have investigated a compact circular cylindrical jet and a compact slab jet in some detail. The pressure field excited by longitudinal quadrupoles within the jet is modified by a factor $(1-M_r)^{-5}$, but even higher powers of the Doppler factor accompany unsteady convection. Quadrupoles normal to the jet axis are altered in a more complicated way by the shrouding effect of the surrounding jet. We found that when the jet is lighter than it is compact, the sound can scale on extremely low powers of the Mach number. This may be relevant to the 'excess noise' problem where it is known that jet noise is less sensitive to velocity variations than Lighthill's eighth power law predicts.

When an elastic membrane with an initial displacement is suddenly tugged it makes a loud cracking noise. The motion of such a sheet has been determined in Chapter 4. We found that a tension wave propagates supersonically through the sheet. The sheet is stationary ahead of this front and behind it, it supports the transverse vibrations usually associated with a tensioned membrane. In the limit where the fluid loading may be neglected, the flapping sheet is silent except at the tension front and at the tugged end. When the sheet is tugged instantaneously the noise from the tension front has all the characteristics of a supersonically moving line source and the sound on the Mach wedge propagates in an unattenuated beam. However when the tension is applied over a small non-zero time interval the sound field everywhere decays with the inverse square-root of distance from the source. Fluid loading has a considerable effect on a thin sheet; it dampens the motion of the membrane so that eventually it comes to rest.

Some of the problems covered in this thesis actually owe their origin to a need to understand anomalies revealed in the extensive flight testing of Concorde. Those tests led to more accurate and comprehensive measurements of the noise of an aircraft in flight than had previously been possible, and showed, quite definitely that the effect of flight on aircraft noise was neither as simple nor as straightforward as existing theories predicted. When the work described in this thesis was begun, Concorde was about to enter regular passenger service and its noise was a big problem. This provided a definite incentive to theoretical studies aimed at understanding the experimental results. Investigations of the effect of source motion, of the type considered in Chapter 2, have re-emphasized the need for a proper specification of the source process. It is now apparent that the interaction between the sound and the mean flow is a very important element of jet noise. Over the last few years many theories of acoustic-mean flow interaction have been developed. They are invariably based on vortex sheet or laminar shear layer models of the flow, and in general they predict scaling laws which agree well with experimental results. We have been attempting to put these theories on a firmer basis, so that the more complicated issues, such as the determination of the equivalent sources, can be clarified, and the role of the mean flow instabilities understood. Our work shows not only that a real jet may be modelled by suitable sources adjacent to a vortex sheet, but gives also the source strength needed for an exact analogy and puts the role of the instabilities on a firm, though unconventional, footing.

The techniques developed to study the aircraft noise problem are increasingly being applied to other branches of engineering. Our third topic is an example of such an application, and it was undertaken at the request of a printing press manufacturer.

These three topics are all concerned with very practical problems

whose application to manufactured products is immediate. It is this industrial call for knowledge obtained from research that places the work firmly in the realm of Engineering. The techniques we have enjoyed using to answer this call are of course those of an applied mathematician!

REFERENCES

Acton, E.	1976	A modelling of large jet eddies. Ph.D. thesis, Cambridge University
Balsa, T.F.	1976	The far field of high frequency convected singularities in sheared flows, with an application to jet-noise prediction. J. Fluid Mech. 74, 193-208
Batchelor, G.K.	1970	An Introduction to Fluid Mechanics. Cambridge University Press
Bernstein, B. et al.	1958	On the dynamics of a bull whip. J.Acoustic.Soc.Amer. 30, 1112-1115
Brekhovskikh, L.M.	1960	Waves in Layered Media. Academic Press
Broadbent, E.G.	1977	Acoustic ray theory applied to vortex refraction. J.Inst.Maths.Applics. 19, 1-27
Craver, J.K. & Taylor, D.L.	1965	Nondestructive sonic measurement of paper elasticity. Tappi. 48, 142-147
Crighton, D.G.	1975	Scattering and diffraction of sound by moving bodies. J. Fluid Mech. 72, 209-227
Dash, R.	1976a	Radiation through a composite medium. J. Sound Vib. 49, 365-377
Dash, R.	1976b	Radiation from a source near a jet. J. Sound Vib. 49, 379-392
Dowling, A.P.	1975	The refraction of sound by a shear layer made up of discrete vortices. Aero.Res.Coun. R&M 3770
Dowling, A.P.	1976	Convective amplification of real simple sources. J. Fluid Mech. 74, 529-546
Ffowcs Williams, J.E.	1969	Jet noise from aircraft. AGARD Conference Proceedings, No.42, paper 8
Ffowcs Williams, J.E.	1974	Sound production at the edge of a steady flow. J. Fluid Mech. 66, 791-816
Ffowcs Williams, J.E.	1976a	Aerodynamic noise notebook. A.I.A.A. Professional Study Series
Ffowcs Williams, J.E.	1976b	Silencing the printing press. J. Institute of Printing 20, 2-5

Ffowcs Williams, J.E.	1977	The theoretical modelling of aerodynamic noise. Proc. Sixth Canadian Congress of Appl.Mech., Vancouver
Ffowcs Williams, J.E. & Hawkings, D.L.	1969	Sound generation by turbulence and surfaces in arbitrary motion. Phil.Trans.Roy.Soc. 264, 321-342
Ffowcs Williams, J.E. & Lovely, D.J.	1975	Sound radiation into uniformly flowing fluid by compact surface vibration. J. Fluid Mech. 71, 689-700
Ffowcs Williams, J.E. & Lovely, D.J.	1977	An approximate method for evaluating the sound of impulsively accelerated bodies. J.Sound.Vib. 50, 333-343
Goldstein, M.E.	1975	The low frequency sound from multiple sources in axisymmetric shear flows, with applications to jet noise. J. Fluid Mech. 70, 595-604
Graham, E.W. & Graham, B.B.	1971	A note on theoretical acoustical sources in motion. J. Fluid Mech. 49, 481-488
Gottlieb, P.	1960	Sound source near a velocity discontinuity. J.Acoust.Soc.Amer. 32, 1117-1122
Hoch, R. & Hawkins, R.	1974	Recent studies into Concorde noise reduction. AGARD Conference Proceedings, No.131, paper 19
Horio, M. & Onogi, S.	1951	Dynamic measurements of physical properties of pulp and paper by audiofrequency sound. J.Appl.Phys. 22. 971-977
Howe, M.S.	1975	Contributions to the theory of aerodynamic sound, with application to excess jet noise and the theory of the flute. J. Fluid Mech. 71, 625-673
Jones, D.S.	1973	The effect of radiation due to a moving source on a vortex sheet. Proc. R.S.E. 72, 195-205
Kempton, A.J.	1977	Scattering by density gradients. J. Fluid Mech. 83, 495-508
Knott, P.R.	1974	Supersonic jet exhaust noise investigation. AFAPL-TR-74-25
Landau, L.D. & Lifshitz, E.M.	1959	The Theory of Elasticity. Pergamon Press
Lighthill, M.J.	1952	On sound generated aerodynamically. Part I. General Theory. Proc.Roy.Soc. A211, 564-587

Lilley, G.M. 1971 Sound generation in shear flow turbulence. Fluid Dynamics Transactions (Poland) 6, 405-420

Lilley, G.M. 1974 On the noise from jets. AGARD Conference Proceedings, No.131, paper 13

Lowson, M.V. 1965 The sound field of singularities in motion. Proc.Roy.Soc. A286, 559-572

Lush, P.A. 1971 Measurements of subsonic jet noise and comparisons with theory. J. Fluid Mech. 46, 477-500

Lush, P.A. & Fisher, M.J. 1974 Noise from hot jets. AGARD Conference Proceedings, No.131, paper 12

Mani, R. 1976 The influence of jet flows on jet noise. Parts 1 and 2. J. Fluid Mech. 73, 753-793

Morfey, C.L. & Tester, B.J. 1976 Developments in jet noise modelling. J. Sound Vib. 46, 79-103

Morgan, J.D. 1975 The interaction of sound with a subsonic cylindrical vortex layer. Proc.Roy.Soc. A344, 341-362

Morse, P.M. & Feshbach, H. 1953 Methods of Theoretical Physics. Part I. McGraw-Hill

Morse, P.M. & Ingard, K.U. 1968 Theoretical Acoustics. McGraw-Hill

Oldham, K.B. & Spanier, J. 1974 The Fractional Calculus. Academic Press

Pao, A.P. 1969 Noise emission from turbulent shear layers. J. Fluid Mech. 59, 451-479

Phillips, O.M. 1960 On the generation of sound by supersonic turbulent shear layers. J. Fluid Mech. 9, 1-28

Ribner, H.S. 1964 The generation of sound by turbulent jets. Adva. in Appl.Mech. 8, 103-182

Schubert, L.K. 1972 Numerical study of sound refraction by a jet flow. Parts 1 and 2. J.Acoust.Soc.Amer. 51, 439-463

Taylor, K. 1975 Acoustic propagation in a steady potential flow at low Mach number. R.A.E. Tech.Memo. Aero. 1653

Van Dyke, M. 1975 Perturbation Methods in Fluid Mechanics. The Parabolic Press

Warren, C.H.E. 1975 A note on moving multipole sources of sound. J. Sound Vib. 44, 3-13

Wiechert, E. 1900 L'eclairage electrique. Archives Neerlandaises des sciences exactes et naturelles 5, 549-573

APPENDIX 3.A THE EFFECT OF RESONANCES

We now derive a representation for the sound field when the point source excites a neutrally stable mode of the vortex sheet model, and $\bar{H}G^{\dagger}$ is only bounded as $|y|, -\tau \to \infty$. In this case not all the end-point contributions from partial integration are negligible.

The terms evaluated at 'infinity' need to be considered carefully. In order to do this we introduce a bounding surface $B(\tau)$. $B(\tau)$ is initially a sphere of large radius L and is subsequently convected with the flow. The fluid far from the sources is only linearly disturbed and $B(\tau)$ is slightly rippled from its starting position.

We define the Heaviside function H , such that H is unity for points within both ν_0 and $B(\tau)$ and zero elsewhere. $\partial H/\partial y_i$ is therefore non-zero on $B_0(\tau)$, the part of B in the region ν_0 , and also on $S_L(\tau)$, the section of $S(\tau)$ within the bounding surface B (this arrangement is illustrated in Figure 3.A). Equation (2.11) is still valid but now describes the flow within a finite region. We multiply it by $H^T(\tau)$, where H^T is unity for $|\tau| < T$, zero otherwise and rearrange to give

$$\left(\frac{\partial^2}{\partial\tau^2} - c_0^2\frac{\partial^2}{\partial y_i^2}\right)(H^T H\rho') = \frac{\partial^2(H^T H T_{ij})}{\partial y_i \partial y_j} - \frac{\partial}{\partial y_j}\left(H^T p_{ij}\frac{\partial H}{\partial y_i}\right) + \rho_0\frac{\partial}{\partial\tau}\left(H^T v_i\frac{\partial H}{\partial y_i}\right) + \frac{\partial}{\partial\tau}\left(H\rho'\frac{\partial H^T}{\partial\tau}\right) + \frac{\partial H^T}{\partial\tau}\frac{\partial(H\rho)}{\partial\tau}. \tag{A.1}$$

It follows from the definition of $G_0^{\dagger}$ given in (2.15) that

$$H^T H\rho'(\boldsymbol{x}, t) = -\int_{\infty} H^T H\rho'(\boldsymbol{y}, \tau)\left\{\frac{\partial^2 G_0^{\dagger}}{\partial y_i^2} - \frac{1}{c_0^2}\frac{\partial^2 G_0^{\dagger}}{\partial\tau^2}\right\} \mathrm{d}^3\boldsymbol{y}\,\mathrm{d}\tau. \tag{A.2}$$

This can be integrated by parts exactly as before, the end-point contributions vanish because $H^T H$ is zero as $|\boldsymbol{y}, \tau| \to \infty$.

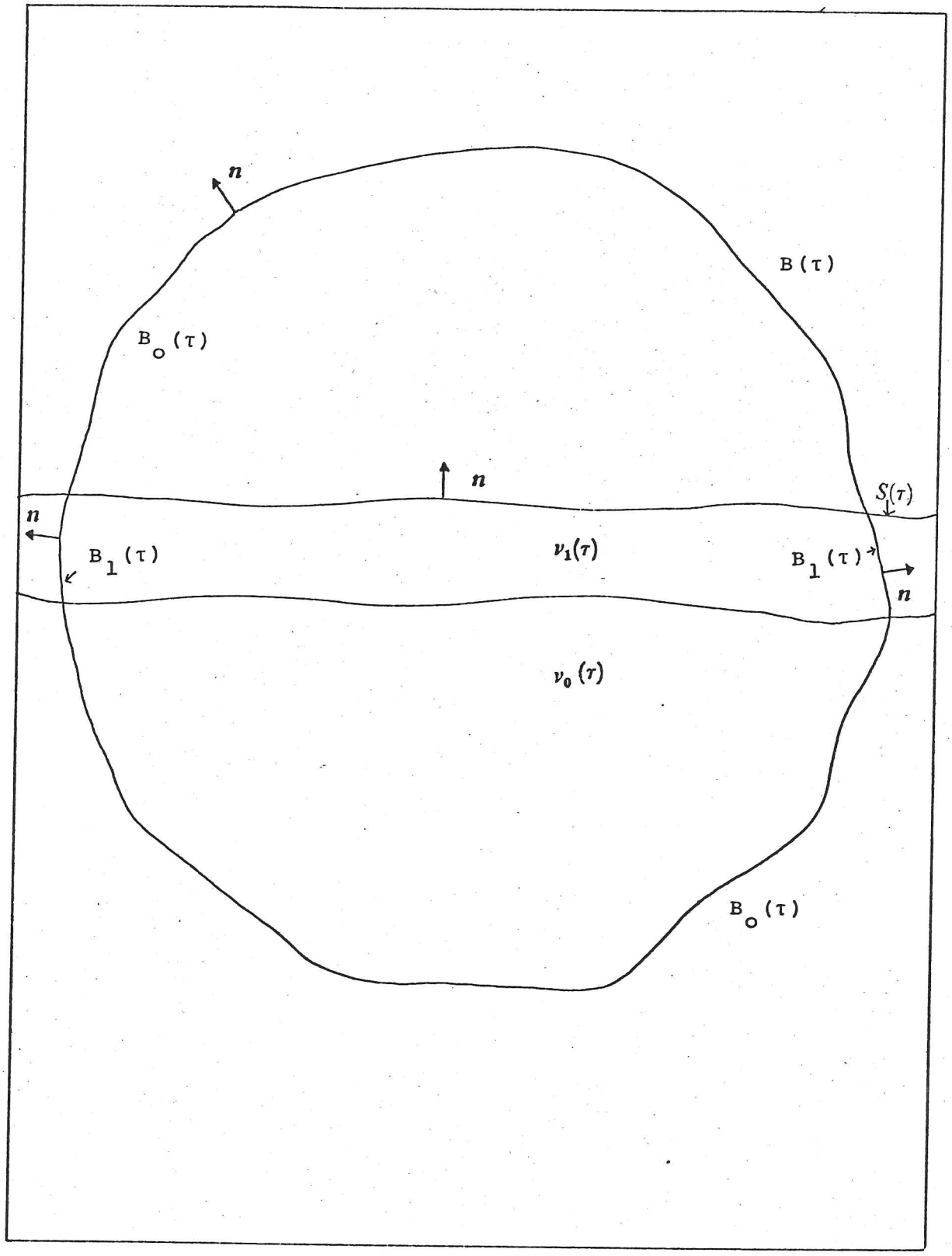

Figure 3.A The bounding surface at infinity

$$H^T H\rho'(x,t) = \int_\infty \frac{G_0^\dagger}{c_0^2}\left\{\frac{\partial^2}{\partial\tau^2} - c_0^2\frac{\partial^2}{\partial y_i^2}\right\} H^T H\rho'(y,\tau)\,\mathrm{d}^3y\,\mathrm{d}\tau. \tag{A.3}$$

We then substitute equation (A.1) into (A.3) and rearrange by partial integration to obtain

$$c_0^2 H^T H\rho'(x,t) = \int_\infty \left\{H^T H T_{ij}\frac{\partial^2 G_0^\dagger}{\partial y_i\,\partial y_j} + H^T p_{ij}\frac{\partial H}{\partial y_i}\frac{\partial G_0^\dagger}{\partial y_j} - H^T\rho_0\frac{\partial G_0^\dagger}{\partial\tau}v_i\frac{\partial H}{\partial y_i}\right.$$
$$\left. + \frac{\partial H^T}{\partial\tau}\left(\frac{\partial(H\rho)}{\partial\tau}G_0^\dagger - H\rho'\frac{\partial G_0^\dagger}{\partial\tau}\right)\right\}\mathrm{d}^3y\,\mathrm{d}\tau. \tag{A.4}$$

The last term of this equation can be simplified because from the definition of H^T,

$$\int_{-\infty}^{\infty} (\partial H^T/\partial\tau)\,K(y,\tau)\,\mathrm{d}\tau = -\{K(y,T) - K(y,-T)\} \tag{A.5}$$

for any function $K(y,\tau)$.

Initially there is no flow, and the perturbed fluid parameters v, $p-p_0$ and ρ' are zero. $G^\dagger$ decays as $\tau\to\infty$, and so if T is sufficiently big (A.4) reduces to

$$c_0^2 H^T H\rho'(x,t) = \int_{-T}^{T}\int\left\{HT_{ij}\frac{\partial^2 G_0^\dagger}{\partial y_i\,\partial y_j} + p_{ij}\frac{\partial H}{\partial y_i}\frac{\partial G_0^\dagger}{\partial y_j} - \rho_0 v_i\frac{\partial H}{\partial y_i}\frac{\partial G_0^\dagger}{\partial\tau}\right\}\mathrm{d}^3y\,\mathrm{d}\tau. \tag{A.6}$$

The first term on the right-hand side is a volume integral over the region of $\nu_0(\tau)$ contained within $B(\tau)$. The last two terms are surface integrals over $B_0(\tau)$ and $S_L(\tau)$.

On $B_0(\tau)$, $G_0^\dagger$ has incoming wave behaviour, and the acoustic parameters have outward wave behaviour. Therefore

$$\frac{\partial G_0^\dagger}{\partial n} = \frac{1}{c_0}\frac{\partial G_0^\dagger}{\partial\tau} + O(L^{-2})$$

and

$$p_{ij} = (p-p_0)\,\delta_{ij} = \rho_0 c_0\, v\cdot n\;\delta_{ij} + O(L^{-2})$$

on $B_o(\tau)$, where n is the normal to the surface $B_o(\tau)$ in the direction shown in Figure 3.A. These conditions ensure that

$$\int_{B_o(\tau)} n_i \left(\rho_0 v_i \frac{\partial G_0^\dagger}{\partial \tau} - p_{ij} \frac{\partial G_0^\dagger}{\partial y_j}\right) dB \sim O(L^{-1}) \quad ,$$

and for large enough values of L,

$$c_0^2 H^T H \rho'(x,t) = \int_{-T}^{T} \int \left\{ H T_{ij} \frac{\partial^2 G_0^\dagger}{\partial y_i \partial y_j} \, d^3y \, d\tau - \int_{-T}^{T} d\tau \int_{S_L(\tau)} n_i \left(\rho_0 v_i \frac{\partial G_0^\dagger}{\partial \tau} - p_{ij} \frac{\partial G_0^\dagger}{\partial y_j}\right) dS \, d\tau. \right.$$

(A.7)

The region in the interior of the jet may be treated in exactly the same way. $\bar{H}$ is defined to be unity for points within both the region ν_1 and the surface B, and zero elsewhere.

We multiply (2.14) by H^T and rearrange

$$\left\{\frac{D_1^2}{D\tau^2} - c_1^2 \frac{\partial^2}{\partial y_i^2}\right\} \{H^T(\bar{H} - H_V)\rho_1'\} = \frac{\partial^2}{\partial y_i \partial y_j} \{H^T(\bar{H} - H_V) T_{ij}'\} - \frac{\partial}{\partial y_j} \left\{ H^T p_{ij} \left(\frac{\partial \bar{H}}{\partial y_i} - \frac{\partial H_V}{\partial y_i}\right)\right\}$$
$$- \rho_1 \frac{D_1^2}{D\tau^2}(H^T \bar{H}) + \rho_1 \frac{D_1}{D\tau}\left(H^T \frac{D_1 H_V}{D\tau}\right) + \frac{\partial H^T}{\partial \tau} \frac{D_1}{D\tau} \{(\bar{H} - H_V)\rho\}$$
$$+ \frac{D_1}{D\tau}\left\{ \frac{\partial H^T}{\partial \tau} (\rho(\bar{H} - H_V) + \rho_1 H_V)\right\}.$$

(A.8)

The definition of $G_1^\dagger$, (2.16), gives

$$0 = \int_\infty H^T(\bar{H} - H_V)\rho_1'(y,\tau) \left\{\frac{D_1^2}{D\tau^2} - c_1^2 \frac{\partial^2}{\partial y_i^2}\right\} G_1^\dagger \, d^3y \, d\tau. \qquad \text{(A.9)}$$

The differential operators can be transferred onto $H^T(\bar{H} - H_V)\rho_1'$ by partial integration; contributions at infinity vanish because $H^T(\bar{H} - H_V)$ is zero as $|y,\tau| \to \infty$.

$$0 = \int_\infty G_1^\dagger \left\{\frac{D_1^2}{D\tau^2} - c_1^2 \frac{\partial^2}{\partial y_i^2}\right\} H^T(\bar{H} - H_V)\rho_1'(y,\tau) \, d^3y \, d\tau. \qquad \text{(A.10)}$$

We substitute (A.8) into (A.10) and rearrange by partial integration, end-point contributions are again zero because $H^T(\bar{H}-H_V)$ is zero as any one of the variables tends to $\pm$ infinity.

$$O=\int_\infty H^T\left\{(\bar{H}-H_V)\,T'_{ij}\frac{\partial^2 G_1^\dagger}{\partial y_i\,\partial y_j}+p_{ij}\frac{\partial G_1^\dagger}{\partial y_j}\left(\frac{\partial \bar{H}}{\partial y_i}-\frac{\partial H_V}{\partial y_i}\right)-\rho_1\bar{H}\frac{\mathrm{D}_1^2 G_1^\dagger}{\mathrm{D}\tau^2}-\rho_1\frac{\mathrm{D}_1 G_1^\dagger}{\mathrm{D}\tau}\frac{\mathrm{D}_1 H_V}{\mathrm{D}\tau}\right\}\mathrm{d}^3y\,\mathrm{d}\tau$$
$$+\int_\infty\frac{\partial H^T}{\partial\tau}\left\{G_1^\dagger\frac{\mathrm{D}_1}{\mathrm{D}\tau}((\bar{H}-H_V)\rho)-\left(\rho(\bar{H}-H_V)+\rho_1 H_V\right)\frac{\mathrm{D}_1 G_1^\dagger}{\mathrm{D}\tau}\right\}\mathrm{d}^3y\,\mathrm{d}\tau. \tag{A.11}$$

As in §3.2, we introduce a function Γ defined in ν_1 by

$$\bar{H}\;\partial^2\Gamma/\partial\tau^2=\bar{H}\;\mathrm{D}_1^2 G_1^\dagger/\mathrm{D}\tau^2,\quad \bar{H}\,\partial\Gamma/\partial\tau\to 0\quad\text{as}\quad\tau\to\infty.$$

The term $-\rho_1\int_\infty H^T\bar{H}\frac{\mathrm{D}_1^2 G_1^\dagger}{\mathrm{D}\tau^2}\mathrm{d}^3y\,\mathrm{d}\tau$ in (A.11) can be written as

$$-\rho_1\int_\infty H^T\bar{H}\frac{\partial^2\Gamma}{\partial\tau^2}\mathrm{d}^3y\,\mathrm{d}\tau=\rho_1\int_\infty\left(H^T\frac{\partial\bar{H}}{\partial\tau}\frac{\partial\Gamma}{\partial\tau}+\frac{\partial H^T}{\partial\tau}\bar{H}\frac{\partial\Gamma}{\partial\tau}\right)\mathrm{d}^3y\,\mathrm{d}\tau$$
$$=\rho_1\int_\infty\left(-H^T v_i\frac{\partial\bar{H}}{\partial y_i}\frac{\partial\Gamma}{\partial\tau}+\frac{\partial H^T}{\partial\tau}\bar{H}\frac{\partial\Gamma}{\partial\tau}\right)\mathrm{d}^3y\,\mathrm{d}\tau.$$

After an application of (A.5), equation (A.11) becomes

$$O=\int_{-T}^{T}\int_\infty\left\{(\bar{H}-H_V)\,T'_{ij}\frac{\partial^2 G_1^\dagger}{\partial y_i\,\partial y_j}+p_{ij}\frac{\partial G_1^\dagger}{\partial y_j}\left(\frac{\partial\bar{H}}{\partial y_i}-\frac{\partial H_V}{\partial y_i}\right)-\rho_1\frac{\mathrm{D}_1 G_1^\dagger}{\mathrm{D}\tau}\frac{\mathrm{D}_1 H_V}{\mathrm{D}\tau}-\rho_1 v_i\frac{\partial\bar{H}}{\partial y_i}\frac{\partial\Gamma}{\partial\tau}\right\}\mathrm{d}^3y\,\mathrm{d}\tau.$$
$$+\left[\int\left\{-G_1^\dagger\frac{\mathrm{D}_1}{\mathrm{D}\tau}((\bar{H}-H_V)\rho)+\left(\rho(\bar{H}-H_V)+\rho_1 H_V\right)\frac{\mathrm{D}_1 G_1^\dagger}{\mathrm{D}\tau}-\rho_1\bar{H}\frac{\partial\Gamma}{\partial\tau}\right\}\mathrm{d}^3y\right]_{\tau=-T}^{T}. \tag{A.12}$$

Initially the flow is at rest and unheated; the velocity everywhere is zero and the density ρ_0. $G^\dagger$ and Γ are zero at $\tau=\infty$. Therefore for a large enough value of T (A.12) may be rewritten as

$$0=\int_{-T}^{T}\int_{\nu}\left\{(\bar{H}-H_{1'})\,T'_{ij}\frac{\partial^2 G_1^{\dagger}}{\partial y_i\,\partial y_j}+p_{ij}\frac{\partial G_1^{\dagger}}{\partial y_j}\left(\frac{\partial \bar{H}}{\partial y_i}-\frac{\partial H_{\nu}}{\partial y_i}\right)-\rho_1\frac{D_1 G_1^{\dagger}}{D\tau}\frac{D_1 H_{1'}}{D\tau}-\rho_1 v_i\,\frac{\partial \bar{H}}{\partial y_i}\,\frac{\partial \Gamma}{\partial \tau}\right\}d^3y\,d\tau$$

$$\left[\int_{\nu}\left\{-\rho_0\bar{H}\frac{D_1 G_1^{\dagger}}{D\tau}+(\rho_0-\rho_1)H_{1'}\frac{D_1 G_1^{\dagger}}{D\tau}+\rho_0 G_1^{\dagger}U_1\left(\frac{\partial \bar{H}}{\partial y_1}-\frac{\partial H_{1'}}{\partial y_1}\right)+\rho_1\bar{H}\frac{\partial \Gamma}{\partial \tau}\right\}d^3y\right]_{-T}. \quad (A.13)$$

$\partial\bar{H}/\partial y_i$ is non-zero on both $S_L(\tau)$ and $B_1(\tau)$ where B_1 is the part of the surface $B(\tau)$ within ν_1, and

$$\int_{\nu}\frac{\partial \bar{H}}{\partial y_i}\left(\frac{\partial G_1^{\dagger}}{\partial y_j}p_{ij}-\rho_1 v_i\frac{\partial \Gamma}{\partial \tau}\right)d^3y=-\int_{B_1(\tau)}n_i\left(\frac{\partial G_1^{\dagger}}{\partial y_j}p_{ij}-\rho_1 v_i\frac{\partial \Gamma}{\partial \tau}\right)dB$$
$$-\int_{S_L(\tau)}n_i\left(\frac{\partial G_1^{\dagger}}{\partial y_j}p_{ij}-\rho_1 v_i\frac{\partial \Gamma}{\partial \tau}\right)d\,S_L. \quad (A.14)$$

The surface $B_1(\tau)$ has a finite area, because although the region ν_1 may be infinitely long, we have insisted that it have a finite cross-section. $G^{\dagger}$ and Γ are bounded, and on $B(\tau)$ the flow parameters v_i, and $p_{ij}\sim L^{-1}$. Therefore the surface integral over $B_1(\tau)$ is negligible if L is large enough, and from (A.13)

$$0=\int_{-T}^{T}\int_{\nu}\left\{(\bar{H}-H_{1'})\,T'_{ij}\frac{\partial^2 G_1^{\dagger}}{\partial y_i\,\partial y_j}-p_{ij}\frac{\partial G_1^{\dagger}}{\partial y_j}\frac{\partial H_{1'}}{\partial y_i}-\rho_1\frac{D_1 G_1^{\dagger}}{D\tau}\frac{D_1 H_{1'}}{D\tau}\right\}d^3y\,d\tau$$

$$-\int_{-T}^{T}\int_{S_L(\tau)}n_i\left(\frac{\partial G_1^{\dagger}}{\partial y_j}p_{ij}-\rho_1 v_i\frac{\partial \Gamma}{\partial \tau}\right)d\,S_L\,d\tau$$

$$\left[\int_{\nu}\left\{-\rho_0\bar{H}\frac{D_1 G_1^{\dagger}}{D\tau}+(\rho_0-\rho_1)H_{1'}\frac{D_1 G_1^{\dagger}}{D\tau}+\rho_0 G_1^{\dagger}U_1\left(\frac{\partial \bar{H}}{\partial y_1}-\frac{\partial H_{1'}}{\partial y_1}\right)+\rho_1\bar{H}\frac{\partial \Gamma}{\partial \tau}\right\}d^3y\right]_{-T}. \quad (A.15)$$

This equation is multiplied by $\beta(x,t)$ and added to (A.7) to obtain the exact result

$$c_0^2 H^T H\rho'(x,t)=\int_{-T}^{T}\int_{\nu}\left\{HT_{ij}\frac{\partial^2 G_0^{\dagger}}{\partial y_i\,\partial y_j}+\beta(\bar{H}-H_{1'})\,T'_{ij}\frac{\partial^2 G_1^{\dagger}}{\partial y_i\,\partial y_j}\right.$$
$$\left.-\beta p_{ij}\frac{\partial H_{1'}}{\partial y_i}\frac{\partial G_1^{\dagger}}{\partial y_j}-\beta\rho_1\frac{D_1 G_1^{\dagger}}{D\tau}\frac{D_1 H_{1'}}{D\tau}\right\}d^3y\,d\tau+\Phi+\Psi, \quad (A.16)$$

where

$$\Phi(x,t) = \int_{-T}^{T}\int_{S(\tau)}\left\{(p-p_0)\left(\frac{\partial G_0^\dagger}{\partial n} - \beta\frac{\partial G_1^\dagger}{\partial n}\right) + n_i e_{ij}\left(\beta\frac{\partial G_1^\dagger}{\partial y_j} - \frac{\partial G_0^\dagger}{\partial y_j}\right) - n_i v_i\left(\rho_0\frac{\partial G_0^\dagger}{\partial \tau} - \beta\rho_1\frac{\partial \Gamma}{\partial \tau}\right)\right\} dS\, d\tau$$

and

$$\Psi(x,t) = \beta\left[\int_\infty\left\{-\rho_0\bar{H}\frac{D_1 G_1^\dagger}{D\tau} + (\rho_0-\rho_1)H_V\frac{D_1 G_1^\dagger}{D\tau} + \rho_0 G_1^\dagger U_1\left(\frac{\partial \bar{H}}{\partial y_1} - \frac{\partial H_V}{\partial y_1}\right) + \rho_1\bar{H}\frac{\partial \Gamma}{\partial \tau}\right\} d^3y\right]_{-T}.$$

This equation is similar to the form obtained earlier (equation (2.24)), but now the integration range is finite and there is an additional term Ψ. Ψ describes any sources present at $\tau = -T$, ; their effect lives forever when vortex sheet resonances are excited.

We choose $G^\dagger$ to satisfy jump conditions across $S(\tau)$ that minimize Φ, and as in (2.30) we pick $G_0^\dagger$ and $G_1^\dagger$ such that

$$\rho_0\,\partial G_0^\dagger/\partial\tau = \beta\rho_1\,\partial\Gamma/\partial\tau \quad \text{and} \quad \partial G_0^\dagger/\partial n = \beta\,\partial G_1^\dagger/\partial n, \tag{A.17}$$

for all y on $S(\tau)$ where $v_i n_i \neq 0$, $p_{ij} \neq 0$.
With this choice of $G^\dagger$, Φ only depends on the viscous stress on the surface $S(\tau)$ (just as in 2.31), and at a high Reynolds number the sound produced by this viscous term is negligible compared with that due to the inertial terms, and we neglect it.

The term Ψ is actually independent of the real flow and depends only on the initial conditions. We denote the initial position of the fluid surface $S(\tau)$ by S_0, and the region contained within S_0 by $V_1^{(0)}$. We then define $\bar{H}_0$ to be a Heaviside function which is unity for points within both $V_1^{(0)}$ and a large sphere of radius L, and zero elsewhere

$$\bar{H}_0(y) = \lim_{\tau\to-\infty}\bar{H}(y,\tau).$$

Similarly the starting position of the surface $\Sigma(\tau)$ is denoted by Σ_0, and we introduce H_{V0}, the Heaviside function which is unity within Σ_0, and zero elsewhere.

Therefore

$$\Psi = \beta\left[\int_\infty \left\{ -\rho_0 \bar{H}_0 \frac{D_1 G_1^\dagger}{D\tau} + (\rho_0-\rho_1) H_{V0} \frac{D_1 G_1^\dagger}{D\tau} + \rho_0 G_1^\dagger U_1 \left(\frac{\partial \bar{H}_0}{\partial y_1} - \frac{\partial H_{V0}}{\partial y_1}\right) + \rho_1 \bar{H}_0 \frac{\partial \Gamma}{\partial \tau}\right\} d^3y\right]_{\tau=-T}$$

$$= \beta \int_{-T}^{T}\int_\infty \frac{\partial}{\partial \tau}\left\{ \rho_0 \bar{H}_0 \frac{D_1 G_1^\dagger}{D\tau} - (\rho_0-\rho_1) H_{V0} \frac{D_1 G_1^\dagger}{D\tau} - \rho_0 G_1^\dagger U_1 \left(\frac{\partial \bar{H}_0}{\partial y_1} - \frac{\partial H_{V0}}{\partial y_1}\right) - \rho_1 \bar{H}_0 \frac{\partial \Gamma}{\partial \tau}\right\} d^3y\, d\tau. \tag{A.18}$$

The right-hand side may be rearranged to give

$$\Psi = -\beta \int_{-T}^{T}\int_\infty \left\{ (\bar{H}_0 - H_{V0})(\rho_0 U_1^2 \delta_{i1}\delta_{j1} - c_1^2(\rho_0-\rho_1)\delta_{ij}) \frac{\partial^2 G_1^\dagger}{\partial y_i \partial y_j} - \rho_1 \frac{D_1 G_1^\dagger}{D\tau} U_1 \frac{\partial H_{V0}}{\partial y_1}\right\} d^3y\, d\tau.$$

From (A.16), we finally obtain our modified vortex sheet analogy,

$$\begin{aligned} c_0^2 H^T H\rho'(x,t) = {} & \int_{-T}^{T}\int_\infty \left\{ HT_{ij} \frac{\partial^2 G_0^\dagger}{\partial y_i \partial y_j} + \beta\left((\bar{H}-H_V)T'_{ij} - (\bar{H}_0 - H_{V0})(\rho_0 U_1^2 \delta_{i1}\delta_{j1} - c_1^2(\rho_0-\rho_1)\delta_{ij})\right) \frac{\partial^2 G_1^\dagger}{\partial y_i \partial y_j}\right\} d^3y\, d\tau \\ & + \int_{-T}^{T}\int_\infty \beta\left\{ \rho_1 \left(U_1 \frac{\partial H_{V0}}{\partial y_1} - \frac{D_1 H_V}{D\tau}\right) \frac{D_1 G_1^\dagger}{D\tau} - \frac{\partial H_V}{\partial y_i} p_{ij} \frac{\partial G_1^\dagger}{\partial y_j}\right\} d^3y\, d\tau \\ & - \int_{-T}^{T}\int_{S(\tau)} n_i e_{ij} \frac{\partial}{\partial y_j}(G_0^\dagger - \beta G_1^\dagger)\, dS\, d\tau. \end{aligned} \tag{A.19}$$

The terms in (A.19) arising from Ψ conveniently ensure that the source terms decay as any one of the variables tends to infinity because

$$G^\dagger \to 0 \quad \text{as} \quad \tau \to \infty,$$

$$(\bar{H}-H_V)T'_{ij} \to (\bar{H}_0 - H_{V0})(\rho_0 U_1^2 \delta_{i1}\delta_{j1} - c_1^2(\rho_0-\rho_1)\delta_{ij})$$

and

$$\frac{D_1 H_V}{D\tau} \to U_1 \frac{\partial H_{V0}}{\partial y_1} \quad \text{as } |y|, -\tau \to \infty.$$

When $G^{\dagger}$ decays at infinity, $\Psi = 0$. Then (A.19) and the previous representation (2.31) are entirely equivalent, either form may be used.

APPENDIX 3.B THE RECIPROCAL THEOREM

When the surface is only linearly disturbed as described in §3.3 we can determine a simple relationship between the reciprocal Green function defined by (2.15) and (2.16) with the jump conditions (3.6) and the direct Green function defined in equations (3.9)-(3.11), for the case when $\bar{H}G^{\dagger}$ decays at infinity.

Throughout this section y is a point within the jet, i.e. in the region $\nu_1^{(0)}$, and x is in the ambient fluid in $\nu_0^{(0)}$. $H_0(z)$ is a Heaviside function such that

$$\begin{aligned} H_0(z) &= 1 \quad \text{for} \quad z \quad \text{in} \quad \nu_0^{(0)} \\ &= 0 \quad \text{for} \quad z \quad \text{in} \quad \nu_1^{(0)}, \end{aligned} \tag{B.1}$$

and $\bar{H}_0(z) = 1 - H_0(z)$.

$H_0(z)$ is independent of z_1, because S_0, the bounding surface between $\nu_0^{(0)}$ and $\nu_1^{(0)}$, is a fixed surface parallel to the z_1-axis.

Now

$$H_0(x)\, G(x,t|y,\tau) = \int H_0(z)\, G(z,s|y,\tau)\, \delta(x-z, t-s)\, \mathrm{d}^3z\, \mathrm{d}s \tag{B.2}$$

$$= -\int H_0(z)\, G(z,s|y,\tau) \left(\frac{\partial^2}{\partial z_i^2} - \frac{1}{c_0^2}\frac{\partial^2}{\partial s^2}\right) G_0^{\dagger}(z,s|x,t)\, \mathrm{d}^3z\, \mathrm{d}s \tag{B.3}$$

from (2.15).

After integration by parts and the use of equation (3.9) we obtain

$$H_0(x)\, G(x,t|y,\tau) = \int \frac{\partial H_0}{\partial z_i} \left\{ G(z,s|y,\tau) \frac{\partial G_0^{\dagger}}{\partial z_i}(z,s|x,t) - G_0^{\dagger}(z,s|x,t) \frac{\partial G}{\partial z_i}(z,s|y,\tau) \right\} \mathrm{d}^3z\, \mathrm{d}s; \tag{B.4}$$

contributions at infinity vanish because G represents an outgoing and $G^{\dagger}$ an incoming wave in the variables (z,s), and G decays as $s \to -\infty$,

$G^\dagger$ as $s \to \infty$.

$H_0(x)$ is independent of x_1 and t, hence

$$H_0(x)\frac{D_1^2}{Dt^2}G(x,t|y,\tau) = \frac{D_1^2}{Dt^2}\{H_0(x)\,G(x,t|y,\tau)\}$$

$$= \int \frac{\partial H_0}{\partial z_i}\left\{G(z,s|y,\tau)\frac{\partial}{\partial z_i}\frac{D_1^2}{Dt^2}G_0^\dagger(z,s|x,t) - \frac{D_1^2}{Dt^2}G_0^\dagger(z,s|x,t)\frac{\partial G}{\partial z_i}(z,s|y,\tau)\right\} d^3z\,ds, \tag{B.5}$$

by differentiating (B.4).

By applying (3.4), we can write

$$H_0(x)\frac{D_1^2}{Dt^2}G(x,t|y,\tau) = \int\int_{S_0} n_i\left\{G(z,s|y,\tau)\frac{\partial D_1^2}{\partial z_i\,Ds^2}G_0^\dagger(z,s|x,t) - \frac{D_1^2}{Ds^2}G_0^\dagger(z,s|x,t)\frac{\partial}{\partial z_i}G(z,s|y,\tau)\right\} dS_0\,ds. \tag{B.6}$$

Then an integration by parts of the last term gives

$$\rho_1 H_0(x)\frac{D_1^2 G}{Dt^2}(x,t|y,\tau) = \int\int_{S_0}\left\{G(z,s|y,\tau)\,\rho_1\frac{D_1^2}{Ds^2}\frac{\partial G_0^\dagger}{\partial n}(z,s|x,t) - G_0^\dagger(z,s|x,t)\,\rho_1\frac{D_1^2}{Ds^2}\frac{\partial G}{\partial n}(z,s|y,\tau)\right\} dS_0\,ds. \tag{B.7}$$

The condition $\bar{H}G^\dagger \to 0$ as $|z, s| \to \infty$ ensures that $G_0^\dagger$ tends to zero at infinity on the surface S_0, and so there are no contributions from the end-points.

Similarly

$$\bar{H}_0(y)G_1^\dagger(y,\tau|x,t) = \int \bar{H}_0(z)\,G_1^\dagger(z,s|x,t)\,\delta(y-z,\tau-s)\,d^3z\,ds \tag{B.8}$$

$$= -\int \bar{H}_0(z)\,G_1^\dagger(z,s|x,t)\left\{\frac{\partial^2}{\partial z_i^2} - \frac{1}{c_1^2}\frac{D_1^2}{Ds^2}\right\}G(z,s|y,\tau)\,d^3z\,ds \tag{B.9}$$

from equation (3.10).

After partial integration this becomes

$$\bar{H}_0(y)\, G_1^\dagger(y,\tau|x,t) = \int \frac{\partial \bar{H}_0}{\partial z_i}\left\{G_1^\dagger(z,s|x,t)\frac{\partial G}{\partial z_i}(z,s|y,\tau) - G(z,s|y,\tau)\frac{\partial G_1^\dagger}{\partial z_i}(z,s|x,t)\right\} \mathrm{d}^3z\, \mathrm{d}s. \tag{B.10}$$

Here we have used equation (2.16)

$$\bar{H}_0(z)\left\{\frac{\partial^2}{\partial z_i^2} - \frac{1}{c_1^2}\frac{\mathrm{D}_1^2}{\mathrm{D}s^2}\right\} G_1^\dagger(z,s|x,t) = 0,$$

and the fact that $\bar{H}G^\dagger \to 0$ as $|z\,,\, s| \to \infty$

It can easily be shown by differentiating (B.10) that

$$\bar{H}_0(y) B\rho_0 \frac{\partial^2 G_1^\dagger}{\partial t^2}(y,\tau|x,t) = \int\int_{S_0}\left\{G(z,s|y,\tau)\, B\,\rho_0 \frac{\partial^2}{\partial s^2}\frac{\partial G_1^\dagger}{\partial n}(z,s|x,t) - B\, G_1^\dagger(z,s|x,t)\,\rho_0 \frac{\partial^2}{\partial s^2}\frac{\partial G}{\partial n}(z,s|y,\tau)\right\} \mathrm{d}S_0\, \mathrm{d}s. \tag{B.11}$$

$G^\dagger$ satisfies the jump conditions (3.6) and G the condition (3.11), and hence we can deduce from (B.7) and (B.11) that

$$B\,\rho_0 \frac{\partial^2}{\partial t^2} G_1^\dagger(y,\tau|x,t) = \rho_1 \frac{\mathrm{D}_1^2 G}{\mathrm{D}t^2}(x,t|y,\tau), \tag{B.12}$$

x is in the far-field and so this expression simplifies

$$B\,\rho_0\, G_1^\dagger(y,\tau|x,t) = \rho_1 \quad (1-M_r)^2 G(x,t|y,\tau), \tag{B.13}$$

or equivalently when B is written explicitly as $B = \beta(1-M_r)^2\rho_1/\rho_0$, (B.13) reduces to the required reciprocal identity

$$\beta\, G_1^\dagger(y,\tau|x,t) = G(x,t|y,\tau). \tag{B.14}$$

APPENDIX 4.A THE DERIVATION OF THE ELASTIC EQUATIONS OF MOTION

We determine the elastic equations of motion of a thin plate of uniform thickness d. The undeformed plate lies in the plane $y_3 = 0$ and $y_1 \geq 0$, $\infty \geq y_2 \geq -\infty$. $\xi(y_1,y_2,\tau)$ denotes the vertical displacement and $u_i(y_1,y_2,\tau)$, $i = 1,2$, the in-plane deformation.

Landau and Lifshitz (II §14) derive an expression for the elastic potential energy in such a plate and show that, neglecting the bending resistance, the elastic potential energy may be written

$$\tfrac{1}{2} d e_{ij} \sigma_{ij} \qquad (i \text{ and } j \text{ are summed over } 1 \text{ and } 2) \tag{A.1}$$

where e_{ij} is the total strain tensor given by

$$e_{ij} = \tfrac{1}{2}\left(\frac{\partial u_i}{\partial y_j} + \frac{\partial u_j}{\partial y_i}\right) + \tfrac{1}{2}\frac{\partial \xi}{\partial y_i}\frac{\partial \xi}{\partial y_j} \quad , \tag{A.2}$$

and σ_{ij} is the stress tensor set up in the plate by this strain

$$\sigma_{ij} = \frac{E}{1+\nu} e_{ij} + \frac{E\nu}{1-\nu^2} e_{kk} \delta_{ij} \quad . \tag{A.3}$$

δ_{ij} is the two-dimensional Kronecker δ

$$= \begin{cases} 1 & \text{if } i = j \\ 0 & \text{if } i \neq j. \end{cases}$$

If we have an applied force P per unit area acting normal to the sheet in the positive y_3-direction, and a force per unit length T_i applied around the boundary, as shown in Figure 4.A, then the total potential energy V is given by

$$V = \int\int \left\{ \tfrac{1}{2} d e_{ij} \sigma_{ij} - P\xi \right\} dy_1 dy_2 - \oint T_i u_i d\, ds \quad , \tag{A.4}$$

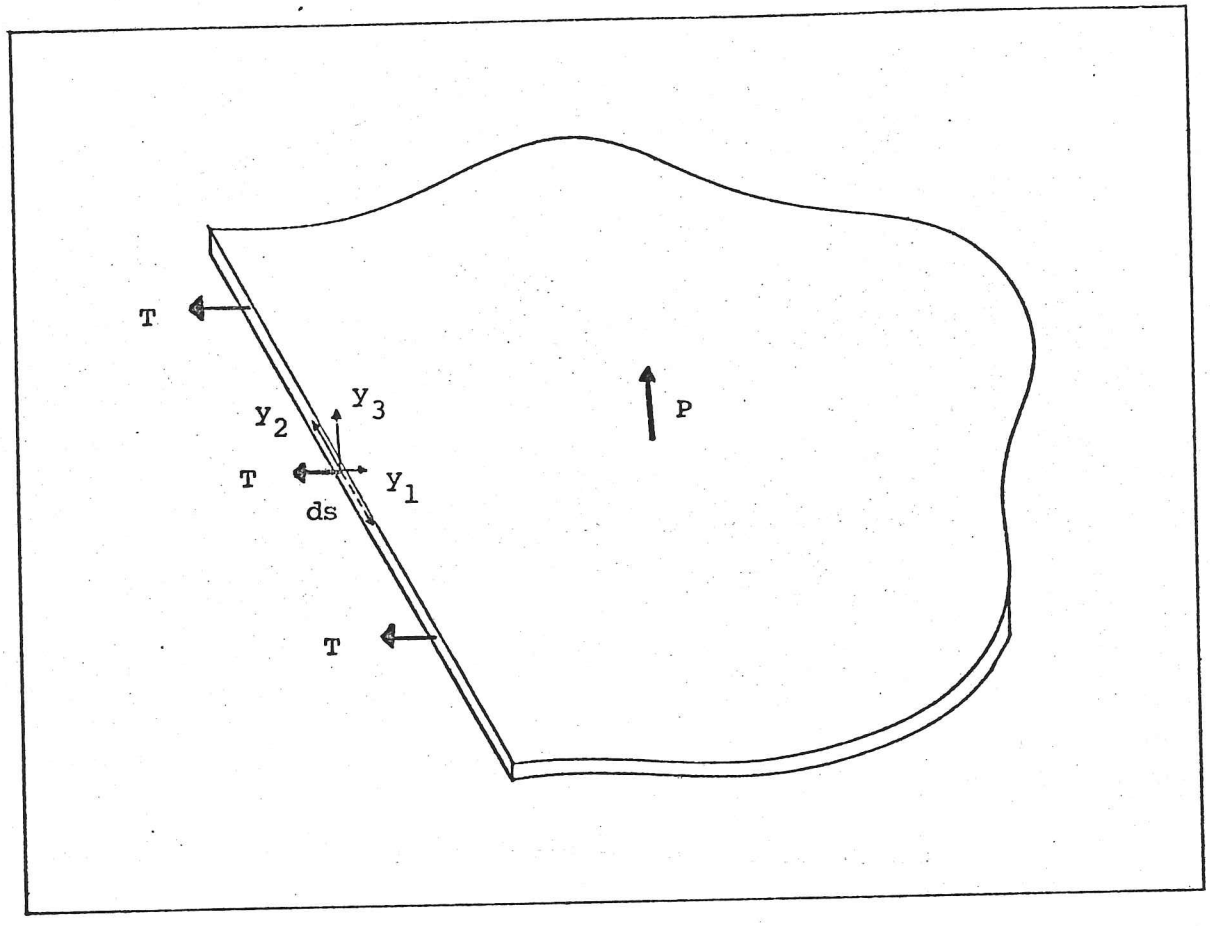

Figure 4.A The geometry of the plate

where the first integral is over the plate area and the second is round its circumference.

The total kinetic energy, U , is equal to

$$\iint \tfrac{1}{2}\rho_M d\left\{\left(\frac{\partial \xi}{\partial \tau}\right)^2 + \frac{\partial u_i}{\partial \tau}\frac{\partial u_i}{\partial \tau}\right\} dy_1\, dy_2 \quad . \tag{A.5}$$

Now Hamilton's principle states that in any mechanical system the variation in the integral of U-V is zero for arbitrary variations in ξ and u_1 ;

$$\delta \int_{t_1}^{t_2} (U-V)dt = 0 \quad . \tag{A.6}$$

Hence

$$\int_{t_1}^{t_2} dt \iint \left(\delta\xi \left\{ -\rho_M d \frac{\partial^2 \xi}{\partial \tau^2} + d \frac{\partial}{\partial y_j} \left(\sigma_{ij} \frac{\partial \xi}{\partial y_i} \right) + P \right\} + \delta u_i \left\{ -\rho_M d \frac{\partial^2 u_i}{\partial \tau^2} + d \frac{\partial \sigma_{ij}}{\partial y_j} \right\} \right) dy_1 dy_2$$

$$- \int_{t_1}^{t_2} dt \oint \left(\delta\xi \sigma_{ij} n_j \frac{\partial \xi}{\partial y_i} d + \delta u_i \left\{ \sigma_{ij} n_j d - T_i d \right\} \right) ds = 0 \quad . \tag{A.7}$$

Since this is true for arbitrary $\delta\xi$ and δu_i we obtain the equations of motion

$$\rho_M \frac{\partial^2 u_i}{\partial \tau^2} - \frac{\partial \sigma_{ij}}{\partial y_j} = 0 \tag{A.8}$$

and

$$\rho_M d \frac{\partial^2 \xi}{\partial \tau^2} - d \frac{\partial}{\partial y_j} \left(\sigma_{ij} \frac{\partial \xi}{\partial y_i} \right) = P \quad . \tag{A.9}$$

When the boundary $y_1 = 0$ is tugged with a prescribed force per unit length $-T(\tau)$ in the 1-direction the boundary conditions are from (A.7)

$$\sigma_{11}(0, y_2, \tau) = T(\tau) \qquad \text{and} \qquad \xi(0, y_2, \tau) = 0 \quad . \tag{A.10}$$

We linearize the expression (A.3) for σ_{ij} by neglecting the term quadratic in ξ . This term describes the additional stress caused by the bending of the plate and is negligible in comparison with that due to the external stretching force applied on the circumference.

Then

$$\sigma_{ij} = \frac{E}{2(1+\nu)} \left(\frac{\partial u_i}{\partial y_j} + \frac{\partial u_j}{\partial y_i} \right) + \frac{E\nu}{1-\nu^2} \frac{\partial u_k}{\partial y_k} \delta_{ij} \quad . \tag{A.11}$$

When we substitute this form of σ_{ij} into (A.8) and (A.9) and remember that here the problem is independent of y_2 these equations reduce to those used in the main text;

$$\rho_M \frac{\partial^2 u_1}{\partial \tau^2} = \frac{E}{1-\nu^2} \frac{\partial^2 u_1}{\partial y_1^2} \quad , \tag{A.12}$$

$$u_2 = 0 \quad , \tag{A.13}$$

$$\rho_M d \frac{\partial^2 \xi}{\partial \tau^2} - d \frac{\partial}{\partial y_1} \left(\sigma_{11} \frac{\partial \xi}{\partial y_1} \right) = P \quad , \tag{A.14}$$

where

$$\sigma_{11} = \frac{E}{1-\nu^2} \frac{\partial u_1}{\partial y_1} \quad . \tag{A.15}$$

APPENDIX 4.B SIMPLIFICATION OF THE INTEGRAL DESCRIBING THE FAR-FIELD DENSITY

From equation (2.19) we have

$$(\rho-\rho_o)(\underset{\sim}{x},t) = I_1 + I_2 \quad , \tag{B.1}$$

where

$$I_1 = \frac{\rho_o}{2\pi c^2}\frac{\partial}{\partial t}\int_{y_1=0}^{\infty}\int_{y_2=-\infty}^{\infty}\left[\frac{g_1(y_1+\beta\tau)H(\tau-y_1/\alpha)}{|\underset{\sim}{x}-\underset{\sim}{y}|}\right]dy_1\,dy_2 \quad , \tag{B.2}$$

and

$$I_2 = \frac{\rho_o}{2\pi c^2}\frac{\partial}{\partial t}\int_{y_1=0}^{\infty}\int_{y_2=-\infty}^{\infty}\left[\frac{g_2(y_1-\beta\tau)H(\tau-y_1/\alpha)}{|\underset{\sim}{x}-\underset{\sim}{y}|}\right]dy_1\,dy_2 \quad . \tag{B.3}$$

The square brackets denote that the function they enclose is to be evaluated at a retarded time $\tau = t-|\underset{\sim}{x}-\underset{\sim}{y}|/c$.

In the integral I_1 , we change the integration variable to $\underset{\sim}{\eta} = \underset{\sim}{y}+\underset{\sim}{\beta}\tau$ with $\underset{\sim}{\beta} = (\beta,0,0)$. The Jacobian of the transformation is

$$\frac{|\underset{\sim}{x}-\underset{\sim}{y}|}{|\underset{\sim}{x}-\underset{\sim}{y}| + (x_1-y_1)\beta/c} \quad .$$

Hence

$$I_1 = \frac{\rho_o}{2\pi c^2}\frac{\partial}{\partial t}\iint_D\left[\frac{g_1(\eta_1)H(\tau\{1+\beta/\alpha\}-\eta_1/\alpha)}{|\underset{\sim}{x}-\underset{\sim}{\eta}+\underset{\sim}{\beta}\tau| + (x_1-\eta_1+\beta\tau)\beta/c}\right]d\eta_1 d\eta_2 \tag{B.4}$$

where now

$$\tau = t - |\underset{\sim}{x}-\underset{\sim}{\eta}+\underset{\sim}{\beta}\tau|/c \quad . \tag{B.5}$$

D is the image of the region $y_1 \geq 0$, $\infty \geq y_2 \geq -\infty$, $y_3 = 0$ mapped into the $\underset{\sim}{\eta}$-plane as shown in Figure 4.B. The boundary of D corresponds to $y_1 = 0$ and hence $\eta_1 = \beta\tau$ on this boundary or alternatively $\eta_1-\beta t = |\underset{\sim}{x}-\underset{\sim}{\eta}+\underset{\sim}{\beta}\tau|$.

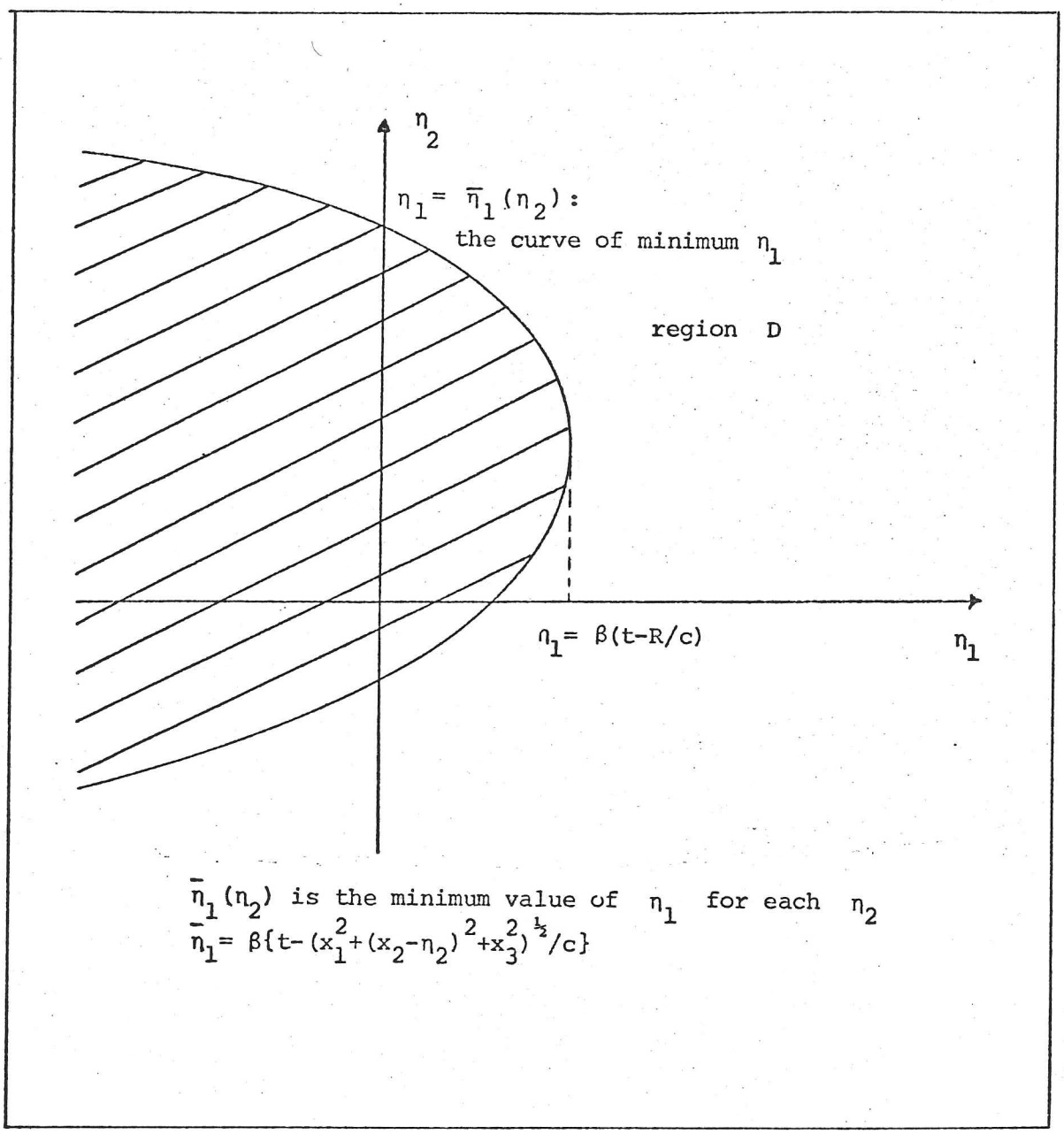

Figure 4.B The boundary of the region D

We can evaluate the time derivative in (B.4). The integrand varies with t only through τ and in addition we must differentiate the limits of integration.

From a differentiation of (B.5) with respect to time, we find

$$\left.\frac{\partial\tau}{\partial t}\right|_{\underset{\sim}{\eta}} = \frac{|\underset{\sim}{x}-\underset{\sim}{\eta}+\underset{\sim}{\beta}\tau|}{|\underset{\sim}{x}-\underset{\sim}{\eta}+\underset{\sim}{\beta}\tau| + (x_1-\eta_1+\beta\tau)\beta/c} \quad . \tag{B.6}$$

Then

$$I_1 = -\frac{\rho_o \beta}{\pi c} \int_{\tau=-\infty}^{t-R/c} \frac{g_1(\beta\tau)H(\tau)d\tau}{\{c^2(t-\tau)^2-R^2\}^{\frac{1}{2}}(1+\beta\cos\theta/c)}$$

$$+ \frac{\rho_o(1+\beta/\alpha)}{2\pi c^2} \iint_D \left[\frac{g_1(\eta_1)\delta(\tau\{1+\beta/\alpha\}-\eta_1/\alpha)}{|\underset{\sim}{x}-\underset{\sim}{\eta}+\underset{\sim}{\beta}\tau|(1+\beta\cos\theta/c)^2} (1+O(\ell/|\underset{\sim}{x}|)) \right] d\eta_1 d\eta_2 \quad , \qquad (B.7)$$

where

$$R = (x_1^2+x_3^2)^{\frac{1}{2}} \quad , \quad \cos\theta = \frac{x_1}{c(t-\tau)} \quad , \quad \cos\Theta = \frac{x_1-\eta_1+\beta\tau}{|\underset{\sim}{x}-\underset{\sim}{\eta}+\underset{\sim}{\beta}\tau|} \quad ,$$

and ℓ is the length scale over which h varies.

We rewrite the second integral in (B.7) in terms of the stationary coordinates (y_1,y_2) ;

$$\iint_D \left[\frac{g_1(\eta_1)\delta(\tau\{1+\beta/\alpha\}-\eta_1/\alpha)}{|\underset{\sim}{x}-\underset{\sim}{\eta}+\underset{\sim}{\beta}\tau|(1+\beta\cos\psi/c)^2} \right] d\eta_1 d\eta_2 = \int_{y_1=0}^{\infty} \int_{y_2=-\infty}^{\infty} \left[\frac{g_1(y_1+\beta\tau)\delta(\tau-y_1/\alpha)}{|\underset{\sim}{x}-\underset{\sim}{y}|+(x_1-y_1)\beta/c} \right] dy_1 dy_2 .$$

The y_2-integral can be evaluated using the δ-function

$$= 2c \int_{y_1=0}^{\infty} \frac{g_1(y_1\{1+\beta/\alpha\})H\left(t-y_1/\alpha-\{(x_1-y_1)^2+x_3^2\}^{\frac{1}{2}}/c\right)}{\left\{c^2(t-y_1/\alpha)^2-(x_1-y_1)^2-x_3^2\right\}^{\frac{1}{2}}(1+\beta\cos\phi/c)} dy_1 \quad ,$$

where $$\cos\phi = \frac{x_1-y_1}{c(t-y_1/\alpha)} \quad .$$

When g_1 is expressed in terms of the initial vertical displacement h from equation (2.16)

$$I_1 = -\frac{\rho_o \beta^2 H(t-R/c)}{2\pi c(1+\beta/\alpha)} \int_{\tau=0}^{t-R/c} \frac{h'(\beta\tau\{1+\beta/\alpha\}^{-1})d\tau}{\{c^2(t-\tau)^2-R^2\}^{\frac{1}{2}}(1+\beta\cos\theta/c)} .$$

$$+ \frac{\rho_o \beta}{2\pi c} \int_{y_1=0}^{\infty} \frac{H\left(t-y_1/\alpha-\{(x_1-y_1)^2+x_3^2\}^{\frac{1}{2}}/c\right)h'(y_1)dy_1}{\left\{c^2(t-y_1/\alpha)^2-(x_1-y_1)^2-x_3^2\right\}^{\frac{1}{2}}(1+\beta\cos\phi/c)} (1+O(\ell/|\underset{\sim}{x}|)) \quad .$$

(B.8)

The integral I_2 may be treated similarly. We introduce a moving coordinate system $\underset{\sim}{\eta}^* = \underset{\sim}{y} - \underset{\sim}{\beta}\tau$ and once again the time derivative may be evaluated to give

$$I_2 = -\frac{\rho_o \beta^2 H(t-R/c)}{2\pi c(1+\beta/\alpha)} \int_{\tau=0}^{t-R/c} \frac{h'(\beta\tau\{1+\beta/\alpha\}^{-1})d\tau}{\{c^2(t-\tau)^2-R^2\}^{\frac{1}{2}}(1-\beta\cos\theta/c)}$$

$$-\frac{\rho_o \beta}{2\pi c} \int_{y_1=0}^{\infty} \frac{H\left(t-y_1/\alpha-\{(x_1-y_1)^2+x_3^2\}^{\frac{1}{2}}/c\right)h'(y_1)dy_1}{\left\{c^2(t-y_1/\alpha)^2-(x_1-y_1)^2-x_3^2\right\}^{\frac{1}{2}}(1-\beta\cos\phi/c)} (1+O(\iota/|\underset{\sim}{x}|)) \quad . \tag{B.9}$$

By adding (B.8) and (B.9) we finally obtain

$$(\rho-\rho_o)(\underset{\sim}{x},t) = I_1 + I_2$$

$$= -\frac{\rho_o \beta^2 H(t-R/c)}{\pi c(1+\beta/\alpha)} \int_{\tau=0}^{t-R/c} \frac{h'(\beta\tau\{1+\beta/\alpha\}^{-1})d\tau}{\{c^2(t-\tau)^2-R^2\}^{\frac{1}{2}}(1-\beta^2\cos^2\theta/c^2)}$$

$$-\frac{\rho_o \beta^2}{\pi c^2} (1+O(\iota/|\underset{\sim}{x}|)) \int_{y_1=0}^{\infty} \frac{H\left(t-y_1/\alpha-\{(x_1-y_1)^2+x_3^2\}^{\frac{1}{2}}/c\right)h'(y_1)\cos\phi dy_1}{\left\{c^2(t-y_1/\alpha)^2-(x_1-y_1)^2-x_3^2\right\}^{\frac{1}{2}}(1-\beta^2\cos^2\phi/c^2)}. \tag{B.10}$$